Université catholique de Louvain

Earth and Life Institute – Earth and Climate (ELI-C)

Ghent University

Department of Green Chemistry and Technology – Faculty of Bioscience Engineering

---

Soil erosion and nutrient availability in tropical forests of the Congo Basin

---

Simon BAUMGARTNER

Doctoral thesis for a joint PhD in

Science at Université catholique de Louvain
and
Bioscience engineering at Ghent University

PhD committee:
Prof. Kristof van Oost, UC Louvain (supervisor)
Prof. Pascal Boeckx, UGent (supervisor)
Prof. De Keersmaecker Marie-Laurence, UC Louvain (Chairperson)
Prof. Johan Six, ETH Zürich
Dr. Marijn Bauters, UGent
Prof. Vanacker Veerle, UC Louvain
Prof. Bouillon Steven, KU Leuven

French translation of the title:

L'érosion des sols et la disponibilité des nutriments dans les forêts tropicales du bassin du Congo

Dutch translation of the title:

Bodemerosie en beschikbaarheid van voedingsstoffen in tropische bossen in het Congobekken

Summary

The importance of tropical forests in the global climate system is widely known. Through their high productivity they represent a significant global carbon reservoir. Preserving this function needs a continuous supply of nutrients, mainly nitrogen (N) and phosphorus (P). However, the availability and biogeochemical cycling of these nutrients is highly variable in space and time and the understanding of different nutrient loss pathways is still lacking. The influence of soil erosion on the availability of these nutrients in pristine forests of the tropics is not well understood. To gain a better mechanistic understanding of the aquatic loss processes of N and P, we monitored different headwater streams in three distinct tropical forests of the Congo Basin and determined the influence of soil erosion on soil N. This knowledge is important to assess the response of these ecosystems to changing climate and land use.

To assess the importance of soil erosion in tropical forests and export of sediments and nutrients from drainage basins, the first part of the thesis focussed on the fundamental understanding of the dynamics and drivers of sediment export in headwater streams of a tropical lowland forest and a deciduous Miombo woodland. We used high temporal resolution turbidity data and analysed the turbidity-discharge hysteresis patterns during storm events. Although these forest systems are situated in very old and stable landscapes, the obtained sediment yields were substantial and comparable to forests in more geomorphic active sites of the tropics. Although the Miombo only experiences a five-month wet season, similar annual sediment export was found as for the lowland forest, due to the lower vegetation cover. Furthermore, results showed that storm events exported 30% and 68% of the annual sediment yield in the lowland and the Miombo, respectively.

In Chapter three, it was shown that soil erosion and storm events also play a crucial role in aquatic nutrient export from these forest ecosystems. At both sites, N and P were dominantly exported in particulate or dissolved organic forms and the yields of those nutrient constituents were driven by intense discharge pulses due to storm events. This highlights the need to include samples of those events in a sampling campaign to get reliable annual export yields. This was not possible for the montane forest monitoring site (Chapter four), resulting in a large uncertainty in the sediment and nutrient yield estimates. However, best estimates of the long-term baseflow dataset highlighted the same trend to the importance of particulate and dissolved organic N and P export. Although these losses are significant, there is no indication that erosion leads to local nutrient limitations in the N and P rich montane and lowland forests. The goal of Chapter five was to evaluate if soil erosion influences soil N at the catchment scale. For this, stable isotope signatures of soil N have been analysed as an integrator of N cycling processes. Results showed that only in the Miombo woodland, stable isotopic signatures of soil N were influenced by topography and soil erosion, indicating erosional effects on N cycling.

In the last part of this thesis, the influence of land use in the lowlands on aquatic sediment and nutrient export was examined. Results from a field campaign, during which baseflow was intensively sampled, revealed that there was significant higher export of dissolved organic N and particulate inorganic P, while the yields of nitrate were lower in an agricultural catchment compared to the pristine forest catchment. Continuous sensor measurements indicated that our findings most probably underestimated these differences because of the lack of storm event data.

The results of this thesis highlight the importance of particulate N and P losses from pristine tropical forests and their inclusion in biogeochemical studies are important, even in so believed low erosive ecosystems. The predicted increase in rainfall intensity and the ongoing loss of primary forests will further enhance the importance of these processes.

Résumé

L'importance des forêts tropicales dans le système climatique mondial est largement connue. Grâce à leur forte productivité, elles représentent un réservoir de carbone à l'échelle mondiale. La préservation de cette fonction nécessite un approvisionnement continu en nutriments, principalement en azote (N) et en phosphore (P). Cependant, la disponibilité et le cycle biogéochimique de ces nutriments sont très variables dans l'espace et dans le temps. La compréhension des différentes voies de perte de nutriments demeure insuffisante. De ce fait, l'influence de l'érosion des sols sur la disponibilité de ces nutriments dans les forêts vierges des tropiques est moins comprise. Afin d'acquérir une meilleure compréhension mécaniste des processus de perte aquatique de N et de P, nous avons suivi différents cours d'eau de tête dans trois forêts tropicales distinctes du Bassin du Congo et déterminé l'influence de l'érosion du sol sur le N du sol. Ces connaissances sont importantes pour évaluer la réponse de ces écosystèmes aux changements climatiques et à l'utilisation des terres.

Dans le but d'évaluer l'importance de l'érosion des sols dans les forêts tropicales et l'exportation de sédiments et de nutriments depuis les bassins versants, la première partie de la thèse s'est concentrée sur la compréhension fondamentale de la dynamique et des moteurs de l'exportation de sédiments dans les cours d'eau de tête d'une forêt tropicale de plaine et d'une forêt de Miombo à feuilles caduques. Nous avons utilisé des données de turbidité à haute résolution temporelle et analysé les modèles d'hystérésis de turbidité-débit pendant les événements de tempête. Bien que ces systèmes forestiers soient situés dans des paysages stables, les rendements sédimentaires obtenus étaient substantiels et comparables à ceux des forêts situées dans des sites géomorphologiques plus actifs des tropiques. Bien que le Miombo ne connaisse qu'une saison humide de cinq mois, l'exportation annuelle de sédiments était similaire à celle de la forêt tropicale de plaine, suite à de la couverture végétale plus faible. De plus, les résultats de cette étude ont révélé que 30% et 68% des rendements annuels de sédiments respectivement dans la forêt tropicale de plaine et le Miombo ont été exportés suite aux événements de tempête.

Dans le chapitre trois, il a été montré que l'érosion du sol et les tempêtes jouent également un rôle crucial dans l'exportation des nutriments aquatiques de ces écosystèmes forestiers. Sur les deux sites, N et P ont été principalement exportés sous forme de particules ou d'éléments organiques dissous. Les rendements de ces éléments nutritifs ont été déterminés par des impulsions de décharge intenses dues aux tempêtes. Cela souligne la nécessité d'inclure ces paramètres dans une campagne d'échantillonnage afin d'obtenir des rendements d'exportation annuels fiables. Cela n'a pas été possible pour le site de surveillance de la forêt montagnarde (chapitre quatre), ce qui a entraîné une grande incertitude dans l'estimation des rendements en sédiments et en nutriments. Cependant, les meilleures estimations de l'ensemble de données sur le débit de base à long terme ont mis en évidence la même tendance à l'importance de l'exportation de N et P organiques particulaires et dissous. Bien que ces pertes soient importantes, rien n'indique que l'érosion entraîne

des limitations locales de nutriments dans les forêts de montagne et de plaine riches en N et en P. Le chapitre cinq avait pour objectif d'évaluer l'effet de l'érosion du sol sur l'azote du sol à l'échelle du bassin versant. Pour cela, les signatures isotopiques stables de l'azote du sol ont été analysées en tant qu'intégrateur des processus de cycle de l'azote. Les résultats ont montré que dans la forêt de Miombo en particulier, les signatures isotopiques stables de l'azote du sol ont été influencées par la topographie et l'érosion du sol, ce qui indique les effets de l'érosion sur le cycle de l'azote.

La dernière partie de cette thèse avait pour objectif d'examiner l'influence de l'utilisation des terres sur les sédiments aquatiques et l'exportation de nutriments dans les forêts de basse altitude. Les résultats d'une campagne de terrain, au cours de laquelle le débit de base a été intensivement échantillonné, ont révélé l'existence d'une exportation significativement plus élevée de N organique dissous et de P inorganique particulaire, alors que les rendements de nitrate étaient plus faibles dans un bassin versant agricole par rapport au bassin versant forestier vierge. Les mesures des capteurs continus ont indiqué que nos résultats ont très probablement sous-estimé ces différences en raison du manque de données sur les événements de tempête.

Les résultats de cette thèse soulignent l'importance des pertes de N et P particulaires des forêts tropicales vierges. Leur inclusion dans les études biogéochimiques est importante, même dans des écosystèmes que l'on croit peu érosifs. L'augmentation prévue de l'intensité des précipitations et la perte continue de forêts primaires contribueront à renforcer l'importance de ces processus.

Samenvatting

Het belang van tropische bossen voor het globale klimaatsysteem is algemeen bekend. Door hun hoge productiviteit assimileren deze bossen enorme hoeveelheden koolstof en vormen zij dus een belangrijk globaal reservoir voor CO_2 in de globale koolstofcyclus. Om deze functie in stand te houden is een voortdurende toevoer van nutriënten nodig, voornamelijk stikstof (N) en fosfor (P). De beschikbaarheid en biogeochemische cyclus van deze nutriënten is echter zeer variabel in ruimte en tijd en het inzicht in de verschillende routes waarlangs nutriënten verloren gaan, is nog steeds beperkt. Ook de invloed van bodemerosie op de beschikbaarheid van deze nutriënten in ongerepte bossen in de tropen is niet goed begrepen. Om een beter mechanistisch inzicht te krijgen in de aquatische verliesprocessen van N en P, bestudeerden we verschillende bovenlopen in drie verschillende tropische wouden van het Congobekken en bepaalden we de invloed van erosie op N in de bodem. Deze kennis is belangrijk om de respons van deze ecosystemen op een veranderend klimaat en landgebruik te in te schatten.

Om het belang van bodemerosie en sedimentexport in tropische wouden te bestuderen, richtte het eerste deel van dit doctoraat zich op de fundamentele kennis van de dynamiek en de drijvende krachten van sedimentexport in bovenlopen van een tropisch laaglandbos en een Miombo-bos. We gebruikten gegevens met een hoge temporele resolutie van de troebelheid van het water en analyseerden de hysteresispatronen van troebelheid versus debiet tijdens stormen. Hoewel deze bossystemen zich in geomorfologisch stabiele landschappen bevinden, waren de berekende hoeveelheden sedimentexport aanzienlijk en vergelijkbaar met bossen in meer geomorfisch actieve gebieden in de tropen. Hoewel de Miombo slechts een nat seizoen van vijf maanden kent, werd een vergelijkbare jaarlijkse sedimentexport gevonden als voor het laaglandbos, als gevolg van de lagere vegetatiebedekking. Bovendien toonden de resultaten het belang van stormen op de sedimentexport, die respectievelijk 30% en 68% van de jaarlijkse sedimentexport in het laagland en de Miombo voor hun rekening namen.

In een volgend hoofdstuk werd aangetoond dat bodemerosie en stormen ook een cruciale rol spelen in de aquatische export van nutriënten in deze bosecosystemen. Op beide locaties werden N en P overwegend geëxporteerd als fijn materiaal, of als opgeloste organische vormen. De geëxporteerdehoeveelheid van deze nutriënten werd bepaald door intense debieten als gevolg van stormen. Dit onderstreept de noodzaak om stalen tijdens dergelijke gebeurtenissen te verzamelen om betrouwbare berekening van de jaarlijkse hoeveelheid geëxporteede nutriënten te maken. Dit was niet mogelijk voor het deel van het studiegebied gelegen in een bergachtig gebied, wat resulteert in een grote onzekerheid voor de berekende hoeveelheden geëxporteerde sedimenten en nutriënten. De beste berekeningen van de dataset verzameld tijdens basisdebieten op lange termijn wezen echter op dezelfde tendens voor het belang van de export van organische N en P uit fijn materiaal en opgeloste organische stof. Hoewel deze verliezen aanzienlijk zijn, zijn er geen aanwijzingen dat erosie leidt tot lokale tekorten in nutriënten in de N en P

rijke geheuvelde en laagland bossen. In hoofdstuk 5 was het doel om te evalueren of erosie een effect heeft op N in de bodem op de schaal van stroombekkens. Hiervoor zijn kenmerkende verhoudingen in stabiele isotopen van bodem N geanalyseerd als een benadering van processes gerelateerd aan de cyclus van N in bodems. Alleen in het Miombo-bos werden de verhoudingen in stabiele isotopen van bodem N beïnvloed door topografie en bodemerosie, wat wijst op een effect van erosie op de N cyclus.

In het laatste deel van dit doctoraat werd de invloed van landgebruik in de laaglanden op de aquatische sediment- en nutriëntenexport onderzocht. De intensieve bemonsteringscampagne van het basisdebiet toonde aan dat er een significant hogere export was van opgelost organisch N en anorganisch P in fijn materiaal, terwijl de hoeveelheid geëxporteerd nitraat lager was in rivier in een landbouwgebied vergeleken met een rivier in een ongerepte bos. Continue metingen met sensors suggereren dat onze resultaten deze verschillen onderschatten vanwege het gebrek aan gegevens over export tijdens stormen.

De resultaten van dit proefschrift onderstrepen het belang van N- en P-verliezen als fijn materiaal uit ongerepte tropische bossen en de opname daarvan in biogeochemische studies zijn belangrijk, zelfs in ecosystemen waar erosie geacht wordt mininimaal te zijn. De voorspelde toename van de neerslagintensiteit en het voortdurende verlies van oerbossen zullen het belang van deze processen nog doen toenemen.

Zusammenfassung

Die Bedeutung tropischer Wälder für das globale Klimasystem ist allgemein bekannt. Durch ihre hohe Produktivität stellen sie ein bedeutendes globales Kohlenstoffreservoir dar. Die Aufrechterhaltung dieser Funktion erfordert eine kontinuierliche Zufuhr von Nährstoffen, vor allem von Stickstoff (N) und Phosphor (P). Die Verfügbarkeit und der biogeochemische Kreislauf dieser Nährstoffe sind jedoch räumlich und zeitlich sehr variabel, und die verschiedenen Wege des Nährstoffverlusts sind noch nicht ausreichend bekannt. Der Einfluss der Bodenerosion auf die Verfügbarkeit dieser Nährstoffe in Urwäldern in den Tropen ist nicht gut verstanden. Um ein besseres mechanistisches Verständnis der aquatischen N- und P-Verluste zu erlangen, haben wir verschiedene Quellbäche in drei verschiedenen tropischen Wäldern des Kongobeckens beobachtet und den Einfluss der Bodenerosion auf die Bodennährstoffe bestimmt. Dieses Wissen ist wichtig, um die Reaktion dieser Ökosysteme auf Klima- und Landnutzungsänderungen zu bewerten.

Um die Bedeutung der Bodenerosion in tropischen Wäldern und den Export von Sedimenten und Nährstoffen aus Entwässerungsgebieten zu bewerten, konzentrierte sich der erste Teil der Arbeit auf das grundlegende Verständnis der Dynamik und der Triebkräfte des Sedimentexports in Oberläufen eines tropischen Tieflandwaldes und eines sommergrünen Miombo-Waldes. Wir verwendeten zeitlich hoch aufgelöste Trübungsdaten und analysierten die Hysteresemuster von Trübung und Abfluss während Sturmereignissen. Obwohl sich diese Waldsysteme in stabilen Landschaften befinden, waren die erzielten Sedimenterträge beträchtlich und vergleichbar mit Wäldern in geomorphologisch aktiveren Gebieten der Tropen. Obwohl der Miombo-Wald nur eine fünfmonatige Regenzeit erlebt, wurde aufgrund der geringeren Vegetationsbedeckung ein ähnlicher jährlicher Sedimentexport wie im Tieflandwald festgestellt. Darüber hinaus zeigten die Ergebnisse, dass Sturmereignisse 30 % bzw. 68 % des jährlichen Sedimentaustrags im Tiefland und im Miombo-Gebiet ausmachen.

In Kapitel 3 wurde gezeigt, dass Bodenerosion und Sturmereignisse auch eine entscheidende Rolle für den aquatischen Nährstoffexport aus diesen Waldökosystemen spielen. An beiden Standorten wurden N und P überwiegend in partikulärer oder gelöster organischer Form exportiert, und die Ausbeute an diesen Nährstoffbestandteilen wurde durch intensive Abflussimpulse aufgrund von Sturmereignissen bestimmt. Dies unterstreicht die Notwendigkeit, Proben dieser Ereignisse in eine Probenahme-Kampagne einzubeziehen, um zuverlässige jährliche Exportwerte zu erhalten. Dies war bei der Überwachungsstelle im montanen Wald (Kapitel 4) nicht möglich, was zu einer großen Unsicherheit bei den Sediment- und Nährstofferträgen führte. Die besten Schätzungen der langfristigen Basisdaten zeigen jedoch denselben Trend zur Bedeutung des partikulären und gelösten organischen N- und P-Exports. Obwohl diese Verluste beträchtlich sind, gibt es keinen Hinweis darauf, dass die Erosion zu einer lokalen Nährstofflimitation in den N- und P-reichen montanen und Tieflandwäldern führt. Ziel des fünften Kapitels war

es zu untersuchen, ob die Bodenerosion Auswirkungen auf den Stickstoffgehalt des Bodens auf der Ebene des Einzugsgebiets hat. Zu diesem Zweck wurden stabile Isotopensignaturen des Stickstoffs im Boden als Indikator für die Prozesse des Stickstoffkreislaufs analysiert. Die Ergebnisse zeigten, dass nur in den Miombo-Wäldern die stabilen Isotopensignaturen des Boden-N durch die Topographie und die Bodenerosion beeinflusst wurden, was auf erosive Auswirkungen auf den N-Kreislauf hinweist.

Im letzten Teil dieser Arbeit wurde der Einfluss der Landnutzung im Tiefland auf den aquatischen Sediment- und Nährstoffexport untersucht. Die Ergebnisse einer Feldkampagne, bei der der Grundwasserabfluss intensiv beprobt wurde, zeigten, dass in einem landwirtschaftlich genutzten Einzugsgebiet ein deutlich höherer Export von gelöstem organischem N und partikulärem anorganischem P zu verzeichnen war, während die Nitratausbeute im Vergleich zu einem unberührten Waldeinzugsgebiet geringer war. Kontinuierliche Sensormessungen zeigten, dass unsere Ergebnisse diese Unterschiede höchstwahrscheinlich unterschätzten, da keine Daten zu Sturmereignissen vorlagen.

Die Ergebnisse dieser Arbeit unterstreichen die Bedeutung der partikulären N- und P-Verluste aus tropischen Urwäldern, und ihre Einbeziehung in biogeochemische Studien ist wichtig, selbst in vermeintlich wenig erosiven Ökosystemen. Die prognostizierte Zunahme der Niederschlagsintensität und der fortschreitende Verlust von Primärwäldern werden die Bedeutung dieser Prozesse noch verstärken.

Abbreviations

BNF	biological nitrogen fixation
CRB	Congo River Basin
CUE	carbon use efficiency
DEM	digital elevation model
DIN	dissolved inorganic nitrogen
DIP	dissolved inorganic phosphorus
DOC	dissolved organic carbon
DON	dissolved organic nitrogen
DOP	dissolved organic phosphorus
DRC	Democratic Republic of the Congo
EC	erosion coefficient
ET	evapotranspiration
fDOM	fluorescent dissolved organic matter
GHG	greenhouse gas
GPP	gross primary production
HI	hysteresis index
LAI	leaf area index
LSI	landslide hazard index
LUC	land-use change
MAP	mean annual precipitation
m a.s.l.	meters above sea level
MAT	mean annual temperature
NPP	net primary production
NSE	Nash-Sutcliffe efficiency
PIP	particulate inorganic phosphorus
POM	particulate organic matter
PN	particulate nitrogen
Q	discharge
TDN	total dissolved nitrogen
TDP	total dissolved phosphorus
TN	total nitrogen
TP	total phosphorus
TPP	total particulate phosphorus
TSS	total suspended sediments

Table of Contents

Part I - Introduction

Chapter 1: Introduction

1.1. Global C cycle

One of the biggest challenges facing humankind in the 21st century are the risks accompanied by climate change. The effects of climate change are already visible today: longer periods of drought in some regions, increase in storm durations and intensities in other regions, more frequent wildfires and melting of glaciers, just to name a few (IPCC, 2021). Climate change is mainly driven by the increase of greenhouse gas (GHG) concentrations in the atmosphere, changing the energy balance of Earth's surface. Anthropogenic activities, such as the combustion of fossil fuels and land use change, increase the atmospheric concentrations of the three main GHGs since the pre-industrial era: carbon dioxide (CO_2, 47% increase), methane (CH_4, 156% increase) and nitrous oxide (N_2O, 23% increase) (IPCC, 2021).

For a better understanding of the impacts of changing GHG concentrations in the atmosphere, climate and earth system models are used. These models mainly describe the interactions of the atmosphere, ocean, land, and biosphere for an estimation of global or regional climates. The global biogeochemical carbon (C) cycle describes the fluxes and storage of C compounds between reservoirs of the earth system, mainly the atmosphere, oceans and the terrestrial and aquatic biosphere (Falkowski et al., 2000; Houghton, 2003). Fluxes and redistribution of C between the different reservoir can vary immensely in space and time. While geochemical weathering of carbonate minerals alters reservoirs on millennial timescales, the burning of fossil fuel is changing the sizes of C reservoirs on a much faster timescale. Fluxes between the terrestrial biosphere and the atmosphere are the largest C fluxes in the global C cycle (Photosynthesis: 120 Pg C yr^{-1}; Soil and Plant respiration: ~117 Pg C yr^{-1}) (Houghton, 2003), however, these land-to-atmosphere fluxes are far more variable and uncertain than other fluxes in the C cycle. Thus, a better mechanistical understanding of terrestrial ecosystems in the global C cycle is needed. Furthermore, this also helps to increase the accuracy of earth system models.

1.2. Role of tropical forests in the global C cycle

The magnitude of terrestrial C fluxes can vary highly between different ecosystems. Generally, tropical forests play an important role in the global C balance and C fluxes are higher compared to any other vegetation type, due to extent and the high productivity of these ecosystems. Besides being a hotspot for biodiversity (Gardner et al., 2009), tropical forests account for roughly 55 % of the total C stored in forested areas (Pan et al., 2011) and accounts roughly of one third of the metabolic activity of the land surface (Malhi, 2012). The annual C uptake of tropical forests by photosynthesis is estimated to be 72 Pg C (Beer et al., 2010). However, this large amount of sequestered C is partially released again to the atmosphere via autotrophic and heterotrophic respiration and fires. The respiration rates are high in tropics due to high temperature and soil moisture (Davidson et al., 2004).

The question if tropical forests are a net source or net sink of atmospheric C is still highly debated. The productivity of trees is believed to rise with increasing atmospheric CO_2 concentrations (CO_2 fertilizer effect; Lapola et al., 2009), although this effect can be limited due to increasing mortality of trees caused by changes in regional climate patterns, mainly droughts and increase in temperature (Brienen et al., 2015; Hubau et al., 2020). Especially climate change and land use changes in the tropics can have a huge influence on the C storage of tropical forests, with the potential to release large amounts of C stored into the atmosphere (Baccini et al., 2019).

Furthermore, geographical bias is fuelling uncertainties in modelling C fluxes of tropical forests globally. Research has been done primarily in tropical forests of Latin-America and South-East Asia. This region-specific measured C stocks and fluxes is frequently upscaled to the whole tropics, including the tropics of central Africa. However, more evidence is showing that differences between the Latin-American and African tropics are crucial: different structures (Banin et al., 2012), nutrient depositions (Bauters et al., 2018; Bauters et al., 2021) and different species composition (Slik et al., 2015) results in contrasting biomass and C stocks (Lewis et al., 2013) and sink strength (Hubau et al., 2020). More biogeochemical research is needed in tropical forests for a better understanding of their role in the global C cycle. This is especially true for the African tropics, where the lack of long-term measurements of biogeochemical processes are fuelling uncertainties in the understanding of the global C cycle (Ciais et al., 2011).

1.3. Nutrients interaction with the C cycle

The scale of different processes and biogeochemical fluxes within forests is dependent on forest functioning, however, forest functioning also requires nutrients. In forested ecosystems, the allocation of photosynthates to biomass is dependent on the nutrient availability (Vicca et al., 2012). The availability of nutrients is an important factor to determine the net primary production (NEP), i.e., the total amount of C assimilated by photosynthesis (gross primary production, GPP) minus the C lost due to autotrophic respiration. Furthermore, lack of nutrients can counteract the possible increase in GPP due to the CO_2-fertilization effect by limiting the biomass production (Fernández-Martínez et al., 2014). Therefore, adding nutrient dynamics into earth system models is important to mirror these mechanistic interdependencies and to identify potential feedbacks between the land biosphere and atmosphere (Wang et al., 2010). For example: the coupling of C and nitrogen (N) and phosphorus (P) cycles in earth system models reduces projected primary productivity between 19-74% compared to the same models without the nutrient coupling (Thornton et al., 2007; Wieder et al., 2015). A global assessment of the carbon use efficiency (CUE, i.e. the ratio between GPP and NEP) showed that CUE is positively correlated with nutrient availability, meaning that C is stored on longer terms in nutrient rich forests compared to forests that are limited in nutrients (Fernández-Martínez et al., 2014). Main nutrients for forest functioning are N and P, however, also the deficiency of other elements (such as calcium (Ca), magnesium (Mg), potassium (K), and iron (Fe)) can lead to limitations (Kaspari & Powers, 2016).

Thus, understanding the availabilities and dynamics of these nutrients within terrestrial ecosystem is crucial to improve our understanding and future behaving of land-climate interactions within changing environments.

1.4. N cycle

N is the most important nutrient for forest functioning since N is crucial for the building of proteins in all organisms. The two major inputs into tropical forest ecosystems are via atmospheric deposition and the biological fixation of atmospheric dinitrogen (N_2) gas (Fig 1.1). N_2 is a highly unreactive gas, due to the triple bond between the two N atoms and is the most abundant component in atmospheric air. Thus, N_2-fixation is an important process that converts non-reactive N_2 into ammonia (NH_3) which can be used by most organisms. N_2-fixing species are microorganism, some of them are in symbiosis with plants, especially legumes. Those N_2-fixing species can have a huge effect in C sequestration (Levy-Varon et al., 2019). Although N_2-fixing plants are highly abundant in the tropics (Houlton et al., 2008), there is evidence that N_2-fixation by legumes varies largely spatially, with more fixation in disturbed forests while in old-growth tropical lowland forests, N_2-fixation is almost completely downregulated (Barron et al., 2011; Bauters et al., 2016).

Another important input of N into a forested ecosystem is via N deposition, the path of atmospheric N input into a system (Fig 1.1). These inputs are widely diverse globally, because most of atmospheric N species that are deposited, are sourced from anthropogenic activities, such as industrial and agricultural practices. Thus, these enhanced N inputs have been mostly appointed to economically developed regions (Matson et al., 1999). Furthermore, mostly reactive N species (nitrogen oxides NO_x, ammonium NH_4^+, nitrate NO_3^- and N_2O) are being considered. However, also remote areas, with no close vicinity to high input agriculture or industry, such as remote regions in the tropics, can potentially be subjected to high atmospheric N inputs. This is due to high content of organic N in the deposited load. It has been shown that Savanna fires are the source of the organic N which is transported into remote places of the tropics. Thus, even pristine forests, such as the Congo Basin, are influenced by high atmospheric depositions of N (Bauters et al., 2018).

In the soil, mainly inorganic N forms are available for uptake by plants, although there is evidence that plants are capable to incorporate some organic forms of N directly (Neff et al., 2003). Still, the focus in biogeochemical studies lies on inorganic forms of N since they are more readily available for plant uptake. Soil microbes are responsible for controlling the amounts of organic and inorganic N forms in soils. Organic N is mineralized by microbes to the better available ammonium (NH_4^+) which then can be transformed to nitrate (NO_3^-) via nitrification, which is also a process controlled by microbes. NO_3^- on the other hand, can be reduced to N_2 which is lost out of the soil via outgassing. Also, the intermediate products of denitrification, nitrogen dioxide (NO_2), nitric oxide (NO) and N_2O can be lost out of the soil via outgassing. Dissolved organic N (DON) and inorganic N (DIN) can be exported out of the ecosystem by leaching, when organic and inorganic N-forms get into solution with soil water (Fig 1.1). Leaching losses are driven by the N status of a forest. It was

shown that in N-rich forests leaching is dominated by DIN, whereas under N-limited conditions, more DON gets lost via leaching (Hedin et al., 2009). The N status of a forests is also driving outgassing of N, as gaseous N losses correlates positively with the N-richness of an ecosystem (Hedin et al., 2003).

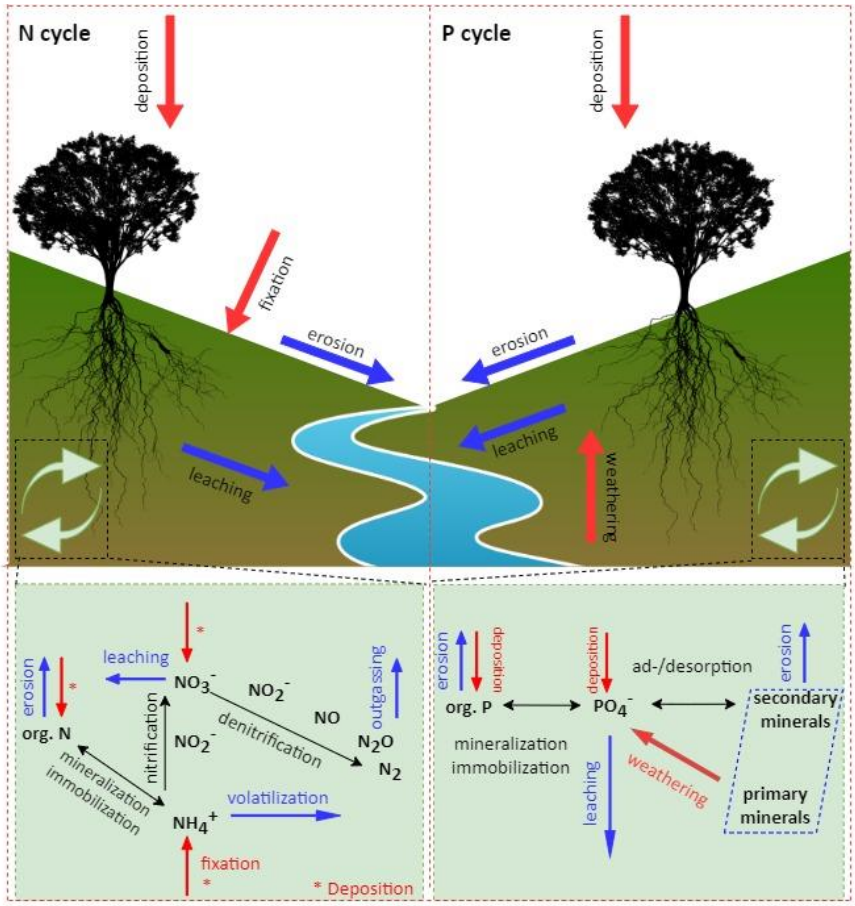

Fig. 1.1 Top: input (red arrows) and output (blue arrows) vectors of nitrogen (N) and phosphorus (P) in and from forest ecosystems. Green arrows indicate internal fluxes within the system. Bottom: detailed N and P cycles within soils.

1.5. P cycle

The biogeochemical cycle of P does not involve an important gaseous component, in contrast to the cycle of N. Thus, there is no atmospheric "fixation" of P and inputs into tropical forests ecosystem are mainly derived from weathering of P-containing bedrocks (Walker & Syers, 1976) and from atmospheric deposition of P containing dust particles (Chadwick et al., 1999) (Fig. 1.1). At early stages of soil development, the weathering of primary minerals are the main sources for plant available phosphate-P (PO_4^-). However, with soil-age, the P inputs from rock-weathering are getting smaller and depletion of soil P is expected. P-depleted soils are common in tropical forests, since these forests commonly exists on old and highly weathered soils. The high temperatures and rainfalls further increase the weathering rates in these regions. However, not all tropical soils are equally weathered. Soils in more geomorphic active sites (such as the montane tropics) have much younger soils and the forests ecosystems there are believed to experience an N limitation rather than P limitation. Soil P that is available for plants portrays only a tiny fraction of the total soil P. The majority of soil P is related to soil minerals (primary and secondary) and organic matter, thus the availability of soil P is regulated over longer terms by biological and geochemical processes (Hou et al., 2018). Biological processes control the mineralization/immobilization between organic P and PO_4^-, while geochemical processes include, beside the weathering of P containing primary minerals, also the ad- and desorption of available P to secondary minerals (Fig. 1.1). Since P is mainly limited in tropical forest soils, internal recycling of organic P is an important mechanism to maintain ecosystem functioning. The speed of decomposition of organic matter, and thus organic P, is dependent on the quality and chemical composition. However, Organic P contains rather divers chemical compounds and is source dependant and thus can vary also greatly within tree stands and species (Townsend et al., 2008). Mineralization is mainly conducted by soil microbes, where organic P is transformed into plant available inorganic P (orthophosphates such as $H_2PO_4^-$ and HPO_4^{2-}). However, also abiotic P mineralization is possible and can be happening through photolytic and hydrolytic reactions, although photolytic reactions may not be an important process, given the low light availability on tropical forest floors (Baldwin et al., 2005). The P availability can be further reduced by P sorption of organic and inorganic forms to secondary minerals. Sorption processes can strongly affect P cycling in forest soils, since available P gets immobilized and this process is especially important in highly weathered soils, due to the high abundance of 1:1 clays and Al and Fe oxides (Sollins et al., 1988). The sorption capacities of clays are dependent on the electric charges of its surfaces, these on the other hand depend strongly on soil pH. Thus, small changes in soil pH can have huge effects on P availability (Sollins et al., 1988). Soil aggregates (mainly formed by weathered clays) can stabilize organic P as well, resulting in a physically protection of soil P and can contribute to low soil P availability (Six et al., 2002). The remaining available P in the soil solution is mobile and thus susceptible to leachate and high losses into groundwater and surface streams are reported in tropical forests (Lewis et al., 1986).

1.6. Influence of erosion on biogeochemical cycles

In tropical forests there is the paradigm, that N is accumulated over time due to the long forming of the predominant old soils. An excess in N cycle is resulting in high aquatic losses of DIN, mainly of the soluble and easily leachable NO_3^-. But due to newer findings, this paradigm has been challenged. Cycling of organic N might be more important than expected. DON dominated aquatic N export was found at different tropical forest sites. DON export can act as a "N-leak" and is rather biologically independent, since it does not change with changing biological activity and/or seasons, compared to DIN (Hedin et al., 1995; Neff et al., 2003). Furthermore, soil erosion and the resulting export of particulate N (PN) can dominate the aquatic N export, in tropical forests within geomorphologically dynamic landscapes (Taylor et al., 2015). There is evidence that erosion can limit the N availability within tropical forest catchments in steeper slopes, where eroding forces are strong (Weintraub et al., 2015). High uplift rates and rainfall intensities generate landscapes that are seen as geomorphologically active or dynamic sites.

While for N, significant reduction of soil stocks are possible (Weintraub et al., 2015), the opposite can be true for rock-derived nutrients. In the case of P, soil erosion that removes topsoil, is exposing regolith to weathering and thus can increase the P input from weathering the primary minerals (Quinton et al., 2010). This implies that there can be a high spatial variability in P availability within a landscape, where slope positions are more prone to be replenished by rock-derived nutrients, such as P, since more and more bed rock is exposed compared to flat and depositional areas. However, this is as well dependent on the depth of bedrock. In deep weathered soils, in stable regions with low uplift and erosion rates, long-term P depletion is expected (Porder et al., 2007). On a landscape level, erosion and the resulting transport of soil particles can lead to transport of rock derived nutrients to soils in depositional areas, whereas it can lead to depletion in areas where erosion outpaces the mineral weathering and the release of biologically available P, which can ultimately result in reduced P availability (Porder et al., 2007).

Soil erosion is defined as all the processes that are displacing soil particles. There are different forms of soil erosion: wind, chemical and physical erosion. In this thesis, the focus lies on physical erosion by water and will be referred as simply "soil erosion" unless stated differently. Soil erosion involves three different actions: detachment of soil particles, transport of soil particles and the subsequent deposition of the moved particles and each of these phases of soil erosion can affect the nutrient allocation in soils (Berhe et al., 2018). The rate and magnitude of soil erosion by water in natural systems is dependent on different factors, which are also important to assess soil erosion with models, for example the Revised Universal Soil Loss equation (RUSLE). The most important factors are:

(i) rainfall quantity and intensity: the duration and intensity of a rainfall event defines the erosional potential of the event. Raindrops falling on the soil surface can break down soil aggregates and detach soil particles. Furthermore, long lasting rainfall events can lead to overland flow, especially in soils that are not well draining, increasing the transport of detached soil particles (Smith & Wischmeier, 1957).

(ii) slope gradient and length: steeper slopes within a landscape increases the risk of soil erosion as water runoff is accumulating and water velocity is increasing with increasing slope (Smith & Wischmeier, 1957).

(iii) soil cover: soil cover acts as a protection against erosion by decreasing the impact energy of raindrops and by slowing down the runoff movement (Benkobi et al., 1994).

(iv) soil characteristics: physical and chemical characteristics of the soil can have an influence on how much soils are able to resist soil erosion. Mainly texture, structure, organic matter content and permeability can influence the susceptibility of soils to erosion (Schwab et al., 1994).

1.7. Study site: The Congo River Basin

The Congo River Basin (CRB) consists of the area that is draining into the Congo River, the second largest river in Africa. The topography of the CRB is like a bowl, with a vast area in the centre ranging elevation between 300-400 m above sea level, surrounded in the north and the south by elevated regions and bordered in the east by the high elevations of the Albertine Rift region. The CRB spans from the Upper Congo in the eastern highlands and the Kasai in the south, to the Oubangi in the north down to the lower Congo in the west, where the Congo rivers is flowing into the Atlantic. In total, the CRB spans an area of 3.7 M km^2 (Alsdorf et al., 2016) and hosts the second largest tropical forests of the world, after the Amazon, however, ecological and biogeochemical research has been mostly absent from this region, leaving a blank spot on the map in terms of baseline data for global earth system models (Verbeeck et al., 2011).

Rainfalls in the CRB range from ~1900 mm yr^{-1} at the centre of the Basin to ~1100 mm yr^{-1} at the northern and southern borders of the basin (Alsdorf et al., 2016). Seasonality in precipitation follows a north-south movement, with peaks in the north from July to September and peaks in the south from January to March, while the equator region experiences two rainfall peaks each year with a smaller rainfall peak from March to May and a more pronounced rainy season from September to November (Bultot, 1971). Evapotranspiration within the CRB ranges from 800 mm in the southern Lualaba Basin to 1200 mm in the eastern Oubangi Basin, and generally transpires between 75% to 85% of the annual precipitation (Bultot and Griffiths, 1972). The mainstem of the Congo River at Kinshasa-Brazzaville has an annual discharge of around 40'660 m^3s^{-1} (Alsdorf et al., 2016).

Understanding biogeochemical processes in these forests is important since the pristine forests of the Congo Basin are under increasing anthropogenic pressure. Land use change from pristine forests to shifting agricultures influences biogeochemical processes in those ecosystems, i.e. change in soil respiration (Houghton, 1999), loss of soil organic C (Guo & Gifford, 2002) and availability of soil nutrients (Templer et al., 2005). These forests of the Congo Basin provide livelihoods to more than 70 million people and the population in the Democratic Republic of the Congo (DRC) alone is projected to increase up to 197 million people in the year of

2050 (Tyukavina et al., 2018). This increase of population comes hand in hand with increase in demand of food and energy. To supply this demand, loss of primary forests is uninventable to produce charcoal and providing farmable land. Thus, the loss of forests in the Congo Basin is primarily driven by shifting agriculture (Curtis et al., 2018), mainly by nonmechanized small-scale clearing for agriculture, such as slash-and-burn agriculture (84% of total forest loss between 2000 and 2014; Tyukavina et al., 2018). However, differences in drivers for deforestation vary locally, for example: in the DRC clearing through smallholder farming practices are dominating, whereas forest losses through more industrialized practices are mainly common in coastal regions on the Gulf of Guinea (Tyukavina et al., 2018). This dominance of subsistence farming within the Congo Basin is also an important difference to tropical forests of the Amazon Basin and Southeast Asia, where more agro-industrial clearing is driving forest losses (Tyukavina et al., 2018). Between 2000 and 2010, alone in the DRC a reported 2.3% of the total forested area was lost (Potapov et al., 2012).

In this thesis we focus on three of the most abundant forest types of the Congo Basin: lowland tropical forest, montane tropical forest and the Miombo woodland, a dry savannah type of forest. Together this forest types represent more than 70 % of the Congo Basins area (Verhegghen et al., 2012). The lowland consists of broad-leaved evergreen closed canopy trees, while the montane site consists of a broad-leaved semi-deciduous forest and the Miombo of broad-leaved deciduous trees. Only one major type of forest has been left out in this thesis: the inundated swamp forests of the cuvette central, which cover up to 5 % of the Congo Basin area. The lowland forest site selected for this thesis is representative for most of the broad-leaved evergreen forests of the central CRB (Réjou-Méchain et al., 2021), as soils were classified as Ferralsols which is the dominant soil type of these forests (Fig. 1.2; Jones et al., 2013) and also the lithology in the centre of the CRB is uniform and soils are formed on aeolian sediments (Fig 1.2, Bow et al., 2009).

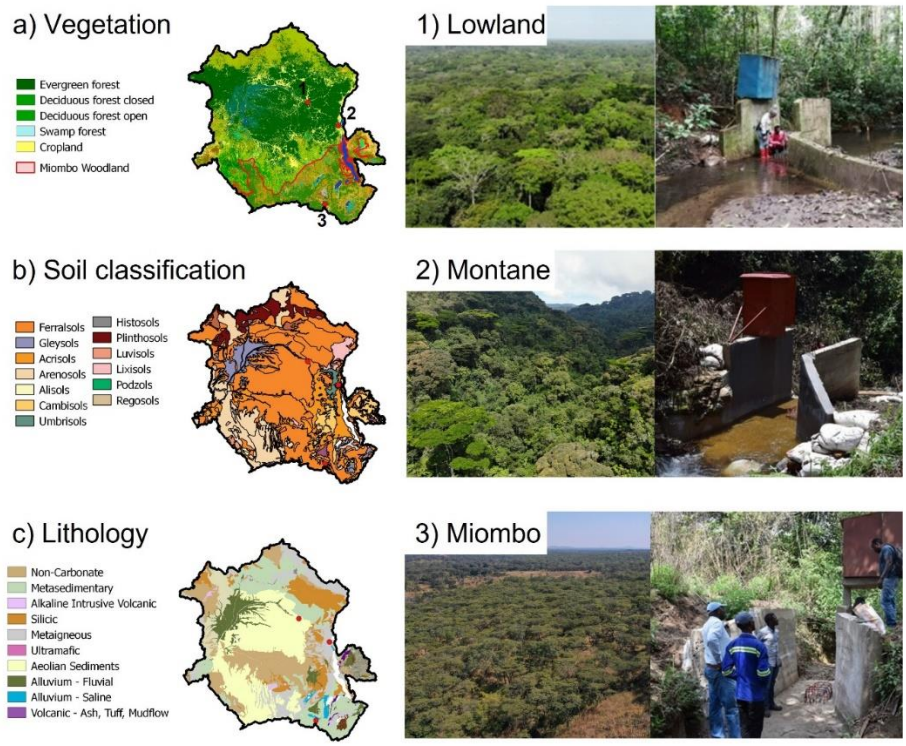

Fig. 1.2 a) Map of the different vegetation ecosystems within Congo River Basin (CRB) (source: Olson et al., 2004). b) soil types within the CRB (source: Jones et al., 2013). c) Map of the surface lithology within the CRB (source: Bow et al., 2009). Red dots indicate the location of the monitoring sites installed for this thesis (right). Photos on the right show the installed flumes and the different forests of the sampling sites (Drone photos taken by Van Oost, K. and Drake, T.).

1.8. Outline of thesis and research questions

Problem statement

The current paradigm of the nutrient status of tropical forests are that old soils in the lowlands are rich in N and poor in rock-derived P, whereas in the more geomorphic active (with steeper slopes) montane forests the rejuvenating of the soils lead to richer P conditions, while being relative poorer in N. However, especially the high N status of lowland forests are highly debated and causing a paradoxical situation (N paradox of tropical forests): A N-rich ecosystem, where N is cycled in excess (meaning that there are high DIN losses), needs to have a N input that is sustaining these high N losses. It is believed that biological N fixation (BNF) is responsible for the high N inputs, however, BNF is mostly downregulated in N-rich environments, since it is not energetic favourable for plants to sustain BNF when there is a surplus of available N. Hedin et al. (2009) proposed the “leaky nitrostat”

concept for tropical forests, where N inputs via BNF can be flexibly up- and down-regulated in N-poor niches within an ecosystem. This induced N_2-fixation appears in N-poor environments created by disturbances such as soil erosion, fires, and tree fall.

Another steady N supply into lowland forests and thus another explanation for the N-paradox, could be high N inputs via atmospheric deposition. High atmospheric deposition loads have been observed in temperate forests, however, in the remote tropical lowland forests, these deposition loads were believed to be low, since there is no adjacent industry and intense fertilized agriculture. Nonetheless, high atmospheric depositional loads were measured in central African forests due to high organic N related to biomass burning in savannahs (Bauters et al., 2018).

Most of the time, all these assumptions lack robust quantification of all processes and fluxes of the N cycle. While Hedin et al., (2009) stated there is apparent lack of N input into lowland forests, Bauters et al. (2019) conducted a study in African forests to thoroughly quantify N fluxes and found that there is an imbalance towards N inputs (due to high N depositions) and there is a lack of N outputs in these forests. Although these findings seem contradictory, regional differences are important and different processes can act in different tropical systems. Furthermore, there are still processes neglected in most studies about nutrient cycles in forested systems. The description of biogeochemical cycles of the main nutrients (N and P) are often lacking the quantification of the influence of erosion on said nutrients. These processes did not receive a lot of attention, especially in forests, due to the main believe that the dense vegetation cover fully protects soils from physical erosion.

In this thesis we aim to connect physical and geomorphological processes with the biogeochemistry of tropical forests (Fig. 1.3). The main objective of this thesis is to assess the influence of erosion on N and P cycles for three different forest ecosystems within the Congo Basin. A better understanding on all the processes playing part in the nutrient cycling of tropical forests is crucial to assess the role of these ecosystems in the global C balance. First, the dynamics of suspended sediment transport is analysed for a better understanding of erosional processes and sediment source allocation in these tropical forest ecosystems (part I). The aim of the second part was to see if erosional processes can cause N limitation on an ecosystem level, and therefore be responsible for N-poor niches on a landscape scale.

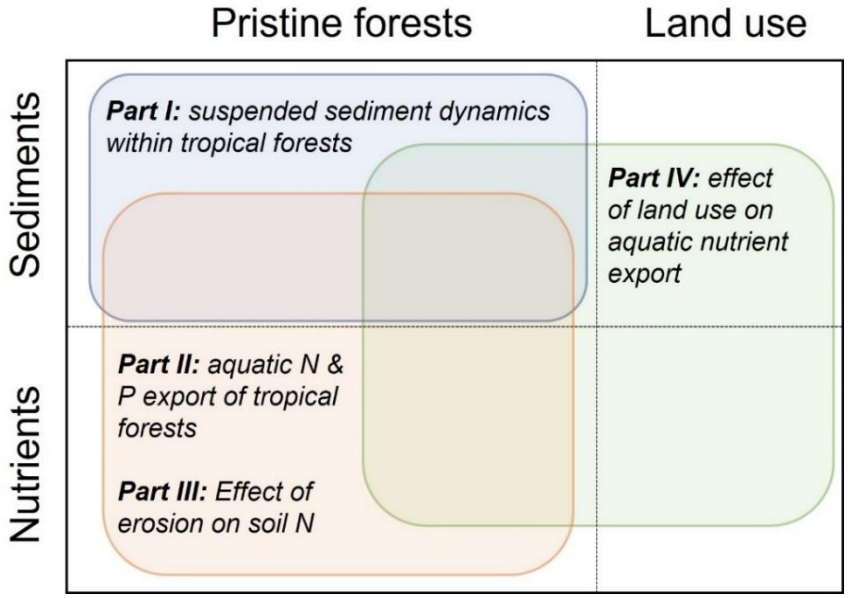

Fig. 1.3 Schematic overview of the different chapters of this thesis.

In the third part, annual aquatic N and P losses were quantified to see how important particulate forms of N and P losses are compared to the dissolved forms and if the previously found imbalance in the N budget of the central African forests can be closed by including PN export. In the last part of the thesis the effect of land use on the aquatic nutrient export is assessed at a paired watershed study in the lowlands of the Congo Basin.

There is scarce evidence of influence of erosion on N cycle but only from geomorphic active sites in Latin America and Southeast Asia (Hilton et al., 2013; Taylor et al., 2015; Weintraub et al., 2015). However, the magnitude of this process and possible implication on N status of tropical forests of the Congo Basin remains unknown and even less work has been done on the export of P.

Part I: Suspended sediment dynamics within tropical forests

The first part of the thesis focuses on the physical processes of sediment export out of the tropical forests. With the help of turbidity-discharge and hysteresis analysis the underlying processes for sediment export were analysed. Sources of sediments were appointed by chemical analysis of the particulate organic matter (POM) fraction of the sediments. Through quantification of total sediment export this part builds the fundament for assessing possible influences of erosion on forest functioning and nutrient export, explored in the next chapter.

The specific research questions of Part I are:

- How do annual sediment yields of tropical forests of the Congo Basin differ between a lowland forest and a Miombo woodland?

- What are the drivers of sediment exports in forested headwater streams?
- What are the temporal and ecosystem level variations in source areas for eroded sediments?

Part II: Aquatic N and P export of tropical forests

The second part tries to incorporate erosional processes on nutrient (N and P) budgets of the three tropical forest ecosystems of the Congo Basin, by quantifying total aquatic nutrient exports with focus on the particulate N (PN) and total particulate P (TPP) export and how they compared to dissolved organic and inorganic N and P losses. The main goal was to see how important particulate nutrient exports are as a loss vector of nutrients in these forest ecosystems.

The specific research questions of Part II are:

- How important are sediment associated nutrient exports compared to the loss of dissolved nutrients?
- What are the differences in this importance between contrasting forest sites?
- Can particulate nutrient exports from forested watersheds close the imbalance in the nutrient budgets?

Part III: Effect of erosion on soil N

In the third part of the thesis the focus lies on N availabilities in the three distinct tropical forests. In this part soil N has been studied and with the help of stable isotopic signatures of soil N ($\delta^{15}N$) differences in soil cycling between sites was tried to assess. Furthermore, the effect of soil erosion on N availabilities was studied on a local scale, to see if N availabilities are dependent on the topography of the forest sites.

The specific research questions of Part III are:

- How do the three distinct tropical forest sites differ in N cycling?
- Does topography affect soil $\delta^{15}N$ signatures in tropical forests of the Congo Basin and thus indicate an influence of erosion on N cycling?

Part IV: Effect of land use on aquatic nutrient export

For the last part of the thesis, we focused on the effect of land use change on aquatic nutrient export. For this, a paired watershed study was conducted in the lowlands of the Congo Basin. Through a yearly monitoring of aquatic N and P losses, differences between nutrient exports of a pristine catchment and a catchment that is used for agriculture, have been assessed.

The specific research questions of Part IV are:

- How does aquatic nutrient export change under changing land use within the catchment?

- How much higher is the importance of erosion on nutrient exports in a deforested headwater catchment compared to a pristine catchment in the lowlands of the Congo Basin?
- What are the implications of this in terms of the projected deforestation within the Congo Basin?

Part II - Suspended sediment dynamics within tropical forests

Chapter 2: Fluvial sediment export from pristine forested headwater catchments in the Congo Basin

This chapter was originally published as: Baumgartner, S., Bauters, M., Barthel, M., Alebadwa, S., Bahizire, N., Sumaili, C., Ngoy, D., Kongolo, M., Bazirake, B. M., Ntaboba, L. C., Six, J., Boeckx, P., Van Oost, K., & Drake, T. W.: Fluvial sediment export from pristine forested headwater catchments in the Congo Basin. *Geomorphology*, 398, 2022.

Abstract

Studies on sediment export from tropical forest watersheds are scarce. Of the assessments that do exist, most are of larger rivers or are model-based and lack validation with measured data. Understanding the mechanisms of sediment export dynamics in forested headwaters is important for assessing downstream effects and as a baseline for net impacts of land-use change. To that end, we quantified annual total suspended sediment (TSS) yields in forested headwater catchments of two major forest types in central Africa (tropical lowland forest and subtropical Miombo woodland) and analyzed turbidity-discharge hysteresis over one hydrological year. We measured TSS yields of 0.24 ± 0.09 t ha^{-1} yr^{-1} in the Miombo woodland and 0.25 ± 0.05 t ha^{-1} yr^{-1} in the lowland forest catchment. The Miombo woodland experienced similar TSS yields as the lowland forest despite a shorter, five-month, rainy season and lower annual precipitation. In the Miombo forest, sparser vegetation cover, seasonal fires that remove understory vegetation and high rainfall intensity during the rainy season therefore resulted in similar TSS yields. As a result of these differences in vegetation and rainfall, approximately 68% of TSS was exported during storm events in the Miombo woodland and 30% in the lowland forest. Both sites showed mainly clockwise hysteresis (positive hysteresis index) patterns of sediment export. In the Miombo woodland, the hysteresis index (i.e., the magnitude and direction of hysteresis) increased with the ongoing rainy season, indicating source limitation already after one month of rain. In the lowland forest, the predominant clockwise hysteresis was more likely caused by the increasing contribution of baseflow during the falling limb of an event, whereas during the rising limb there is a quick flushing of surface material available in the forest. These findings based on hysteresis analysis were further supported by C:N ratio and $\delta^{13}C$ analyses of particulate organic matter (POM). POM C:N ratios increased and $\delta^{13}C$ signatures decreased with increased discharge in the lowland forest, indicating the mobilization of topsoil sediments during rain events. In contrast, the Miombo exhibited no shifts in C:N ratios nor in the $\delta^{13}C$ signature. Despite the pristine nature of these forests and their assumed negligible sediment yields, our results demonstrate that erosion is a significant loss process in tropical forests and call for future research to examine its role in forest functioning and biogeochemical cycling.

2.1. Introduction

The aquatic lateral export of mineral particles via erosion is associated with a loss of nutrients and carbon (C) and influences the biogeochemical processes of soil-plant systems (Quinton et al., 2010; Van Oost et al., 2007; Vercruysse et al., 2017; J. R. Williams et al., 1984). The common assumption is that soil stocks in pristine systems are in equilibrium, i.e., the rate of soil loss via erosion is the same as the rate of new soil formation. It was shown that for mature soils, formed from uniform bedrock parent material, soil formation and soil erosion are practically at steady state (Phillips, 2010). In these pristine systems, the sediment fluxes in rivers are dominantly controlled by climate and topography (Ludwig et al., 1996). Sites altered by human activities (e.g., agriculture, deforestation, and mining) are often severely affected by erosion, as the removal of the protection provided by vegetation cover leads to soil loss (Baharuddin, 1988). However, some work has shown that even undisturbed forests are prone to high sediment yields, especially in geomorphic active sites in the tropics (Zimmermann et al., 2012). As such, particulate export of nutrients and C influence local biogeochemical cycles and ecosystem functioning even in pristine ecosystems (Taylor et al., 2015; Weintraub et al., 2015). Nevertheless, they are often neglected when assessing aquatic exports, resulting in an imbalance while quantifying budgets of nutrients in forest ecosystems (Bauters et al., 2019).

Tropical ecosystems are especially affected by erosion because of high precipitation rates and intensities (Bagalwa et al., 2021; Labrière et al., 2015). The Congo Basin is home to some of the most pristine tropical and subtropical forests, covering distinct forest types. While the erosion potential is high in montane forests in the eastern parts of the Congo basin because of the combination of high rainfall erosivity and steep topography (Bagalwa et al., 2021), physical erosion is reported to be much lower in the dense lowland forests in the central part of the basin (Borrelli et al., 2017). In contrast to both the montane and lowland forests, the subtropical Miombo woodlands in the south of the Congo Basin have a sparser vegetation cover (especially during the dry season, where the understory vegetation is lost to seasonal fires) compared to other tropical forests, leaving their surface layers less protected against heavy rainfall. Assessments of soil loss in pristine ecosystems in central Africa are rare. To our knowledge there are no studies of sediment export from forested watersheds in the Congo Basin. Moreover, the only other assessments of suspended sediment exports in the Congo Basin are either model-based with very little ground truthing (Borrelli et al., 2017), or set on large rivers (i.e., Congo; Coynel et al., 2005).

Erosion and sediment transport are key processes controlling the export of sediments and nutrients from river catchments. To understand factors controlling erosion, it is crucial to gain a mechanistic understanding of the underlying processes of sediment export and gain insights into sources of the suspended sediments within headwater streams. In tropical headwater catchments, storm events drive surface runoff and sediment transport processes, with the bulk of sediment export driven by a few events (Lloret et al., 2013). Analyzing hysteresis patterns between total suspended sediments (TSS) export and discharge (Q) during storm events (i.e., the time lag between Q and TSS pulses) is a helpful tool to understand mechanisms and dynamics of sediment transport in headwater catchments (Lloyd et al., 2016b). The

shape of the hysteresis loop can provide insights into the underlying drivers at play, as described by Williams (1989), for example: a clockwise hysteresis loop is often times associated with a quick flushing of sediments and subsequent depletion of sediment sources. Furthermore, chemical tracers within suspended sediments are a helpful tool for source appointment. In particular, stable isotope signatures of C ($\delta^{13}C$) and the C:N ratio of the particulate organic matter (POM) associated with the suspended sediments are widely used to determine the source material by comparing the signatures of the suspended POM with the signatures of different source material (Emery et al., 1967; Fry & Sherr, 1989; Lamb et al., 2006).

Focusing on sediment losses in pristine headwaters is crucial to (i) understand the role of physical erosion in nutrient and C export, (ii) have a baseline to assess effects of possible deforestation and land-use change in these regions and (iii) understand the role of storm events on sediment yields for assessing erosional processes under changing climate. Thus, the overall aim of this study was to provide insights in the dynamics of suspended sediment export from pristine forested headwater catchments of the Congo Basin. The specific objectives were (i) to quantify and compare the yearly TSS export of two different forest ecosystems within the Congo Basin (lowland forest and Miombo woodland) and (ii) to get a mechanistic understanding of the underlying drivers of TSS export. To answer these objectives, we measured annual TSS export from headwater streams in different forests of the Congo Basin and analyzed hysteresis patterns during storm events. Furthermore, we used C stable isotopes and C:N ratios to identify the sources of the POM associated with the sediments.

2.2. Material and Methods

2.2.1. Study site

The tropical lowland forest catchment is situated in the Yoko forest reserve, approximately 30 km south of the city of Kisangani in the Democratic Republic of the Congo (DRC). The Yoko forest reserve consists mainly of mixed lowland tropical forest and monodominant forest of Gilbertiodendron dewevrei. Reported mean annual precipitation is ~ 1825 mm and the mean annual temperature is ~24°C (Bauters et al., 2019). The rainfall pattern is characterized by two wet seasons, a short one from March to May and a prolonged one from August to November, with drier periods between the wet seasons (Fig. 2.1). Soils in the lowland forest are classified as deeply weathered Ferralsols (Van Ranst et al., 2010) with a loamy sand texture (Baumgartner et al., 2020). The catchment area has been estimated using the 30 m Shuttle Radar Topographic Mission (SRTM) derived digital elevation model (DEM, NASA JPL) and the GPS (GPSMAP 60CSx, Garmin, accuracy <5 m) coordinates of the flume position. The catchment area was 311 ha and altitude ranges from 440 to 475 m a.s.l. with an average slope of ~4° (Appendix A1).

The catchment in the Miombo woodland is situated approximately 50 km north of the city of Lubumbashi, DRC. The catchment is characterized by Miombo woodland vegetation, where the dominant tree genera are Brachystegia, Julbernadia and Isoberlinia (Campbell, 1996). Pristine Miombo is very scarce in the region; hence, the

selected catchment included minor areas of anthropogenic impact, mostly caused by small-scale agriculture and charcoal production, which is representative for the Miombo in the region (Fig. 2.1, Campbell (1996)). Furthermore, natural and anthropogenic seasonal fires during the prolonged dry season from May to September are common in the Miombo woodlands. Mean annual precipitation is ~1226 mm and mean annual temperature is ~21°C (Fick & Hijmans, 2017). Streamflow stops at the beginning of the dry season (April) and starts again at the onset of the rainy season (November). The catchment area was 588 ha, with an elevation range from 1257 to 1311 m a.s.l., and an average slope of 3.9° (Appendix A1). Soils in the Miombo catchment are classified as Acrisols and Cambisols (Chapter 5).

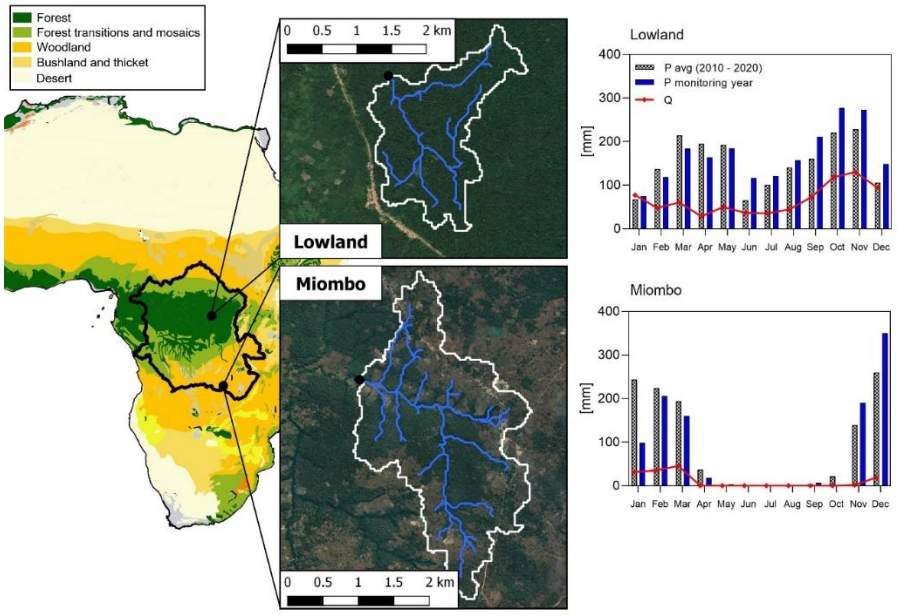

Fig. 2.1 Location of the study sites. Black line delineates the Congo Basin. Black dots in the headwater catchment plots indicate the location of the flumes and white lines delineate the catchments of the study sites. Graphs on the right side show monthly average precipitation (gray) and monthly precipitation (blue) during the monitoring year at the lowland and the Miombo catchment. Red lines indicate measured monthly discharge during the monitoring period in mm. Precipitation data are derived from GPM satellite data for the period 2010-2020 (grey bars) and for the discharge monitoring period (blue bars) (Huffman et al., 2019). Vegetation map adapted from White (1983).

2.2.2. Discharge monitoring

At the two sites, concrete flumes with a fixed width were installed to obtain a robust water level – discharge (Q) relationship (Appendix A1). At each catchment outlet point, a pressure transducer (CS451, Campbell Scientific, UK) connected to a datalogger (CR1000, Campbell Scientific, USA) was installed to the base of the flume measuring water level at 5-min intervals. Q was measured weekly (Miombo woodland; total of 10 measurements) and bi-weekly (lowland forest; total of 34 measurements) using a mechanical flowmeter (Model 2030, General Oceanics Inc., USA) and was subsequently linked to the simultaneous water level measurement from the pressure transducer (Appendix A2). To calculate Q values for each individual water level measurement, a rating curve was applied, where a linear relationship between water level and Q was obtained (Appendix A2). At the Miombo site, only Q measurements up to 0.4 m were available (Appendix A2). The Q - water level relation shown in Appendix A2 indicates that a power function or a second order polynomial function would fit better. However, we verified the use of a linear function by calculating Q values for high water levels with the Manning's equation:

$$Q = \frac{A * Rh^{\frac{2}{3}} * \sqrt{S}}{n} \quad \text{(Eq. 2.1)}$$

where A is the flow area (m^2), Rh is the hydraulic radius (m, cross-sectional area of waterbody divided by wetted perimeter), S is the channel slope (m/m, 0.007 for channel in Miombo) and n is Manning's roughness coefficient. The roughness coefficient n for the flume was obtained from the manual Q measurements during low flowing conditions (0.02 s $m^{-1/3}$). Applying Eq. (1) for water levels > 0.4 m and comparing the calculated Q with obtained Q values from the different possible models of the rating curve, we corroborated that the linear Q ~ water level model produces the most reasonable Q values at high water level conditions (Appendix A3).

Weather stations (ATMOS 41 All-in-one, Meter Environment, Pullman, USA) from the Trans-African HydroMeteorological Observatory (TAHMO, www.tahmo.org) were installed in an open canopy area in close vicinity to the flumes. Although these weather stations provide high temporal precipitation data (5 min), occasional data gaps occurred because of sabotage, malfunctioning, and/or battery failure. To complement the weather station data, GPM satellite precipitation data was downloaded from the NASA web archive (Huffman et al., 2019).

2.2.3. Total suspended sediments monitoring

Turbidity was measured simultaneously with water level (OBS 3+, Campbell Scientific, UK) at the Miombo site, whereas at the lowland site a separate turbidity probe with an internal logger (YSI-EXO2, Xylem, USA) was installed measuring at a lower frequency of 15-min intervals. The same probe also measured conductivity and fluorescent dissolved organic matter (fDOM) at 15-min intervals (only used for water level data gap filling, see Section 2.2.4). Biofouling on optical sensors tend to decrease turbidity, fDOM and conductivity values over time. As it is difficult to re-calibrate the sensors during field deployment, the EXO2 probe at the lowland site was equipped with a wiper, which cleaned the sensors prior to every measurement.

The OBS 3+ sensor at the Miombo site did not have a wiper, hence the sensor was cleaned manually every field visit.

Water samples for total suspended sediment (TSS) analysis were taken in 2L HDPE bottles at a fortnightly (lowland site) to weekly (Miombo site) frequency. In addition to the weekly and fortnightly sampling, autosamplers (6712 Portable Sampler, Teledyne ISCO, US) were installed to collect TSS samples during storm event conditions. The autosamplers were also connected to the CR1000 datalogger and automatic sampling triggered when the water level reached a certain threshold (0.175 m at the lowland site and 0.35 m at the Miombo site). These thresholds were selected based on water level measurements prior to the sampling campaign at the same sites. The sampler could pump up to 24 x 1 L PVC bottles that were replaced during each field-visit. In total we obtained 50 storm event samples from the lowland stream and 55 from the Miombo stream. All water samples were filtered in the laboratories of the University of Kisangani and the University of Lubumbashi on pre-weighed glass fiber filters (0.7 µm GF/F, Whatman, US). The filters were then dried at 60°C for 48 h and weighed again to calculate the TSS concentration by dividing the sediment mass by the volume of water filtered. The sampling periods covered a full hydrological year, i.e., from 1 April 2019 to 31 March 2020 in the lowland forest and during the wet season from 22 November 2019 until 30 April 2020 in the Miombo woodland. The Miombo site is running an intermittent stream, i.e., with flow only during the rainy season. During the dry season, no surface water is present in the Miombo woodland stream and thus sampling was only conducted during the wet season. In total we obtained 77 TSS samples from the lowland site (28 during campaign/baseflow sampling and 49 storm event samples from the autosampler) and 69 TSS samples from the Miombo site (13 campaign/baseflow samples and 56 storm event samples).

2.2.4. Filling data gaps

The datalogger and the autosampler were powered with a rechargeable 12V battery, which was replaced and recharged at every field visit. However, because of battery failure and theft, data loss occurred at both sites. At the lowland site, we obtained a total of 6690 h (>75%) of water level measurements with the pressure transducer. At this site, the EXO2 sonde was independently powered, thus providing turbidity, conductivity and fDOM measurements for the times when the datalogger failed. As these three parameters are well corelated with water height, the missing data gaps in the water level measurements were filled using a machine learning algorithm (random forest; RF). For each month with missing water level data, a separate model was applied with a training dataset from the respective month, containing the complete dataset, i.e., water level, turbidity, fDOM, and conductivity values. To build the RF models, we used the R software (R Core Team, 2021) with the *randomForest* package (Liaw & Wiener, 2002). The models were run with the number of variables selected at each node set to 1 and the number of trees set to 500. To validate model predictions, Nash-Sutcliffe efficiency (NSE) was calculated for each model (Nash & Sutcliffe, 1970). Model performance for each month was excellent, with all the models exceeding NSE > 0.99. Only during nine hours of the monitoring period from

the lowland forest site, both loggers (CR1000 datalogger and EXO2 sonde) were not operational. Therefore, no data was available for this period. As no rainfall occurred at that day, a linear gap filling for missing water level and turbidity values was applied.
At the Miombo site, data was missing for two short periods. i.e., four days from 10 to 14 February 2020 and six days from 7 to 13 March 2020, because of malfunctioning of the power supply. As no additional logger was placed in the Miombo site, modelling of the missing Q data was not possible. Because during the first data gap no rainfall was measured and the water was stagnant before and after the logger failure, we assumed that no Q occurred during this time. During the second data gap, no large rain events occurred either, so a linear gap-filling for the Q data was applied.

2.2.5. TSS yield calculation

Because turbidity values tend to decrease over time owing to possible biofouling at the sensor and the difficulty to re-calibrate the sensors during field deployment, we applied a RF model to the data with Q and turbidity as predictors for TSS concentration, yielding an excellent NSE of 0.82 and 0.89 for lowland and Miombo data, respectively. Total sediment export per 5 min interval was calculated using the TSS concentration (obtained from the turbidity values, in mg l^{-1}), multiplied with the water Q (in m^3 s^{-1}) and then integrated over the whole 5 min period. TSS yields for each site were calculated by dividing yearly sediment exports (t yr^{-1}) by the catchment area (ha^{-1}). At the Miombo forest site, the turbidity sensor experienced a malfunction after 26 January 2020 (Fig. 2.3, middle panel), thus a second RF model with only Q as TSS predictor was applied and used for the times when turbidity values were not available (November 2019) or not reliable (27 January 2020 and onwards). To calculate the variance and standard deviation of the TSS predictions from the RF models, we used the *randomForestCI* package in R (Wager, 2014).

2.2.6. Hysteresis calculation

Because of the large number of storm events in the lowland forest, a digital filter signal processing technique from the R package *EcoHydRology* (Fuka et al., 2015) was used to separate the discharge hydrograph into event flow and baseflow. Baseflow is the part of the hydrograph that sustains the discharge between precipitation events and reacts slowly to such events. A rainfall-runoff event in the lowland catchment was identified as a storm event, when (1) peak event flow was at least 10% higher than baseflow (Messina & Biggs, 2016), and 2) the event lasted at least 45 min to have sufficient logger measurements. As baseflow in the Miombo catchment was more stable during the whole season, we classified a storm event when Q surpassed a threshold value of 0.15 m^3 s^{-1} and the event lasted at least for 45 min. For each storm event, a numerical hysteresis index (HI) was calculated to analyze sediment export dynamics during a storm event. The HI calculation reported by Lloyd et al. (2016b) was used, where turbidity and Q data is normalized, allowing for a better comparison of different events:

$$Normalized\ Q_i = \frac{Q_i - Q_{min}}{Q_{max} - Q_{min}} \quad \text{(Eq. 2.2)}$$

$$Normalized\ C_i = \frac{C_i - C_{min}}{C_{max} - C_{min}} \quad \text{(Eq. 2.3)}$$

where Q_i and C_i are the discharge and turbidity values at timestep *i* and Q_{min}/Q_{max} and C_{min}/C_{max} are the minimum, respective maximum, discharge, and turbidity value of the event. The HI is calculated at different percentiles of the Q (Q_i):

$$HI_{Q_i} = C_{RL\_Q_i} - C_{FL\_Q_i} \quad \text{(Eq. 2.4)}$$

where C_{RL_Qi} is the turbidity value on the rising limb at percentile I of Q and C_{FL_Qi} is the turbidity value on the falling limb at the same Q value. Q_j values are defined as:

$$Q_i = k(Q_{max} - Q_{min}) + Q_{max} \quad \text{(Eq. 2.5)}$$

where k is the interval at which calculations were made (for HI every 5% of Q, k = 0.05, 0.1, …, 0.95). The HI of the whole event (HI_{Event}) is defined as the sum of all HI values at each percentile:

$$HI_{Event} = \sum_{i=0.05}^{1} HI_{Q_i} \quad \text{(Eq. 2.6)}$$

The HI gives a number between -1 and 1 for each event, where a negative value indicates an anti-clockwise hysteresis loop, positive value a clockwise hysteresis loop, and values around 0 indicate no hysteresis or an eight-shaped pattern. Hysteresis analysis has been used for decades (e.g., Heidel, 1956; Klein, 1984) and different processes cause the different hysteresis patterns and are summarized in the literature (Malutta et al., 2020).

2.2.7. Chemical analysis

C and N content and $\delta^{13}C$ signatures of TSS were measured using an elemental analyser (Automated Nitrogen Carbon Analyzer; SerCon; Crewe, UK) interfaced with an isotope ratio mass spectrometer (IRMS; 20-20; SerCon; Crewe, UK). $\delta^{13}C$ values are reported in the delta notation against the reference standard Pee Dee Belemnite (VPDB). C:N ratios reported in this study are mass weight calculated ratios.

2.3. Results

2.3.1. Hydrology

During the monitoring period between April 2019 and March 2020, the total runoff from the lowland forest catchment was 665 mm at an annual rainfall of 2031 mm, resulting in a runoff coefficient of 0.33 and an interception plus evapotranspiration of ~1366 mm, assuming no changes in water storage. Rainfall during the monitoring period was higher than the average rainfall amount during the period 2010 - 2020

(1825 mm, Fig. 2.1). From June 2019 until January 2020, the monthly rainfall exceeded the average rainfall between 19% (November 2019) up to 79% (June 2020) (Fig. 2.1).

During the wet season 2019/2020, the Miombo woodland catchment had a runoff coefficient of 0.13 with a runoff of 133 mm and a total rainfall of 1036 mm (Fig 2.1), resulting in an interception plus evapotranspiration of ~900 mm. Despite the above-average rainfall during November and December 2019, the year of the monitoring campaign was slightly drier (8% less precipitation) than the average year between 2010 – 2020, mainly because of a dry January 2020 (Fig. 2.1).

2.3.2. TSS export

We obtained total annual TSS yields (obtained yield ± SE of RF prediction) of 0.25 ± 0.05 t ha^{-1} yr^{-1} from the lowland forest catchment and 0.24 ± 0.09 t ha^{-1} yr^{-1} for the Miombo woodland catchment. The lowland forest catchment experienced 68 distinct storm events during the observation period. In total, these storm events lasted for 413 h, i.e., during 4.7% of the total monitoring period (Fig 2.2). However, despite representing only 4.7% of the monitoring period, storm events were responsible for 29.9% of the total exported sediments in the lowland forest.

At the Miombo woodland site, 21 storm events occurred during the wet season of 2019/2020 (Fig. 2.3). These events lasted for a total of 212 h, equivalent to 7.4% of the total observation period. During these storm event conditions, 68.3% of the total annual TSS yield was exported from the catchment. Before the 5th and 9th event of the season in the Miombo catchment, turbidity values increased steadily over several days, although no water Q was observed (Fig 2.3, orange rectangles). During this period, we observed stagnant water in the flume (Q = 0); thus, TSS export and yield were not affected. Evaporation of the stagnant water was probably the reason for the increasing turbidity values during this period.

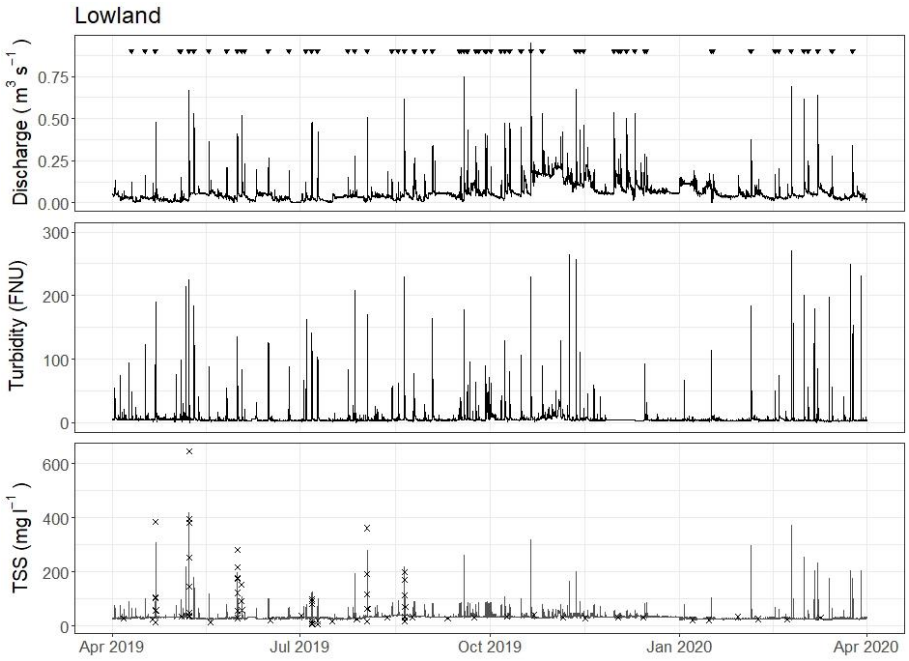

Fig. 2.2 Measured discharge (top) and turbidity (middle) values for the lowland forest site. The bottom panel shows the modelled TSS values (grey line) and the measured values (black crosses). Black triangles in top panel indicate the presence of storm event conditions.

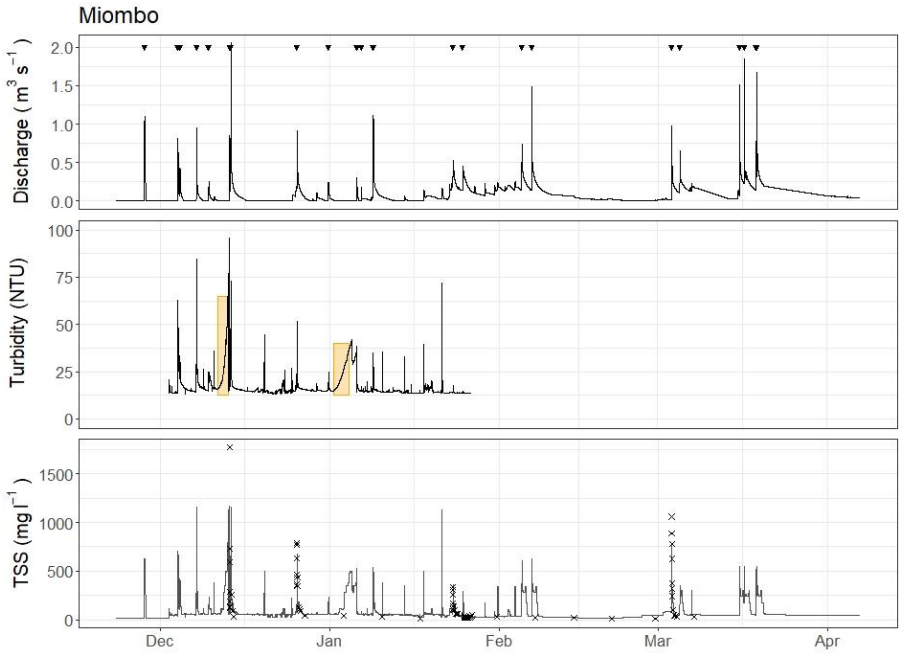

Fig. 2.3 Measured discharge (top) and turbidity (middle) values for the Miombo woodland site. The bottom panel shows the modelled TSS values (grey line) and the measured values (black crosses). Black triangles in top panel indicate the presence of storm event conditions. Orange rectangles in the turbidity plot highlight the conditions where turbidity increased during stagnant water conditions (see Section 3.2).

2.3.3. Hysteresis

From the 68 events measured in the lowland forest, 55 (81%) showed pronounced clockwise hysteresis with a mean HI value of 0.42 (Fig 2.4). Only one event showed an anti-clockwise hysteresis, although it was one of the smallest events with peak Q of 0.03 $m^{-3}\,s^{-1}$ and a total event time of 90 min. The only event with no hysteresis pattern was also a short event (45 min), however, peak Q reached 0.15 $m^{-3}\,s^{-1}$. The remaining 11 events showed a figure eight-shaped hysteresis pattern (Fi. 2.4).

For the 21 events in the Miombo woodland, hysteresis patterns changed over the course of the rainy season. While the first event exhibited almost no hysteresis (HI = -0.04), the next three events showed a figure eight-shaped pattern, and the two consecutive events showed a clockwise pattern (Fig. 2.5). Only two events showed an anti-clockwise hysteresis pattern, although these were only small events with maximum Q values of 0.17 and 0.77 $m^{-3}\,s^{-1}$.

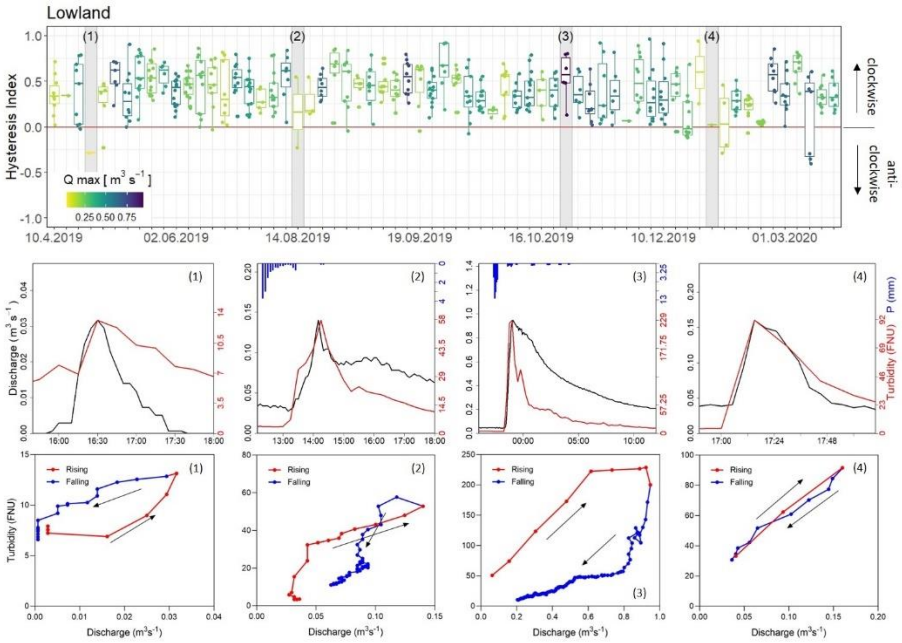

Fig. 2.4 Hysteresis Indexes (HI) for the 68 storm events measured in the lowland forest. Boxplots show the HI values for all flow-percentiles of each individual event. Positive HI values indicate clockwise hysteresis, whereas anti-clockwise hysteresis is indicated by negative HI values. Panels in the middle row show discharge (black line), turbidity (red line), and rainfall (blue bars) for selected events representative for the different hysteresis categories (1 = anti-clockwise; 2 = eight-shaped; 3 = clockwise; 4 = no hysteresis). For the same events, the turbidity-discharge hysteresis is plotted in the panels at the bottom. Red lines indicate the turbidity values on the rising discharge limb, while the blue lines indicate the turbidity values on the falling discharge limb. The HI indexes for the four representative events are highlighted in grey in the top panel.

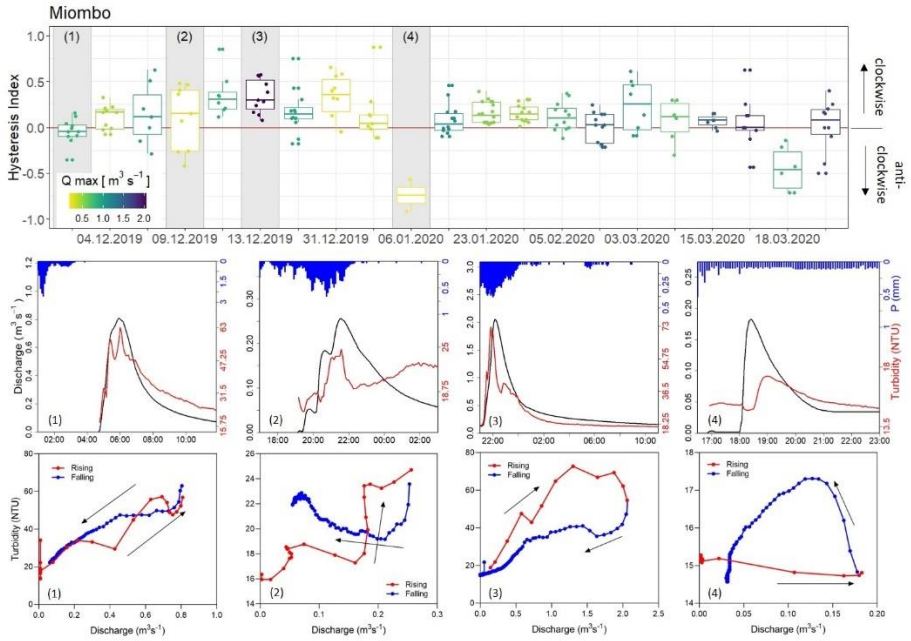

Fig. 2.5 Hysteresis Indexes (HI) for the 21 storm events measured in the Miombo woodland. Boxplots show the HI values for all flow-percentiles of each individual event. Positive HI values indicate clockwise hysteresis, whereas anti-clockwise hysteresis is indicated by negative HI values. Panels in the middle row show discharge (black line), turbidity (red line), and rainfall (blue bars) for selected events representative for the different hysteresis categories (1 = no hysteresis; 2 = eight-shaped; 3 = clockwise; 4 = anti-clockwise). For the same events, the turbidity-discharge hysteresis is plotted in the panels on the bottom. Red lines indicate the turbidity values on the rising discharge limb, while the blue lines indicate the turbidity values on the falling discharge limb. The HI indexes for the four representative events are highlighted in grey in the top panel.

2.3.4. C:N ratios and $\delta^{13}C$ signatures

POM of TSS samples from the lowland stream exhibited C:N ratios between 6.9 and 17.0 with an average value of 12.6 ± 2.1 (average ± standard deviation) and from the Miombo stream between 7.3 and 12.2 with an average value of 9.2 ± 1.0. The POM of the lowland stream was more depleted in the $\delta^{13}C$ isotope with average values of -30.0 ± 0.9‰ compared to the average values of -24.5 ± 2.0‰ of the Miombo stream (Fig 2.8).

Table 2.1 Literature values of annual sediment yields from forested tropical and subtropical catchments.

Forest type	Country	TSS yield (t ha^{-1} yr^{-1})	Reference
Mountain ash forest	Australia	0.05	Grayson et al. (1993)
Hill Dipterocarp forest	Malaysia	0.1	Baharuddin & Abdul (1994)
Hill Dipterocarp forest	Malaysia	0.1	Toriman et al. (2009)
Hill Dipterocarp forest	Malaysia	0.04-0.22	Baharuddin & Abdul (1994)
Tropical montane forest	Kenya	0.215	Stenfert Kroese et al. (2020)
Hill Dipterocarp forest	Malaysia	0.3	Malmer (1996)
Lower Montane Rainforest	Malaysia	0.54	Lai (1993)
Tropical montane forest	American Samoa	0.45 - 1.43	Messina & Biggs (2016)
Hill Dipterocarp forest	Malaysia	3.14	Clarke & Walsh (2006)
Tropical forest	Brazil	0.1	Anache et al. (2017)
Tropical rainforest	Thailand	0.06-0.35	Douglas (1999)
Tropical rainforest	Guyana	0.05-0.7	Fritsch & Sarrailh (1986)
Tropical lowland forest	Panama	1.0-2.0	Zimmermann et al. (2012)
Tropical lowland forest	Costa Rica	1.51	Taylor et al. (2015)
Tropical rainforest	Thailand	3.23	Ziegler et al. (2014)
Tropical lowland forest	**DRC**	**0.25**	**this study**
Cerrado woodland	Brazil	0.1	Oliveira et al. (2015)
Miombo	Malawi	0.07-0.6	Hecky et al. (2003)
Savannah/Miombo	South Africa	0.55	Baade et al. (2012)
Miombo	**DRC**	**0.24**	**this study**

2.4. Discussion

2.4.1. Sediment export

Reported sediment yields from tropical and subtropical forested catchment range from 0.05 – 3.23 t ha^{-1} yr^{-1} (Table 2.1). The yields from the lowland forest and the Miombo woodland are in the same order as yields from comparable ecosystems. Higher values were found in tropical lowland forests in Panama (Zimmermann et al., 2012) and Costa Rica (Taylor et al., 2015); however, these regions have steeper catchments and more intense rainfalls compared to the lowland forest site from this study.

It has been reported that the nutrient status of the forest ecosystems can influence erosion. In nutrient limited ecosystems, thicker root layers (Sayer et al., 2006) and lower litter quality (Kaspari & Yanoviak, 2009) results in slower decomposition and thus function as a protection against soil erosion. However, the Miombo woodland and the lowland forest in our study areas are not limited in N Chapter 5). It is more likely that the presence or absence of overland flow impacts the annual sediment yields. Zimmermann et al. (2012) showed that overland flow has an immense influence on sediment yields in forested catchments and that sites with higher TSS yields most likely experience overland flow. However, during our study period we did not see any indications of occurrence of overland flow in the lowland forest catchment. Because Ferralsols are generally well-draining because of low clay contents and therefore more likely to have vertical flow paths (Elsenbeer, 2001), less overland-flow was expected in the lowland forest catchment. Furthermore, the sandy texture of these Ferralsols in the lowland forest further enable the rapid drainage of water during high precipitation events. On the other hand, Acrisols (soil type of the Miombo woodland catchment) are more likely to experience horizontal flow paths caused by the perching of water on the clay rich Bt horizon, making overland flows more likely in the Miombo woodland catchment. Although the annual yield in the Miombo is similar to that of the lowland forest, the fact that all these sediments are exported during only four months of streamflow shows that sediment yield intensity is three times higher in Miombo and overland flow might be an important process for the generation of 0.24 t ha^{-1} of exported TSS within only four months. Because the annual precipitation in the Miombo catchments is condensed into four months during the wet season, the resulting higher rainfall intensity most likely increases TSS yields. The largest event at the Miombo site (Q_{max} = 2.05 m^3 s^{-1}) lasted for about 17 h (0.6% of total time of annual Q), but exported 0.02 t ha^{-1} of TSS, which is more than 9% of the annual TSS yield. Although storm events played an important role in TSS export in the lowland forest as well, the few intense rainfalls at the Miombo catchment had an even larger influence on the TSS export, i.e., 68% of TSS was exported during storm event conditions in Miombo vs. only 30% in the lowland forest. For the whole Congo River Basin, a sediment yield of 0.083 t ha^{-1} yr^{-1} has been reported by Mushi et al. (2019). If it is accepted that our two catchments are representative of the Congo Basin, sediment yields of headwater catchments in this study are an order of magnitude larger, meaning that high sediment loads are diluted in the larger tributaries or main stem of the Congo and/or that sediments are

deposited in the riverbeds or floodplains. High deposition rates are probable in the *Cuvette Centrale,* a topographical depression in the center of the CRB (Mushi et al., 2019).

2.4.2. Drivers and sediment sources

Hysteresis

In both catchments, TSS export is primarily driven by storm events, with disproportionate TSS yields during storm event conditions compared to baseflow conditions. For a better understanding of the TSS-Q relations, we analyzed the hysteresis patterns of each storm event individually (Fig. 2.4 & Fig. 2.5). Most events in both catchments showed clockwise hysteresis between turbidity and Q (81% in the lowland forest and 52% in the Miombo woodland). A clockwise hysteresis is the most common type of hysteresis pattern in small headwater catchments and is normally associated with a quick flushing of in-channel or nearby sediment sources (Sidle & Campbell, 1985; Smith & Dragovich, 2009; Wood, 1977). The exhaustion of sediment sources has also been shown to enhance clockwise hysteresis (Smith & Dragovich, 2009). Another indicator for source limitation of sediments is that events with double peaks showed no hysteresis on the second peak in the lowland forest (Fig. 2.6), meaning that most of the sediments already were flushed during the first peak. However, because the HI in the lowland forest for all events were similar throughout the year and TSS loads did not decrease, source limitation is probably not the only possible interpretation for the clockwise hysteresis patterns. An increase in baseflow at the falling limb, bank erosion, and sediment yield from areas near river channels are also common interpretations for clockwise hysteresis (Malutta et al., 2020; Sidle & Campbell, 1985; Smith & Dragovich, 2009; Wood, 1977). The changing contributions of event flow and baseflow can also influence the hysteresis patterns. Event flow, which is in general occurring mostly in the upper soil layers, can detach more sediments relative to baseflow. Event flow also contributes more to the total Q during the rising limb relative to the falling limb; in the latter, baseflow becomes more important because of longer water infiltration times into the soil (Bača, 2008). Furthermore, clockwise hysteresis has been attributed to sediment sources in and near stream channels (Hughes et al., 2012). In the lowland forest, channel banks can be steep (compared to the flat topography in the rest of the catchment) and are probably susceptible to soil detachment during heavy rainfalls.

Different explanations for the observed anti-clockwise patterns are possible. For example, anti-clockwise hysteresis can occur when sediment sources are far away from the measurement locations (Hughes et al., 2012) or if water and sediment transport travel times are different , which can be influenced by catchment characteristics such as geology or catchment topography (Brasington & Richards, 2000). However, anti-clockwise hysteresis patterns were not important in our two study streams. Only one event in the lowland forest and two events in the Miombo woodland exhibited anti-clockwise hysteresis. Moreover, all three events were small, with maximum Q just slightly higher than baseflow Q.

The Miombo woodland showed an interesting temporal pattern of hysteresis at the onset of the rainy season: while the first event did not show a strong hysteresis pattern, the HI increased with every subsequent event (Fig. 2.5). At the end of the dry season, litter residues and burned vegetation cover the soil surface in the Miombo and, hence, loose sediment particles are susceptible to transport by overland flow (Appendix A6). Thus, during the first events of the rainy season, sediment sources are not depleted yet and result in a lack of hysteresis. However, over the course of the rainy season, soils become increasingly protected by vegetation and limited in sediment availability, leading to more events with clockwise hysteresis later in the wet season. The same trend is visible for double peak events: a double peak event at the beginning of the wet season showed the same pattern and similar TSS increases during both peaks (Fig. 2.7 left panel), however, only nine days later, TSS concentration during the second peak of a double peak event already considerably decreased compared to during the first peak, although the second peak had a higher max Q (Fig. 2.7 right panel). This indicates that already one month after the onset of the wet season, sediment sources are likely to be depleted and that the positive HIs are indeed indicating sediment source limitation in the Miombo woodland. Thus, our results clearly show that it is important to analyze seasonal TSS-Q hysteresis patterns because even though both of our study sites showed mainly clockwise hysteresis, the temporal patterns of the HIs demonstrate that different processes are responsible for the similar patterns.

Sediment sources and transformations

To get a better understanding of the origin of the TSS in the forested streams, C:N ratios and ^{13}C signatures of the POM of the suspended sediments were analyzed. It is important to state that these analyses are made on the organic fraction, which comprise only a subset of the total suspended material. As a result, while C:N and $\delta^{13}C$ can be used to infer sources of POM, it does not necessarily reflect the sources of the other, non-organic mineral fractions; however, it still captures organic matter (OM) associated with minerals. Differences in C:N ratios can either point to different sources of the POM or different decomposition processes that already occurred (Ziegler et al., 2016).

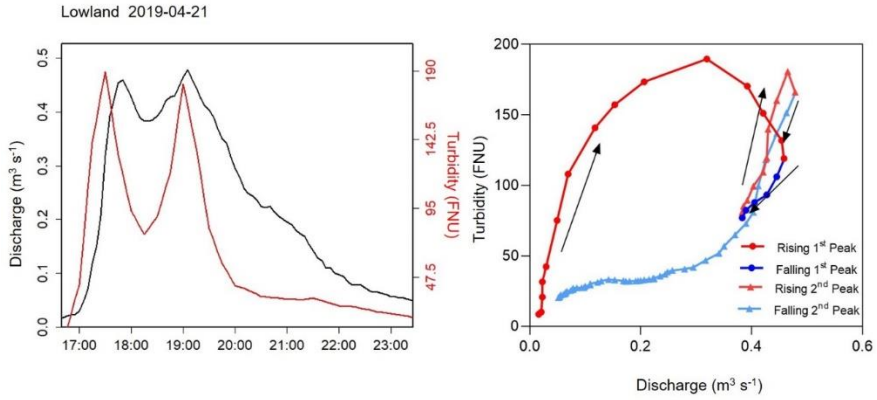

Fig. 2.6 Left: Time series of discharge (black line) and turbidity (red line) values for a double peak event in the lowland forest. Right: turbidity - Discharge hysteresis plot of the same event, red colors indicate turbidity values on the rising limb and blue colors indicate turbidity values on the falling limb. Round dots represent values during the first peak and triangles for the second peak of the event.

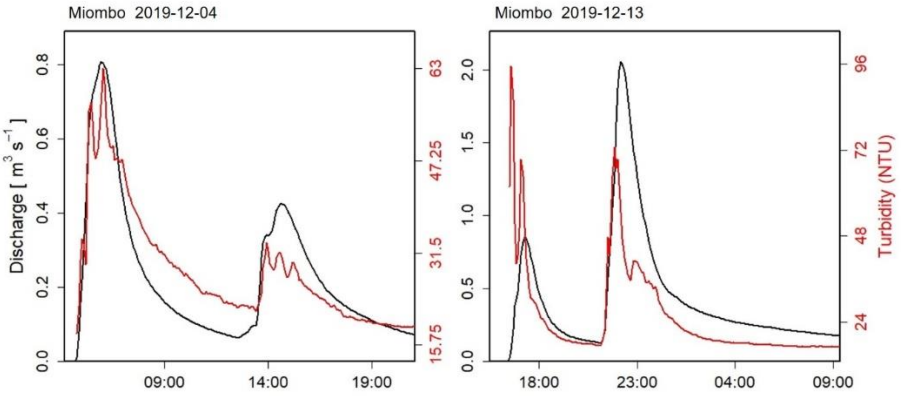

Fig. 2.7 Discharge and turbidity values for two double peak events in the Miombo catchment.

In the lowland forest, C:N ratios of POM increase with higher Q (Appendix A5), indicating shifts of sediment sources during high-flow conditions (from more processed and soil-associated OM, likely from deeper soil layers and riverbanks to topsoil OM, such as litter and fresh leaves). A shift in sources should also be visible in the $\delta^{13}C$ values and indeed a slight trend to more depleted $\delta^{13}C$ values is visible at higher Q (Appendix A5). However, no isotopic values are available for high TSS samples, resulting in a non-significant relationship. On the other hand, in the Miombo woodland there is no trend visible for C:N nor $\delta^{13}C$ (Appendix A5). This reinforces the idea that there is source limitation within events in the Miombo woodland, as no change in POM sources is visible throughout the whole rainy season and no shift of source material occurs between baseflow and storm flow conditions.

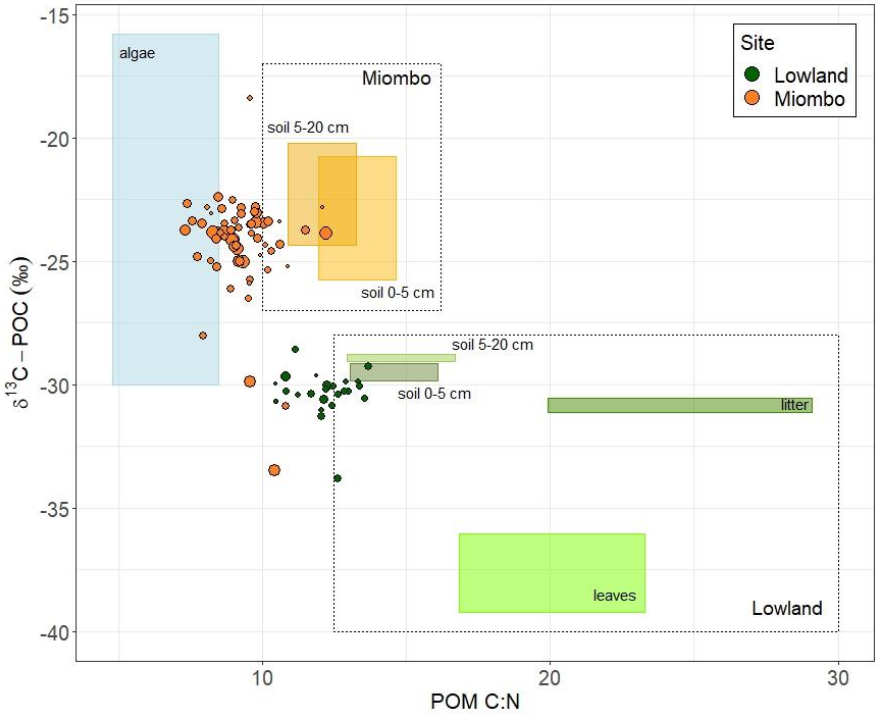

Fig. 2.8 $\delta^{13}C$ values plotted against the C:N ratio of particulate organic matter (POM) from the lowland and Miombo forest site. The size of the dots indicates the discharge during the respective sampling timepoint. Colored boxes indicate the $\delta^{13}C$ values and C:N ratios of potential source material. Values for leaves and litter of the lowland forest were obtained from Baumgartner et al. (2020). Soil $\delta^{13}C$ and C:N values from the lowland and Miombo site were obtained from Chapter 5. Source box for algae values were adapted from Lamb et al. (2006).

In previous studies at the same sites, we reported the ranges of $\delta^{13}C$ and C:N values from different potential source material within our catchments (Baumgartner et al., 2020, 2021). These ranges are plotted together with the values of sediment samples from this study (Fig. 2.8). The lowland and Miombo samples are grouped with distinct $\delta^{13}C$ values, except for four samples from the Miombo site with more depleted $\delta^{13}C$ values compared to the rest of the samples from the same site. The four samples with more depleted $\delta^{13}C$ values are all from the first storm event of the rainy season, likely containing burned litter residues that are depleted in $\delta^{13}C$ (Saiz et al., 2015). The more depleted ^{13}C signature for the lowland site is also visible in the lower $\delta^{13}C$ of soil organic matter (SOM) compared to the SOM in the Miombo woodland. For both sites there is a shift to lower C:N ratios in the POM compared to the soil sources. Lower C:N values can be explained through in-stream partial decomposition of the POM (Ziegler et al., 2016). However, in small headwater streams, extensive decomposition is not likely given the short residence times for water. In the Miombo woodland, the lower C:N ratios could also be due to an algae

origin of the POM (Fig. 2.8). The stagnant water conditions between storm events in the Miombo woodland are ideal conditions for algae biomass to grow and such biomass has been reported to be an important source of POM in tropical rivers (Balakrishna & Probst, 2005). Moreover, the Miombo woodland stream is also more prone to algae growth compared to the lowland stream, as the more closed canopy in the lowland forest likely inhibits algae growth because of sunlight limitation, which is not the case in the Miombo woodland with a more open canopy.

2.5. Conclusion

By measuring sediment yields of two different forested headwater stream catchments within the Congo Basin, we found that sediment yields in the lowland forest and Miombo woodland were similar with 0.25 ± 0.05 t ha^{-1} yr^{-1} and 0.24 ± 0.09 t ha^{-1} yr^{-1}, respectively. TSS export was driven by storm events, with 30% of annual TSS exported during events in the lowland and 68% in the Miombo. Although these forests are pristine and sediment yields have historically been thought to be negligible, our results show that erosion can be an important loss process in tropical forests and its role in forest functioning and biogeochemical cycling may be overlooked and needs to be considered in future research. The analysis of TSS - Q hysteresis helped understand the underlying processes regarding the sediment loss dynamics of lowland forest and Miombo woodland. Even though both sites showed mainly clockwise hysteresis, the underlying processes were different. The Miombo hysteresis likely stemmed from source limitation while the lowland hysteresis more likely resulted from an increase of baseflow during the falling limb. These findings highlight the importance of a temporal coverage for hysteresis analysis. Source limitations in the Miombo woodland is also reinforced by the chemical composition of the POM, where no changes throughout events and seasons were found, contrary to the lowland site, where higher C:N ratios during high flow conditions indicated more topsoil associated OM as source for POM.

Acknowledgments

We thank Héritier Ololo Fundji for assisting and organizing field installations and campaigns, the villagers in Yoko for their support and hospitality during our fieldwork. We are also thankful for Katja Van Nieuland and Samuel Bodé for the help with the analysis of the sediment samples. This research has been funded by the Fonds de la Recherche Scientifique FNRS project numbers T.0059.18 and J.0167.19.

Supporting information

Supporting information to this chapter can be found in Appendix A

Appendix A1: Topographical maps and slope distributions of the two catchments. Colored values are in meters above sea level. Red dots indicate the locations of the concrete flumes (photos at the bottom).

Appendix A2: Rating curves for discharge calculation for the lowland forest catchment (left) and the Miombo woodland catchment (right).

Appendix A3: Comparison between discharge calculated with the Manning's equation and the discharge calculated from the different models obtained from the rating curve in Appendix A2 for the Miombo site. Black is the linear model between water level and Q. Green is the linear model between water level and Q with an intercept 0. Blue is a second order polynomial function between water level and Q and red is a power function between water level and Q. Q were calculated for water levels between 0.5 and 2 m. Grey dashed line indicates the 1:1 line.

Appendix A5: Comparison between measured and predicted TSS values for the lowland forest and Miombo woodland site. Error bars indicate the standard deviation of the random forest prediction.

Appendix A6: C:N ratios of sediments plotted against the discharge (Q) values at the respective sampling points (top figures). $\delta^{13}C$ values of Particulate Organic Carbon plotted against the discharge values at the respective sampling points (bottom figures).

Appendix A7: left photo: Miombo woodland at the end of the dry season after seasonal fires. Right photo: Miombo woodland at the end of the rainy season.

Part III – Aquatic N and P export of tropical forests

Chapter 3: Substantial organic and particulate nitrogen and phosphorus export from stable tropical forest landscapes

After: Baumgartner, S., Bauters, M., Drake, T. W., Barthel, M., Alebadwa, S., Bahizire, N., Bazirake, B. M., Ntaboba, L. C., Six, J., Boeckx, P. & Van Oost, K.: Substantial organic and particulate nitrogen and phosphorus export from stable African tropical forest landscapes. *(under review)*

Abstract

Tropical forest productivity is in part constrained by the availability of important nutrients such as nitrogen (N) and phosphorus (P). The availability of these nutrients results, among other things, from the overall nutrient input-output balance in ecosystems, with aquatic losses being an important loss vector. Traditionally, research has focused mainly on inorganic losses of N and P, whereas the potential contribution of organic and particulate losses to the total nutrient export budget is much less constrained. In this study, we quantified full aquatic N and P exports, including inorganic, organic and particulate forms, from a moist tropical lowland forest and a semi-dry Miombo woodland forest within the Congo Basin. In general, organic and particulate forms of N and P dominated the aquatic exports of both ecosystems. While particulate N (PN) was the highest N loss vector in the lowland stream (3.34 ± 0.66 kg N ha^{-1} yr^{-1}; 44 % of total N (TN)), dissolved organic N (DON) dominated the export in the Miombo stream (1.41 ± 0.28 kg N ha^{-1} yr^{-1}; 47% of TN). Aquatic P export was dominated by dissolved organic P (DOP) in both streams, with yields of 0.29 ± 0.02 kg P ha^{-1} yr^{-1} (65% of total P (TP)) in the lowland and 0.24 ± 0.05 kg P ha^{-1} yr^{-1} (69 % of TP) in the Miombo. The lowland forest showed higher N and P inputs than losses, most likely due to high atmospheric depositions, but the imbalance in the Miombo was lower and might well be because of higher gaseous N losses and N and P losses through seasonal fires. Our data suggests that all organic and particulate species were transport limited and storm events were driving those losses, exporting disproportionally high N and P loads during short periods (16% in the lowland and 29% in the Miombo) of stormflow conditions (32% and 47% of TN and 20% and 40% of TP in the lowland and Miombo, respectively). Our results highlight the need to include particulate and organic forms as important loss vectors in the nutrient balance of tropical forests. A finding of particular importance considering the projected increasing rainfall intensities in many tropical regions which might exacerbate the export of these nutrient forms in the near future and thus potentially impacting the nutrient balance of tropical forests.

3.1. Introduction

Tropical forests play an important role in the global carbon (C) cycle, accounting for roughly 60% of the terrestrial gross primary production (GPP) (Beer et al., 2010; Jung et al., 2020). High primary production rates are counterbalancing the high respiration rates, resulting in a net C uptake of tropical forests of around 1.7 Pg C per year (Harris et al., 2021). The magnitude of both fluxes is partly constrained by the nutrient status

of the ecosystem, where nutrient limitation leads in general to lower carbon use efficiencies in forest ecosystems (Fernández-Martínez et al., 2014). The main nutrients underpinning these C exchange fluxes are nitrogen (N) and phosphorus (P), but their abundance and availability are highly variable in space and time (Chadwick et al., 1999; Hedin et al., 2009). Many tropical forests appear to be limited by N and/or P (Wright, 2019). A long-lasting paradigm has been that highly-weathered soils of tropical forests are abundant in N and limited in rock-derived P, whereas soils in geomorphic active regions are conversely more depleted in N while being rich in P, due to higher soil rejuvenation rates (Hedin et al., 2009).

Traditionally, research has mainly focused on inorganic nutrients, being bioavailable for plant uptake, resulting in the "nutrient retention hypothesis". This hypothesis states that efficient retention of bioavailable and limiting nutrients leads to minimal losses of those nutrients, resulting an accumulation of those nutrients within the ecosystem. Once these nutrients are not limiting biological processes anymore, the outputs of these nutrients should reflect the inputs into the system (Vitousek & Reiners, 1975). Thus, it was postulated that aquatic losses of bioavailable and limiting nutrients can reflect the nutrient status of the ecosystem. However, Hedin et al. (1995) introduced dissolved organic N (DON) as a loss vector without biological control that can profoundly influences the biogeochemical cycling of nutrients in forests. As such, the observation of high DON and dissolved organic P (DOP) losses from unpolluted old-growth forests (Hedin et al., 1995, 2003; Perakis & Hedin, 2002; Vitousek et al., 1998) led to the elaboration of the "leak" hypothesis, which states that besides the high biological need for nutrients, the biologically uncontrolled export of organic forms of nutrient can lead to long-term nutrient limitations (Hedin et al., 2003).

Moreover, this "DON-leak" hypothesis was recently complemented by findings of high losses of particulate N (PN) forms through erosional processes regulated by hydrological controls, that are independent of biological demand (Taylor et al., 2015). Nevertheless, particulate nutrients have been widely neglected in biogeochemical research and studies reporting PN or total particulate P (TPP) are scarce. The few studies that reported PN losses showed that this loss vector can dominate total N (TN) export in a tropical forest (Lewis, 1986; Lewis et al., 1995; Taylor et al., 2015). As the export of organics tend to follow more the hydrological regime, storm events have been identified to be an important driver of particulates and dissolved organic species (Clark et al., 2013; Hoover & MacKenzie, 2009; Lloret et al., 2013; Taylor et al., 2015; Townsend-Small et al., 2008). However, all these studies were conducted in more active landscapes, i.e., sites with high erosional potential, due to steep slopes and/or high rainfall intensities, but the influence of erosion and storm events on nutrient export on old and more stable landscapes, have not been studied yet. The fact that the majority of tropical forests are situated in old stable landscapes with low topography calls for a thorough quantification of N and P losses, including the particulate forms, from old stable forested landscapes of the tropics.

In this study, we assessed the impact of particulate nutrient export on the nutrient budgets of two distinct forest types of the Congo Basin: a lowland tropical forest and a Miombo woodland. These two forest types represent the two most abundant ecosystems of the Congo Basin, with the evergreen lowland forests covering around 35% and the broadleaved deciduous forest (Miombo as a representative type of tropical deciduous forest) covering around 37% (ESA, 2017). In particular we sought to tackle the following research questions: (i) how do N and P exports differ in yield in distinct tropical environmental settings? (ii) what is the contribution of particulate and organic N and P compared to its inorganic species? and (iii) what is the influence of storm events on aquatic N and P losses? To answer these questions, we measured aquatic dissolved and particulate N and P exports from two distinct pristine forest watersheds of the Congo Basin during one hydrological year.

3.2. Material and Methods

3.2.1. Study sites

Aquatic nutrient export and discharge were determined at two representative headwater streams draining a tropical lowland forest and a subtropical woodland catchment (Miombo). The lowland forest catchment is situated in the Yoko Forest Reserve 35 km south of the city of Kisangani (Tshopo province, Democratic Republic of the Congo (DRC); 0.291°N, 25.295°E; Fig. 3.1). The whole catchment area consists of pristine primary mixed tropical forest with patches of monodominant forests, where the species G*ilbertiodendron dewevrei* consists of more than 60% of the basal area. Deeply weathered Ferralsols with loamy sand texture is the main soil type in the lowland forest (Baumgartner et al., 2020; Van Ranst et al., 2010). The lowland forest site experiences two wet seasons, a shorter one from March to May and a more prolonged wet season from August to November with mean annual rainfall of ~1825 mm and mean annual temperature of ~24°C (Bauters et al., 2019; Fig. 3.1). The catchment area was determined using digital elevation models (DEM) derived from the 30 m Shuttle Radar Topographic Mission (SRTM, NASA Jet Propulsion Laboratory). The obtained catchment ranges from 440 – 475 m a.s.l. and has a mean slope of 4.3° with an area of 311 ha (Chapter 5).

The Miombo woodland catchment is situated approximately 50 km north of the city of Lubumbashi (Katanga province, DRC; 11.212° S, 27.233° E; Fig. 3.1). The Miombo woodlands are mosaics of mature forest, shifting cultivation, grazing lands, and regrowing forests (Mayes et al., 2019); thus pristine Miombo woodland is scarce in the region. Dominant tree genera in a Miombo woodland are *Brachystegia, Julbernadia* and *Isoberlinia* (Campbell, 1996). The site has minor anthropogenic impact, mainly from charcoal production and small-scale agricultural practices, which are representative for the Miombo in the region (Campbell, 1996). Moreover, natural and anthropogenic fires during the dry season are common. Soils are classified as Acrisols and Cambisols (Chapter 5). The region experiences a single wet season that starts in October and continues until April, with a mean annual precipitation of ~1230 mm and mean annual temperature of ~21°C (Fick & Hijmans, 2017; Fig. 3.1). The selected stream channel only flows with surface water after the onset of the wet season in November until end of the wet season in April and is dry

during the rest of the year. We determined the catchment area using a 30 m DEM (SRTM, NASA Jet Propulsion Laboratory). The catchment area is 588 ha with an elevation ranging from 1257 to 1311 m a.s.l. and an average slope of 3.9°.

3.2.2 Monitoring and sampling campaigns

At each site, a concrete flume with a fixed width (lowland: 1.6 m; Miombo: 1.4 m; Fig. 3.1) was installed to generate high quality water level – water discharge rating curves. Water level was measured in a 5-min interval with a pressure transducer (CS451, Campbell Scientific, UK) connected to a datalogger (CR1000, Campbell Scientific, UK). Bi-weekly (lowland) and weekly (Miombo) manual discharge measurements were carried out to establish a water level - discharge rating curve for each site using a mechanical flowmeter (Model 2030, General Oceanics Inc., USA). Furthermore, in-stream turbidity sensors were installed and set to record at 5-min interval at the Miombo site (OBS 3+, Campbell Scientific, UK) and at 15-min interval at the lowland site (YSI-EXO2, Xylem, US). At the same time the bi-weekly discharge measurements were conducted, water samples were taken with acid washed 2L- HDPE-bottles. The samples were transported immediately back to the laboratories in Kisangani and Lubumbashi, respectively. In addition to the manual water sampling, autosamplers (6712 Portable Sampler, Teledyne ISCO, USA), equipped with 24 x 1 L PVC bottles, were installed at both sites to obtain water samples during storm event conditions. The autosamplers were connected to the datalogger and triggered when water level reached a certain threshold (0.175 m at the lowland site and 0.35 m at the Miombo site). These thresholds were selected by measuring water level at those streams prior to the monitoring period, which was used to determine water level ranges of the baseflow conditions. Due to logistical constraints, the bottles of the autosampler were only replaced during the bi-weekly or weekly field visits. To minimize biological degradation of the water samples within the autosampler, the empty bottles were prepared with 5 ml of 50 % $ZnCl_2$ solution to stop biological activity in the water samples.

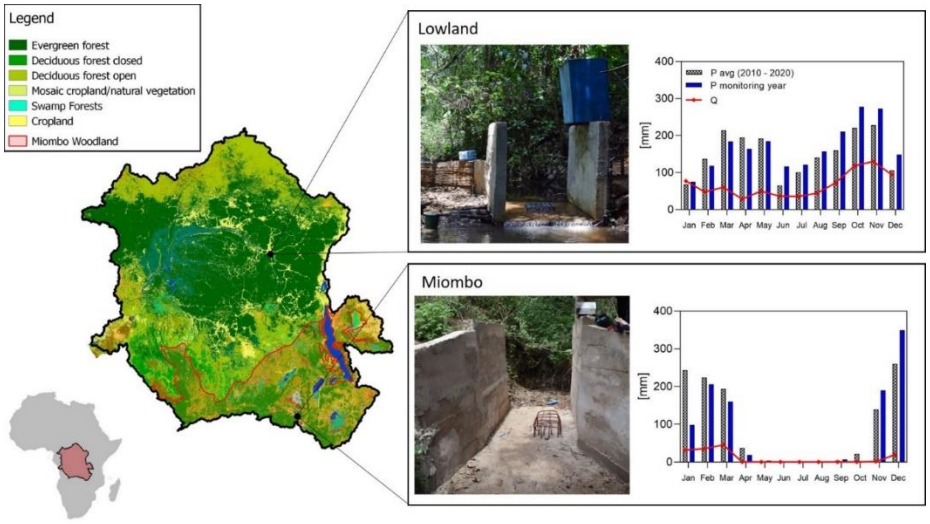

Fig. 3.1 Different ecosystem types within the Congo River Basin and the sampling locations within the lowland forest and the Miombo woodland. Photos show the concrete flumes installed at the two catchments. On the right-hand site are the monthly precipitation rates during the monitoring year (blue) and 10-year average in grey. Precipitation data are derived from GPM satellite data (Huffman et al., 2019). The red line is the discharge measured at the flumes. Map adopted from ESA (2007).

Dissolved nitrous oxide (N_2O) concentration of the stream water was determined using the headspace equilibrium technique. A 12 mL plastic syringe was used to inject 6 mL of air bubble free water into a N_2-pre-flushed 12 mL exetainer (Labco, UK). The pre-flushed exetainer contained 50 µL of 50 % (w/v) $ZnCl_2$ in order to stop microbial activity after water sample injection. The remaining vial headspace was analyzed for N_2O concentration at ETH Zürich, using gas chromatography (456-GC, Scion Instruments, UK) and dissolved gas concentrations subsequently calculated using Henry's law.

Biweekly water sampling and discharge measurements started in November 2018. Monitoring with the full setup (water level, turbidity and autosampler) was done one hydrological year at both sites (lowland: from 01.04.2019 to 31.03.2020; Miombo: from 01.05.2019 to 30.04.2020, sampling only started at onset of streamflow from 22.11.2019 onwards).

3.2.3. Sample analysis

Immediately upon return to the laboratories in Kisangani and Lubumbashi, the water samples were shaken to resuspend sediments and filtered on pre-combusted (450°C for five hours) glass-fiber filters (0.7 µm GF/F, Whatman, USA). For the analysis of the dissolved nutrients, the filtrate was stored in two acid-washed 250 ml HDPE bottles and were immediately frozen. To determine the total suspended sediment (TSS) concentration, particulate C (PC), particulate N (PN) and particulate P, the

water samples were filtered in duplicates on pre-weighted GF/F filters and stored in the freezer. Due to the limited amount of water sample within the autosampler bottles, storm event samples were only filtered for PN and PC analysis, TPP and PIP were only determined for baseflow samples. All the samples were returned for laboratory analysis to Europe in batches every two to four months. All filters were dried at 60°C for 48 h before analysis. TSS concentrations were calculated by dividing the weight difference between the initial and the dried filter after filtration by the amount of water filtered. PC and PN concentrations were determined by measuring the dried GF/F filters on an elemental analyzer (Automated Nitrogen Carbon Analyzer, SerCon; Crewe, UK). To determine TPP concentrations the chemical wet oxidation method by Suzumura (2008) was used. In short, for the TPP extraction, the filters were rinsed with 5 ml of 0.17M Na_2SO_4 solution to remove all dissolved P that was adsorbed to the particles. The filters were afterwards digested in 20ml of 3% $K_2S_2O_8$ at 120°C for 30 minutes using an autoclave. Afterwards, the residues were removed from the digest using a 0.45 µm syringe filter. Before measurement, the digested and filtered solution was diluted with purified water to 1.5% $K_2S_2O_8$ concentration. To get particulate inorganic P (PIP) concentrations, the filters were also rinsed with 5ml of 0.17M Na_2SO_4 solution and then digested with 20 ml of 1M HCl for 24 hours at room temperature on a shaker in the dark (Ehama et al., 2016). The residues were filtered using a 0.45 µm syringe filter. Phosphate (PO_4^{3-}) concentrations in the TPP and PIP digestion solution were measured colorimetrically (see below).

Dissolved nitrate (NO_3^-), ammonia (NH_4+) and PO_4^{3-} concentrations were measured colorimetrically from the filtered water samples using a continuous flow autoanalyzer (AA3, Bran and Luebbe, Germany). NO_3^- concentrations were measured by reducing all NO_3^- to nitrite on a Cu-Cd column, followed by the reaction with *N*-l-naphtylenediamine dihydrochloride to form chromophore. NH_4^+ concentrations were determined by the salycilate-nitroprusside method and PO_4^{3+} concentrations were measured by the reaction of PO_4^{3+} with molybdate and ascorbic acid. Concentrations of NO_3^- and NH_4^+ together are defined as dissolved inorganic N (DIN) and PO_4^{3-} is referred to as dissolved inorganic P (DIP). Total dissolved N (TDN) and total dissolved P (TDP) were measured by converting all N and P in solution into inorganic N and P forms using a 1:1 oxidizing solution of 0.4M NaOH, 0.5M H_3BO_3 and 0.2M $K_2S_2O_8$ and autoclaving it for 1h at 121°C to convert NH_4^+ and dissolved organic N (DON) in NO_3^- and dissolved organic P (DOP) in PO_4^{3-}. DON and DOP were determined by subtracting the inorganic forms of N and P from the TDN and TDP concentrations. TPP and PIP concentrations were only obtained for the samples of the biweekly and weekly sampling campaigns.

3.2.4. Export calculations

To calculate discharge values from the continuously measured water levels, a linear rating curve was applied (Baumgartner et al., 2022). TSS concentrations were already calculated for each turbidity and water level measurement using a random forest approach (see detailed description in Chapter 2). To calculate total export of the particulate nutrient constituents (PN, TPP and PIP), linear regressions with TSS were

applied (Appendix B1). Finally, total PN, TPP and PIP export per 5-min interval was calculated by multiplying the obtained particulate nutrient concentration with the instantaneous discharge value integrated over a 5 min period. Yields were calculated by dividing the yearly particulate nutrient export (kg yr^{-1}) by the catchment area (ha). Due to this "double prediction approach" (TSS via turbidity and then particulate nutrient concentrations via TSS), the uncertainty of the prediction is increasing. To validate model performance, we calculated root mean square errors of the predictions (Appendix B3).

For dissolved nutrient constituents, a linear model with water discharge was applied (Appendix B2). For statistically significant models ($p < 0.05$), the obtained relationship was applied to calculated nutrient concentrations for each discharge measurement. Total exports and yields were then calculated the same way as for particulate nutrient exports and yields. Dissolved nutrient constituents with no significant relation with water discharge, the average concentration was used to calculate annual export and yields, by multiplying the average concentration by the total annual water discharge and yield. Standard errors for the yield calculations include the errors from the double prediction approaches (for particulate nutrients) or the single linear models (for the dissolved nutrients) plus the standard error from the uncertainty in the water discharge calculation with the rating curves that were applied.

3.3. Results

3.3.1. Hydrology

The hydrology and suspended sediment dynamics of the two study sites have been discussed in detail in a previous study (Chapter 2). During the 12-month sampling period from April 2019 to March 2020, the lowland forest site received 2030 mm of rainfall, while the stream exhibited a specific discharge of 795 mm. By difference, interception and evapotranspiration totaled to 1235 mm (Fig. 3.1). During the sampling year, 68 distinct storm events were observed (Chapter 2). These events comprised 4.7% of the monitoring period and were responsible for 16% of water discharge.

The stream at the Miombo woodland site only flows during five months of the wet season. During the 12-month sampling period, this stream exhibited a specific discharge of 133 mm (all between December 2019 and April 2020). Amid the same wet season, 1036 mm of rainfall was measured, resulting in an interception and evapotranspiration of around 900 mm (Fig. 3.1). 21 storm events were identified at the Miombo stream, exporting 29 % of total water discharge during 7.4 % of the wet season.

3.3.2 Particulate nutrient concentrations

PN concentrations in the lowland stream were higher during storm events with measured mean concentration of 2.28 ± 1.09 mg PN-N L^{-1} compared to mean baseflow concentrations of 0.17 ± 0.07 mg PN-N L^{-1} (Fig. 3.2 & Appendix B4). Also, the Miombo stream showed higher mean PN concentrations during storm events

with 1.36 ± 2.05 mg PN-N L^{-1} compared to 0.18 ± 0.11 mg PN-N L^{-1} during baseflow (Fig. 3.2 & Appendix B4). Mean baseflow TPP concentrations were higher in the Miombo stream with 20.52 ± 17.97 µg TPP-P L^{-1} than in the lowland stream with 12.25 ± 6.05 µg TPP-P L^{-1}. While the Miombo stream mainly exported TPP as PIP, the PIP fraction in the lowland stream was only around 41 % of the TPP fraction (Fig. 3.2 & Appendix B4). Particulate nutrient concentrations (PN, TPP, and PIP) all correlated positively with sediment concentrations (Appendix B1). While robust linear relations were obtained for PN at both sites, TPP and PIP correlations with TSS showed higher variability, because no samples for TPP and PIP at high TSS concentrations were available (no storm events).

3.3.3. Dissolved nutrient concentrations

The lowland stream showed mean measured NO_3^- concentrations of 0.17 ± 0.05 mg NO_3^--N L^{-1} for baseflow samples and 0.31 ± 0.18 mg NO_3^--N L^{-1} for storm event samples. NO_3^- values in the Miombo stream were an order of magnitude lower with mean measured concentrations of 0.02 ± 0.04 mg NO_3^--N L^{-1} for baseflow samples and 0.05 ± 0.05 mg NO_3^--N L^{-1} for storm event samples (Appendix B4). While in the lowland stream NH_4^+ concentrations were lower than NO_3^- (0.07 ± 0.04 mg NH_4^+-N L^{-1} during baseflow and 0.12 ± 0.07 mg NH_4^+-N L^{-1} during storm events), the Miombo stream showed higher NH_4^+ concentrations than NO_3^- (0.08 ± 0.07 mg NH_4^+-N L^{-1} during baseflow and 0.22 ± 0.21 mg NH_4^+-N L^{-1} during storm events). In both streams the highest dissolved N concentrations were found as DON, with the lowland stream having mean concentrations of 0.33 ± 0.15 mg DON-N L^{-1} for baseflow samples and 1.05 ± 1.14 mg DON-N L^{-1} for storm event samples and the Miombo stream 0.64 ± 0.86 mg DON-N L^{-1} for baseflow samples and 1.22 ± 1.82 mg DON-N L^{-1} for storm event samples. Only dissolved N species in the lowland site showed a significant positive correlation with water discharge (Appendix B2). On the other hand, the Miombo site showed high variability of DON (0.07 – 5.48 mg DON-N L^{-1}) and DIN (0.01 – 0.75 mg DIN-N L^{-1}) concentrations without a flow dependency (Appendix B2). Dissolved N_2O concentrations ranged from 0.28 to 0.56 µg N_2O-N L^{-1} in the lowland stream and from 0.35 to 0.83 µg N_2O-N L^{-1} in the Miombo stream (Fig. 3.2).

At both sites, DIP samples were mainly below detection limit of the colorimetric technique (DL = 0.01 mg P L^{-1}; Fig. 3.2). At the Miombo site, only one sample exceeded the detection limit with 0.02 mg PO_4^{3-}-P L^{-1} at the onset of the rainy season (Fig. 3.2). At the lowland site, eight samples exceeded the detection limit, however there was no relationship with water discharge (Appendix B2). DOP concentrations in the lowland stream showed low variability, with values ranging from 0.01 – 0.20 mg DOP-P L^{-1}, whereas the Miombo stream showed slightly more pronounced variability with values ranging from 0.04 – 0.60 mg DOP-P L^{-1} (Fig. 3.2).

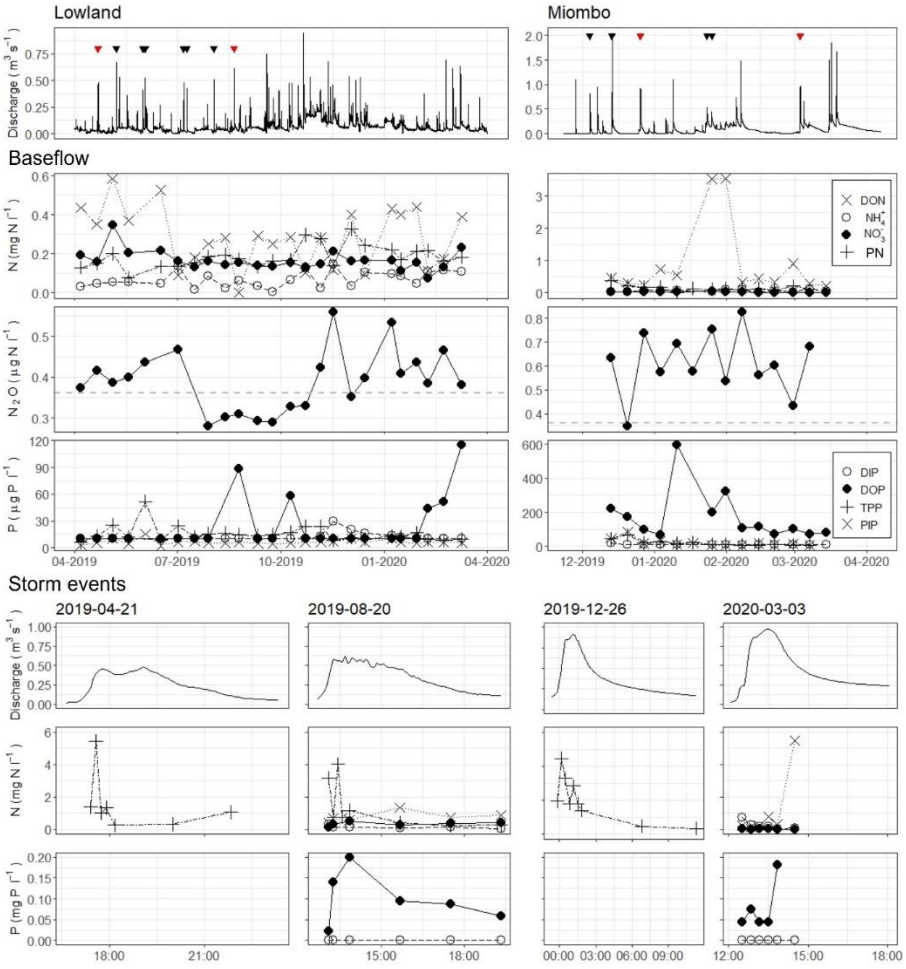

Fig. 3.2 Timeseries for the lowland (left) and Miombo stream (right). Top panel: Timeseries of water discharge with triangles indicate storm events that got sampled. Red triangles indicate the events that are presented in this figure in the lower panels. Middle panels: Timeseries of all the baseflow samples: dissolved and particulate N species (dissolved organic nitrogen – DON, ammonium – NH_4^+, nitrate – NO_3^-, particulate N - PN), dissolved nitrous oxide (N_2O) concentrations, dissolved and particulate P species (dissolved inorganic phosphorus – DIP, dissolved organic phosphorus – DOP, particulate inorganic phosphorus – PIP, total particulate phosphorus – TPP). Lower panels: selected storm events with water discharge, dissolved and particulate N concentrations and dissolved P concentrations.

3.3.4. Nutrient yields

Total N yields of the lowland forest (7.44 ± 1.35 kg N ha^{-1} yr^{-1}) were led by PN (44%; 3.34 ± 0.66 kg N ha^{-1} yr^{-1}) and DON (31%; 2.28 ± 0.47 kg N ha^{-1} yr^{-1}) yields (Fig. 3.3). The smallest proportion of total the N yield was via the DIN fraction (25%) with 1.82 ± 0.21 kg N ha^{-1} yr^{-1} (Fig. 3.3). Total N yields in the Miombo forest were lower with 2.96 ± 0.90 kg N ha^{-1} yr^{-1} (Fig. 3.3). The largest proportion of the TN yield at the Miombo site was the DON fraction (47%; 1.41 ± 0.28 kg N ha^{-1} yr^{-1}), which was only marginally higher than the PN yield (44%; 1.28 ± 0.59 kg N ha^{-1} yr^{-1}). As in the lowland forest, the smallest proportion of N yields at the Miombo site were comprised by DIN (9%) with 0.28 ± 0.04 kg N ha^{-1} yr^{-1} (Fig. 3.3). In the lowland forest catchment, storm events were responsible for 30% of the PN export, 41% of the DON export, and 24% of the DIN export. In the Miombo catchment the storm events were responsible for 65% of the PN export, 32% of the DON export, and 33% of the DIN export (Fig. 3.3). Exports as dissolved N_2O are low and compared to other N exports insignificant. The lowland stream yielded a total of 0.003 kg N_2O-N ha^{-1} yr^{-1} and the Miombo stream 0.001 kg N_2O-N ha^{-1} yr^{-1}.

Total P yields in the lowland stream (0.48 ± 0.08 kg P ha^{-1} yr^{-1}) were dominated by DOP with 0.29 ± 0.02 kg P ha^{-1} yr^{-1} (60%). In the particulate P fraction (TPP; 0.14 ± 0.03 kg P ha^{-1} yr^{-1}; 29% of TP) more organic P was found than PIP (0.06 ± 0.01 kg P ha^{-1} yr^{-1}) (Fig. 3.3). The Miombo site experienced slightly lower total P yields than the lowland site, with 0.35 ± 0.08 kg P ha^{-1} yr^{-1}. The same trend as in the lowland forest was observed in the Miombo woodland, with highest P exports as DOP (0.24 ± 0.05 kg P ha^{-1} yr^{-1}, 68%) followed by TPP (0.10 ± 0.05 kg P ha^{-1} yr^{-1}, 29%) and only a marginal amount as DIP (0.01 ± 0.01 kg P ha^{-1} yr^{-1}, 3%). Particulate P in the Miombo woodland was exclusively exported as PIP (Fig. 3.3). Since the yields for all dissolved P constituents were calculated using average concentrations, the contribution of storm events on P yields, reflect the water discharge during storm event conditions: 16% of all P constituent of the lowland stream and 29% of all P constituents of the Miombo stream were exported during storm events. Storm events were responsible for 30% of the total PIP and TPP export in the lowland stream and for 65% of the total PIP and TPP export in the Miombo stream (Fig. 3.3), even though those predictions might be conservative due to missing TPP and PIP concentration measurements during storm events.

3.4. Discussion

3.4.1. Nitrogen export is dominated by dissolved and particulate organic nitrogen

Across the tropics, reported PN yields (n = 8) are generally less or equal to the PN yields we found for the lowland forest of the Congo Basin. Only for a lowland forest in Costa Rica were reported PN yields significantly larger than those from our lowland site (Taylor et al., 2015); however, with uplift rates from 1.7 up to 8.5 mm yr^{-1} (Weintraub et al., 2015), this lowland forest in the Osa Peninsula is far more geomorphic active than a typical lowland forest sites within the Congo Basin. DON yields from all studies fell within a similar range and varied between 1.21 (lowland forest in Brazil, Lewis et al. (1995)) and 4 kg ha^{-1} yr^{-1} (Montane forest in Venezuela,

Lewis (1986)). Both sites within the Congo Basin lay well within all these reported values (Table 3.1).

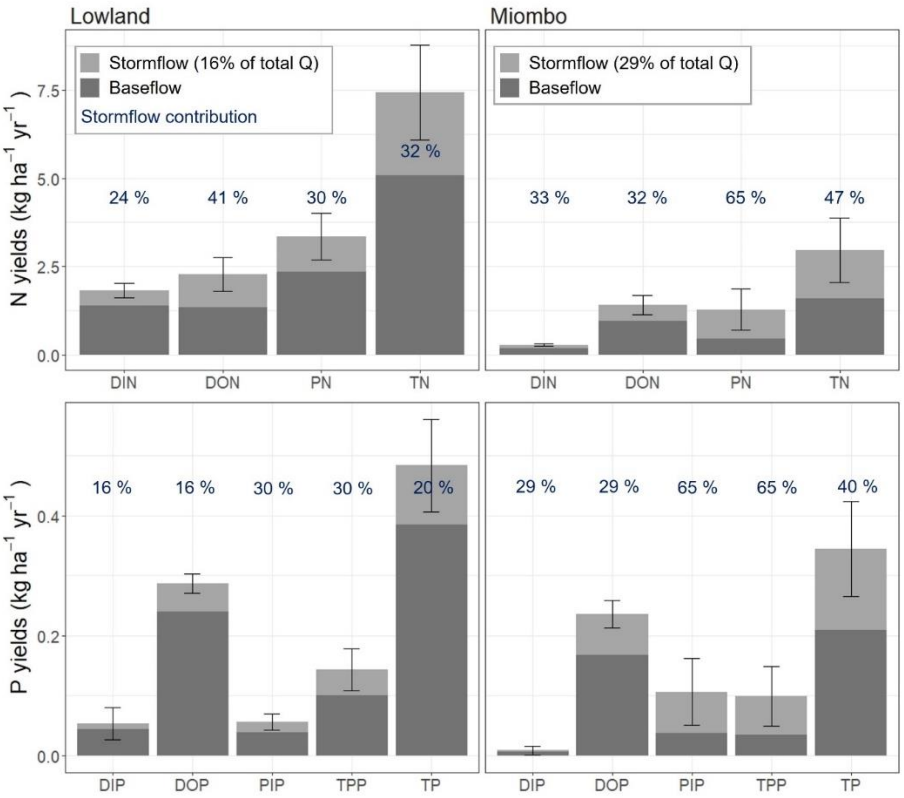

Fig. 3.3 Top: Yields of dissolved inorganic N (DIN), dissolved organic N (DON), particulate N (PN) and total N (TN) during storm- and baseflow conditions at the lowland and Miombo site. Bottom: Yields of phosphate (DIP), dissolved organic P (DOP), particulate inorganic P (PIP), total particulate P (TPP) and total P (TP) during storm- and baseflow conditions at the lowland and Miombo site. Error bars indicating the standard error of the calculated yields. Percentages indicate the share of constituent export during stormflow conditions.

Lowland

Within the DIN losses of the lowland forest, around 70 % is exported as NO_3^- and only 30 % as NH_4^+. Higher losses as NO_3^- are expected, as NH_4^+ is more immobile and usually quickly nitrified to NO_3^- (Fig. 3.2) whereas NO_3^- is more soluble and thus more mobile in soil solution, which makes it prone to leaching (Brookshire et al., 2012). NO_3^- concentrations were stable throughout the year, indicating no shifts in microbial activity (such as nitrification and denitrification) and plant uptake in upslope soils. An increase in NO_3^- concentration was only visible during elevated discharge events (Fig 3.2 & Appendix B2), which has been attributed to increase of water flow in more organic rich soil layers leading to a leaching of soluble N and thus a subsequent increase of lateral NO_3^- transport, a process that is independent of any biological control (Bruijnzeel, 1991; Saunders et al., 2006). In general, dissolved N_2O concentrations are too low to have an impact on TN yields (2.59×10^{-3} kg N_2O-N ha^{-1} yr^{-1}). Nevertheless, N_2O concentrations were lowest between the two wet seasons in July but increased with increasing rainfall in October (Fig. 3.2), which and can be attributed to an increased N_2O production when soil moisture is higher (Davidson, 1993). However, low riverine N_2O concentrations are linked to the low soil N_2O outgassing observed in the same forest, potentially caused by complete denitrification of N_2O to N_2 (Gallarotti et al., 2021).

Our results from the lowland forest in the Congo Basin are the first to corroborate the importance of PN export in apparently low erosive systems and we can show that even for old stable landscapes, sediment export from pristine forests is an important factor for nutrient budgets and biogeochemical cycles. The long-standing paradigm of N-rich lowland tropical forest was mainly justified by high DIN losses from these ecosystems compared to DON losses (Hedin et al., 2003 & 2009; Lewis et al., 1999; Neill et al., 2001; Brookshire et al., 2012). However, more recent observations found exact the opposite pattern: organic losses dominate over inorganic forms in N-rich ecosystems (Bauters et al., 2019; Taylor et al., 2015). We found the same trend during our year-long monitoring of the lowland forest in the central Congo Basin: only 24% of the total N was yielded as DIN, whereas organic forms (including PN) were responsible for 76% the TN export. Our findings show that even in N rich systems, inorganic N forms are cycled tightly, which was already shown in the same lowland forest using a N budgeting approach (Bauters et al., 2019).

Miombo

Dissolved N in the Miombo were dominated by DON, while DIN concentrations were low throughout the wet season, even during storm events. Like the lowland forest, also the Miombo forest showed low aquatic N_2O yields with no influence on TN export (0.98×10^{-3} kg N_2O-N ha^{-1} yr^{-1}). DON concentrations were stable throughout the wet season, with two samples exceeding the usual range of concentrations (0.2 – 0.9 mg l^{-1}) by a factor of 4 (Fig. 3.2). On closer examination, it is obvious that these two samples were collected just hours after the peak discharge of two different storm events. The time lag between the discharge and concentration peak indicates that DON rich waters, sourced from upper soil layers, probably take other flow paths

(with slower response times) than bulk water. Similar to the lowland site, organic forms (i.e., DON and PN) at the Miombo site dominate the N export (Fig. 3.3), however the overall DON and PN yields are lower than from the lowland forest. Although similar total sediment exports from both sites were reported (Lowland: 0.25 t ha^{-1} yr^{-1}; Miombo: 0.24 t ha^{-1} yr^{-1}; Chapter 2), the PN export at the Miombo site was 60% lower compared to the lowland site. This reflects to a general lower N content within the suspended sediments (0.5% vs. 1.3%, respectively), mirroring the overall lower general productivity found in the Miombo, given by the lower density of vegetation and lower overall N inputs (see section 3.4.4).

3.4.2. Dissolved organic phosphorus as the major loss vector, followed by particulate phosphorus

Studies that cover dissolved and particulate forms of organic P export from tropical forest ecosystems are even more scarce than studies covering organic N export (Table 3.1). Reported TPP values range from 0.004 kg ha^{-1} yr^{-1} in a dry forest of Mexico (Campo et al., 2001) up to 0.23 kg ha^{-1} yr^{-1} in a montane forest of Venezuela (Lewis, 1986). All reported values for TPP are within the same order of magnitude as the two measured sites of this study except the dry forest site in Mexico, which is an order of magnitude lower than the Miombo woodland.

Lowland

Roughly 36% of the total P yield of the lowland forest is attributed to particulate P (Fig. 3.3). More than two thirds of this TPP are particulate organic P (POP), whereas only one third is PIP. While PIP concentrations were quite stable during the year (Fig. 3.2) and only showed a marginal increase with increasing water discharge (Appendix B1), POP, and thus TPP, increased more strongly at high flowing conditions. This is an indication that PIP is predominantly exported with baseflow while event-flow adds mainly POP to the suspended sediment fraction.

Table 3.1 Literature values of particulate and dissolved nitrogen and phosphorus yields from tropical forested watersheds

		Yields [kg ha^{-1} yr^{-1}]			
Country	**Forest type**	**PN**	**DON**	**DIN**	**References**
Costa Rica	Lowland	14.6	1.37	0.32	Taylor et al. (2015)
Brasil	Lowland	0.7	2.87	0.2	Lesack (1993)
Brasil	Lowland	0.02 - 2.44	1.21 - 2.48	0.67 - 2.04	Lewis et al. (1995)
Brasil	Montane	2.03 - 3.9	1.3	1.3 - 2.4	Lewis et al. (1995)
Venezuela	Montane	0.75	2.35	2.07	Lewis et al. (1989)
Venezuela	Montane	3.64	4	2.38	Lewis et al. (1986)
Puerto Rico	Montane	1.26	3.78	2.32	McDowell & Asbury (1994)
Kenya	Montane	4			Kroese et al. (2021)
DRC	***Lowland***	***3.25***	***2.28***	***1.82***	***this study***
DRC	***Miombo***	***1.28***	***1.41***	***0.28***	***this study***
Country	**Forest type**	**TPP**	**DOP**	**DIP**	**References**
Malaysia	Lowland	0.05			Malmer (1996)
Malaysia	Lowland	0.1			Malmer (1996)
Venezuela	Montane	0.23	0.177	0.06	Lewis (1986)
Mexico	dry forest	0.004		0.06	Campo et al. (2001)
Puerto Rico	Montane	0.12			Pett-Ridge (2009)
DRC	***Lowland***	***0.16***	***0.29***	***0.05***	***this study***
DRC	***Miombo***	***0.08***	***0.24***	***0.01***	***this study***

DOP is the most important fraction of TP exported from the lowland forest site. Unlike DON, DOP showed no significant correlation with water discharge (Appendix B2). Since a decoupling of these dissolved organic nutrient pools is highly unlikely, this might be an artifact of analytical sensitivity, as DOP concentrations were generally low and close to the detection limit of the measurement.

The DIP concentrations were below the detection limit of 0.01 mg l^{-1} throughout the year, except for six samples at the end of the year 2019, and were not correlated with water discharge, resulting in not detectable concentrations even during storm events (Fig. 3.2 & Appendix B2). The observed concentrations near the detection limit of our method results in high uncertainty of the total DIP export. Low DIP concentrations are expected in old weathered tropical forest soils, due to the low mobility of PO_4^{3-} ions and their fixation by oxides (Sollins et al., 1988).

Miombo

In contrast to the lowland forest, all TPP exported from the Miombo woodland was PIP (Fig. 3.3). PIP concentrations were slightly higher than TPP concentrations for four sampling points (Fig. 3.2), likely because TPP and PIP extractions were done from different filters of the same water sample. Nevertheless, the almost 1:1 correlation between TPP and PIP confirmed that the extraction methods worked well and that mainly PIP is present in TPP (Fig. 3.2). PIP can be in the form of P containing minerals or inorganic P bound to secondary minerals. However, in old-weathered soils of the tropics P inputs from parent material weathering is negligible (Reed et al., 2011) and mobilization of particulate P only occurs through surface runoff (Slomp, 2012). Thus, it is likely that mainly mineral particles and not organic particles were removed from surface soils during rainfall events because export was dominated by PIP. Moreover, in contrast to the highly weathered Ferralsols in the lowland forest, the Acrisols of the Miombo do not show a well-developed organic horizon, leaving the mineral associated P more susceptible to erosion. Soil organic matter accumulation in Miombo woodlands is hindered by seasonal fires and the volatilization of N and P compounds (Campbell, 1996).

DOP was the most important P loss vector in the Miombo woodland (Fig. 3.3), while DIP concentrations were generally low and often below detection limit, hindering a robust quantification of DIP exports (Fig. 3.2). In contrast to DIP losses, DOP losses do not reflect the P status of an ecosystem and can be high even in a P-limited system (Hedin et al., 2003). We observed a generally lower P export compared to the lowland forest. However, the TN losses were even more reduced in the Miombo, resulting in a lower N:P ratio of total nutrient losses from the Miombo (8.5) than from the lowland forest (15.5), which may indicate that the Miombo is relatively more limited in N than in P, compared to the lowland forest (see Chapter 3.4.4).

3.4.3. Storm events disproportionally affect N and P losses

Yields of all N and P constituents at both sites are mostly driven by intense storm event conditions (Fig. 3.3), although these storm conditions only take up a very short time during the whole hydrological year. The influence of short but intense storm

events on sediment and on particulate organic matter (POM) exports of tropical montane forests has been shown (Clark et al., 2013; Lloret et al., 2013; Townsend-Small et al., 2008). Furthermore, also dissolved organic C (DOC) has been reported to be driven by a few storm events in temperate forests (Raymond & Saiers, 2010). The influence of storm events on PN export has been reported for temperate forests (Correll et al., 1999) and in geomorphic active sites of the tropics (Hoover & MacKenzie, 2009; Taylor et al., 2015). However, the influence of storm events on dissolved and particulate forms of N and P in more geomorphic stable regions of the tropics are lacking. In this study we were showed that lowland forest storm conditions of short duration (4.7% of the time) are responsible for 41% of annual DON and 30% of annual PN export (Fig. 3.3). In the Miombo this trend is even more pronounced with events exporting 65% of PN during 6.5% of the time. The same trends are to some extend visible for P exports, although there TPP and PIP are more driven by storm events compared to DOP (Fig. 3.3). However, it is important to state, that TPP and PIP exports were calculated without any storm event samples and are only based on the measured TSS exports, leading to a high uncertainty in those values. The high proportional export of organic constituents also corroborates the idea that there is limited biological control on organic losses and these forms of N and P are mainly transport limited. Thus, particulate, and organic forms of N and P are highly controlled by the hydrological regime, this very much highlights the susceptibility of these systems to possible changes in rainfall patterns. Predictions of future precipitation patterns in central Africa show an increase of heavy rainfalls under all climate scenarios (Haensler et al., 2013), meaning that intensities of single rainfall events are increasing and that the stormflow conditions become even more dominating compared to baseflow conditions. All nutrient forms that are mainly transport limited will tend to follow hydrological regimes and increased aquatic exports of these nutrients are expected with increasing rainfall intensities, possibly increasing the importance of aquatic organic N and P exports under changing climate.

3.4.4. Impact on nutrient budgets

Nitrogen budget

The majority of N inputs and outputs of the same lowland forest in the DRC have been quantified thoroughly by Bauters et al. (2019) and is now complemented by a full quantification of aquatic losses by this study. Bauters et al., 2019 observed high N deposition rates in the lowland forest (18.2 – 53.1 kg ha^{-1} yr^{-1},Table 3.1) which was attributed to fire derived and mainly organic forms of N originating from savanna fires (Bauters et al., 2018). Uncertainty in this value is derived from the difficult distinction between dry deposition and canopy leaching. If we include the complete aquatic N exports from this study, N_2O outgassing of 1.38 kg $N\text{-}N_2O$ ha^{-1} yr^{-1} (Barthel et al., 2022), N_2 outgassing estimated at 7.1 kg ha^{-1} yr^{-1} (Gallarotti et al., 2021) and NO emissions of 7.6 kg N ha^{-1} yr^{-1} (Holtgrieve et al., 2006; Koehler et al., 2009), the high imbalance towards N input is still prominent (-5.2 – 29.7 kg N ha^{-1} yr^{-1}, Table 3.2). While we conclude that PN, although neglected regularly in ecological and biogeochemical research, is an important N loss vector and indeed the highest loss

term in aquatic N losses, it cannot close the N budget of the lowland forest within the Congo Basin. The amount of N received as wet and dry deposition is immensely high, especially considering the remoteness of this site and probably leads to an accumulation of N in this forest.

Although there are no studies available that cover biogeochemical research within the same Miombo ecosystem, reported atmospheric deposition (Bobbink et al., 2010) and N_2-fixation rates (Houlton et al., 2008) from other Miombo forests show that total N inputs into the Miombo likely range from 5 – 11 kg N ha^{-1} yr^{-1} (Table 3.2). Aquatic TN export of 2.97 kg N ha^{-1} yr^{-1} measured in this study together with reported N_2O emissions of 1.6 kg N ha^{-1} yr^{-1} (Rees et al., 2006) are almost counterbalancing the N inputs (Table 3.1), even with N_2 and NO outgassing not been accounted for yet. Furthermore, seasonal fires cause N losses through volatilization and soil N mining is occurring through ongoing agricultural practices and charcoal production (Campbell, 1996; Mayes et al., 2019; P. M. Vitousek et al., 2009). Therefore, the Miombo is potentially more prone to N limitations compared to the lowland forest, which can also be seen in the low DIN losses (Fig. 3.3).

Phosphorus budget

P budgets are less complicated than N as there is no major gaseous form of P. There are only two inputs of P into a forest ecosystem: via weathering of P-containing rocks and through atmospheric deposition. We assume that P inputs through weathering are negligible as these soils are already old and deeply weathered (Reed et al., 2011). High atmospheric P deposition sourced from fires has been found in the lowland forests of the DRC (Bauters et al., 2021). As with N, the observed rates of aquatic P losses are too low to counterbalance high deposition rates (Table 3.2). This indicates that -contrary to widely held assumption - lowland tropical forests of the Congo Basin are likely not P limited.

P deposition for Miombo were obtained from a global modelling study by Wang et al. (2017) and are thus highly uncertain. Even if assuming a conservative P deposition of 0.8 kg ha^{-1} yr^{-1} the aquatic loss term still only accounts for around 40 % of the P input into the Miombo ecosystem (Table 3.2). However, an important landscape-level loss vector within the Miombo ecosystems was not accounted for in this study: seasonal understory fires and resulting loss of dust particles that transport organic forms of N and P from Savanna regions into the central tropics. This is likely a significant loss term, given the observed high N and P deposition within the lowlands which originates from savanna fires (Bauters et al., 2018; Bauters et al., 2021).

Table 3.2 Nitrogen and phosphorus budgets from the lowland forest and Miombo woodland site. All values are in kg ha^{-1} yr^{-1}. References used: 1) Bauters et al. (2019); 2) Bauters et al. (2016); Barthel et al. (2022) ; 4) Gallarotti et al. (2021) ; 5) Holtgrieve et al. (2006); 5) Bobbink et al. (2010) ; 6) Houlton et al. (2008); 7) Rees et al. (2006); 8) Bauters et al. (2021); 9) Wang et al. (2017).

Nitrogen

	Deposition	Fixation	**Inputs**	TDN	PN	N_2O	N_2	NO	**Outputs**	*Imbalance*
Lowland	18.2 - 53.1 [1]	0 [2]	**18.2 - 53.1**	4.1	3.3	1.43	7.1 [4]	7.6 [5]	**23.5**	*-5.3 – 29.6*
Miombo	3.0 - 5.0 [5]	2.0 - 6.0 [6]	**5.0 -11.0**	1.7	1.3	1.2 [7]	*n. a.*	*n. a.*	**4.2**	*0.8 – 6.8*

Phosphorus

	Deposition	**Inputs**	DIP	DOP	TPP	**Outputs**	*Imbalance*
Lowland	3.1 [8]	**3.1**	0.05	0.29	0.16	**0.5**	*2.6*
Miombo	0.8 - 1.6 [9]	**0.8 - 1.6**	0.01	0.24	0.08	**0.33**	*0.47 - 1.27*

3.5. Conclusion

Our study highlights the importance to include aquatic losses of organic and particulate N and P constituents in biogeochemical research of tropical forest ecosystems. Even in stable landforms, such as the lowland forest and Miombo woodland within the Congo Basin, sediment transport had an important influence on the aquatic losses of N and P. Organic and especially particulate forms of N and P are under limited biological control, compared to inorganic forms, and thus those exports follow more the hydrological regime. Therefore, short but intense storm events are driving significant parts of TN and TP exports in both of our study sites. This is especially important in light of the predicted increase in rainfall intensity with climate change for the Congo Basin and thus has the potential to strongly impact N and P exports and impact nutrient cycling in those ecosystems. Moreover, although some systems such as the lowland forest experience high nutrient inputs through atmospheric deposition, inorganic aquatic losses are minimal compared to organic losses, which challenges the current paradigm that nutrient-rich systems encounter high losses of inorganic and bio-available nutrients.

Acknowledgements

We thank the villagers of the Yoko village and around the Lupembashi field-site for their support and hospitality during our field-campaigns. Furthermore, we thank Héritier Ololo Fundji, Degra Ngoy, Claudino Sumaili, Merveille Kongolo, and the CSB at UniKis for the assistance and the organization of the fieldtrips. We are also thankful for Katja Van Nieuland and Samuel Bodé for their help with sample analysis. This research has been funded by the Fonds de la Recherche Scientifique – FNRS (project numbers: T.0059.18 and J.0167.19).

Supporting information

Supporting information to this chapter can be found in Appendix B.

Appendix B1: Particulate nutrient concentrations as a function of total suspended sediment (TSS) concentration at the two forest sites. Round dots represent samples during baseflow campaigns and square dots represent samples taken during storm flow conditions. Blue lines indicate linear regressions with its confidence intervals in grey.

Appendix B2: Dissolved nutrient concentrations as a function of discharge at the two forest sites. Round dots indicate the samples from the baseflow sampling campaign and square dots represent samples during storm-event sampling. Blue lines indicate linear regressions with its confidence intervals in grey. Regression fits are only shown when regressions have a p value < 0.05.

Appendix B3: Comparison of measured particulate nutrients concentrations and predicted concentrations with the doubled modelling approach (turbidity -> TSS -> particulate nutrient concentrations). Values indicate the root mean square errors (RMSE). Dashed line represents the 1:1 line.

Appendix B4: Number of samples taken at baseflow and stormflow conditions for each measurement. Middle columns show the mean values ± standard error of the baseflow and stormflow samples. Root mean square error (RMSE) of model predictions for the constituents which were modelled for yield calculations.

Chapter 4: Sediment and nutrient export from a montane Forest catchment in the Congo Basin: an exploratory study

Abstract

Tropical montane forests are believed to experience different biogeochemical cycling of the main nutrients nitrogen (N) and phosphorus (P) compared to tropical lowland forests. Furthermore, soil erosion rates are reported to be higher in steeper catchments. The differences in nutrient availability and cycling and soil erosion should be reflected in the aquatic exports of these nutrients in headwater streams of these forests. To gain a better understanding of the montane aquatic sediment and nutrient export, a headwater stream, draining pristine tropical montane forest, was monitored for 21 months. Estimated total suspended sediment (TSS) yields were highly uncertain, due to the lack of samples during storm events. Estimates ranged between 0.3 – 1.6 t ha^{-1} yr^{-1}, however, turbidity data indicated the real TSS yields to be more likely at the higher end. Due to the high uncertainty of TSS yields, the estimates of the particulate N (PN) and total particulate P (TPP) showed high variability as well (PN ranged from 1.9 – 12.7 kg N ha^{-1} yr^{-1} and TPP ranged from 0.3 – 1.9 kg P ha^{-1} yr^{-1}). The quantification of dissolved N and P exports were more precise since the influence of storm events on these constituents was not as high as for sediments. Like the lowland forest, the montane forest experienced higher dissolved organic N (DON; 8.0 kg N ha^{-1} yr^{-1}) than dissolved inorganic N (DIN; 2.5 kg N ha^{-1} yr^{-1}) and the same trend was found for P, with dissolved organic P (DOP; 0.8 kg P ha^{-1} yr^{-1}) yields being substantially higher than for phosphate (PO_4^{3-}; 0.3 kg P ha^{-1} yr^{-1}). The montane forest had considerably higher total N and total P exports compared to the lowland forest and Miombo woodland even with the most conservative predictions. However, to get to get more precise predictions of the aquatic sediment and nutrient losses and reduce the uncertainty, the representative sampling of storm events is crucial.

4.1. Introduction

Tropical forest soils exhibit large variations in soil age, uplift- and erosion rates, which results in high differences in biogeochemical cycling of carbon (C) and nutrients between those forests (Townsend-Small et al., 2008). Along an altitudinal gradient, tropical forests tend to change in stand composition and structure, and general productivity is decreasing with increasing altitude (Bauters et al., 2017; Tanner et al., 1998). There is a general believe that while lowland tropical forests are rich in nitrogen (N) and poor in rock-derived phosphorus (P), montane forests of the tropics show more limitations in N than in P (Santiago, 2015; Tanner et al., 1998). Old-weathered soils of most tropical lowland forests are mostly poor in rock-derived P due to long lasting leaching losses and the immobilization of available P in those soils (Hedin et al., 2009). On the other hand, soils of montane forests are generally lot younger and less weathered compared to the lowland soils, because they are situated in sites that are geomorphic more active, with higher uplift rates and steeper slopes. Thus, these forests are prone to higher soil erosion rates and the

steady soil loss increases the rejuvenation of soils, which influences the input of rock derived nutrients (Fisher et al., 2013). As N accumulates over time, less N availability is expected in those montane forests with younger soils. Furthermore, the slower decomposition and mineralization rates at lower temperatures are limiting N availability as well (Kirschbaum, 1995). These high variabilities in processes that are controlling nutrient cycling and -availability, underline the need for biogeochemical research that are capturing spatial variabilities within the tropics.

Only around 3% of the evergreen tropical forest covering the Congo River Basin (CRB) are montane forests in the Albertine Rift region in the east of the CRB (Verhegghen et al., 2012). This region shows distinct differences from the rest of the evergreen forests: steep topography, high elevation, and high anthropogenic pressure on pristine forests. Furthermore, this region experiences high potential rainfall erosivity (Bagalwa et al., 2021). Due to these fundamental differences between lowland and montane forests, aquatic nutrient exports are most likely different as well. Thus, the goal of this chapter is to quantify aquatic losses of sediments and nutrients (N and P) from a headwater draining pristine tropical montane forest and compare those losses to the findings from the lowland and Miombo forest site (Chapters 2 and 3). The montane monitoring site was equipped with the same setup as the Miombo woodland site, however, technical failures and sabotaging of the monitoring material resulted in a very incomplete dataset. Thus, calculating annual yields of sediment and nutrients is challenging and accompanied with a high uncertainty. Still, the obtained data from the montane site is presented here and uncertainties are discussed.

4.2. Material and Methods

4.2.1. Site description

The montane catchment lies within the Kahuzi-Biéga National Park, northwest of the city of Bukavu in the South Kivu province in the east of the Democratic Republic of the Congo (DRC). The monitoring point is situated on the border to the national park, so that the whole catchment is covered by pristine montane tropical mixed forest, intercepted by patches of monodominant bamboo forest. The headwater catchment area was delineated using digital elevation model (DEM) derived from the 30m-Shuttle Radar Topographic Mission (SRTM) and spans an area of 1276 ha, with elevations ranging from 2100 to 2450 m a.s.l. and experiences an average slope of 23° (Fig. 4.1). The main soil types within the catchment are classified as Ferralsols and Acrisols (Bauters et al., 2019) with a sandy loam texture in the upper soil and silty loam texture in deeper soil layers (Baumgartner et al., 2020). The region experiences two peaks of rainfall throughout the year, one in April and one in October, with a prolonged dry season from June to September in between. Mean annual precipitation is 1970 mm and mean annual temperature is ~15°C.

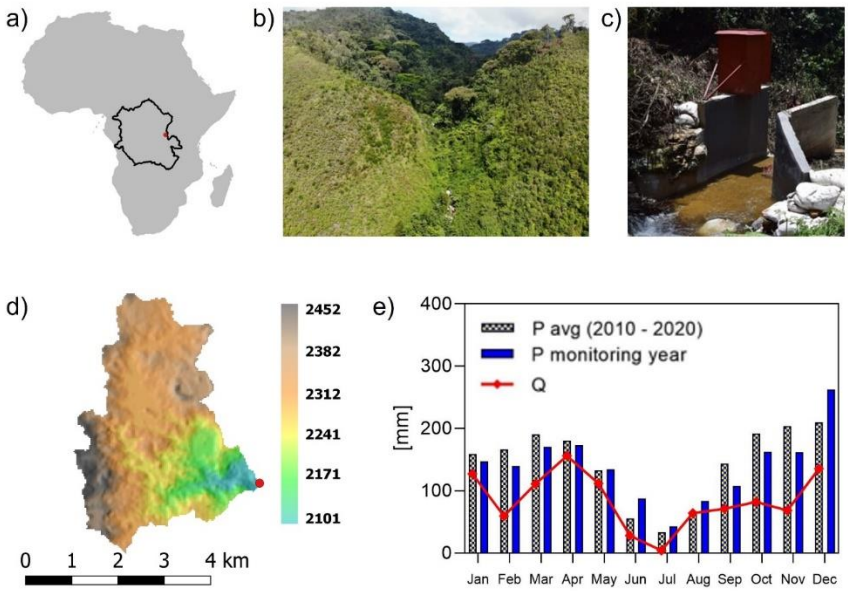

Fig. 4.1 a) Map of Africa with the Congo Basin outlined and the location of the montane forest catchment (red dot). b) drone image over the forest catchment, from outside the national park (image taken by Travis Drake). c) Picture of the flume installed at the montane forest stream. d) Topographical map of the catchment, colors indicate the elevation in meters above sea level (m a.s.l.). DEM source: (DEM, NASA JPL). e) Average monthly precipitation between the years 2010 to 2020 (grey bars), blue bars are the precipitation during the months of discharge monitoring and red line indicates the stream discharge during these monitoring months.

4.2.2. Sampling design

A concrete flume with a fixed width (1.75 m) was built at the monitoring site and at the base of the flume equipped with a pressure transducer (CS451, Campbell Scientific, UK) connected to a datalogger (CR1000, Campbell Scientific, UK), powered by a 12V battery. The pressure transducer measured the water level in 5-min intervals. Biweekly measurements of water discharge (Q) were conducted using a mechanical flowmeter (Model 2030, General Oceanics Inc., USA) to establish a robust water level – Q rating curve. Continuous water level data was obtained starting from 29th of July 2018 until the 27th of April 2020, however, longer periods of data gaps occurred due to battery failure and/or stealing of the datalogger (Fig. 4.2). For two and a half months, starting on the 13th of February 2020, a turbidity sensor (OBS3+, Campbell Scientific, UK) was added to the datalogger and turbidity was measured simultaneously with water level at a 5-min interval. Rainfall data was obtained from GPM satellite precipitation data, downloaded from the NASA web archive (Huffman et al., 2019).

Water samples were taken in a biweekly interval and the sampling and measurement design is described in detail in Chapter 3, section 3.2.2.

4.2.3. Export calculations

Calculate sediment and nutrient yields with an incomplete dataset is challenging and different methods are possible, resulting in a wide range of possible yields. In this chapter, the yields get reported as average values from the different calculation methods, with reported ranges from the lowest to the highest calculated yield.

For TSS yield concentrations, three different calculations were made (T1 – T3): T1) The easiest and most reliable way of calculating TSS yields is by applying a linear correlation of TSS concentrations with measured turbidity values. Since the turbidity values are only available for two and a half months, an extrapolation to annual yields is necessary. T2) a linear relationship between TSS concentrations and water discharge was applied to get TSS values for every 5-min interval of discharge measurement. T3) The average TSS concentration of all manual samples was assumed for a whole hydrological year.

PN, TPP, and PIP yields were also calculated in three different ways: 1 & 2) A linear relationship between TSS and the particulate forms of N and P was obtained to calculate PN, TPP and PIP concentrations for every TSS concentration. Method 1 used the TSS concentration values obtained from T1 (TSS – Turbidity regression), while method 2 used the TSS concentration values obtained from the T2 (TSS – water level regression). 3) For the third method for the average of all measured particulate nutrient concentrations during the monitoring period was assumed (analogue to T3).

Dissolved nutrient yields (DON, DIN, PN, DIP) were calculated with two different approaches: 1) a linear relationship between the dissolved species and water discharge, in terms to calculate dissolved N and P concentrations for every 5-min water discharge value. And 2) assuming average dissolved N and P species from all the manual measurements and applying these values for the whole monitoring period.

All yields for all methods were calculated by multiplying the obtained concentrations with the simultaneous water discharge value, integrating over the 5-min time interval, and divided by the catchment area.

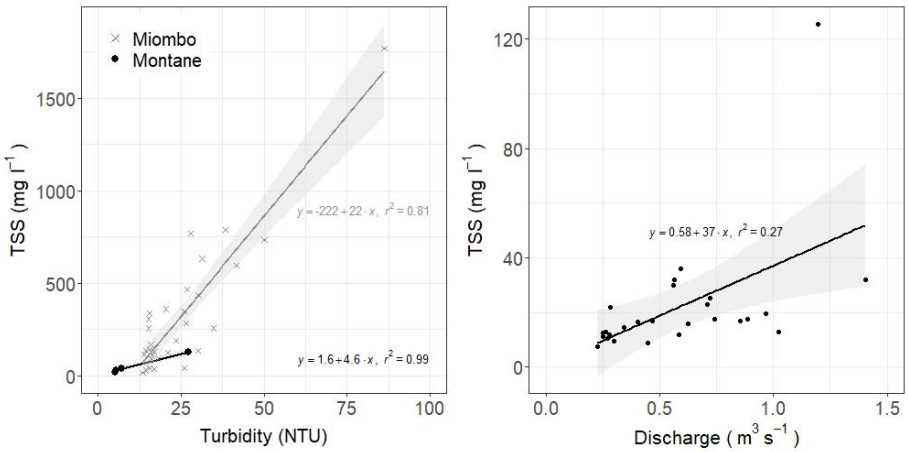

Fig. 4.2 Linear relations between turbidity and total suspended sediments with data from the montane and Miombo site (a) and water discharge and total suspended sediments (b). Black and grey lines indicate the linear regression with its confidence intervals in grey.

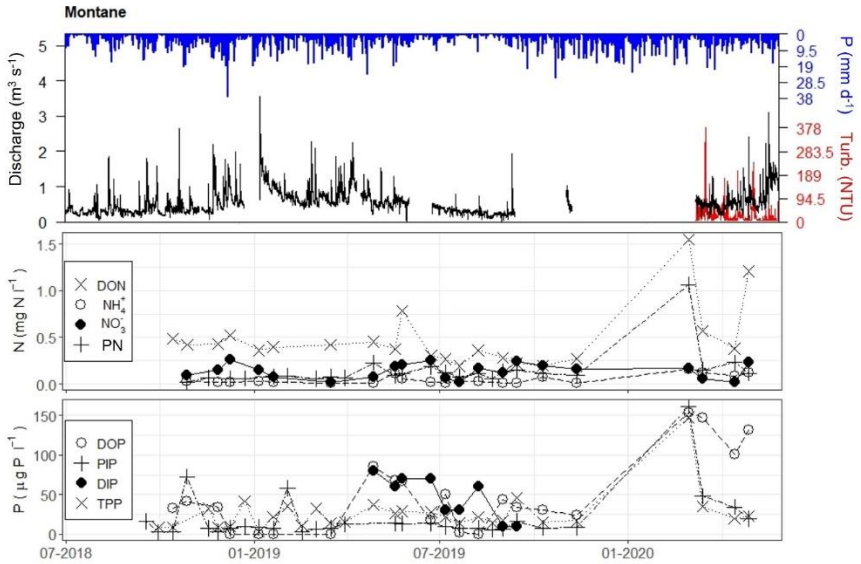

Fig. 4.3 From top panel to bottom panel: Timeseries of water discharge (black line) line and measured turbidity values (red line) and daily precipitation (blue bars); dissolved and particulate N species (dissolved organic nitrogen – DON, ammonia – NH_4^+, nitrate – NO_3^-, particulate N - PN), dissolved and particulate P species (dissolved organic phosphorus -DOP, particulate inorganic phosphorus – PIP, dissolved inorganic phosphorus – DIP, total particulate phosphorus – TPP).

4.3. Results

4.3.1. Hydrology

During the 21 months of monitoring a total of around 14.5 months (69 %) of discharge data is available. During this time, an average annual Q of 1193 mm yr^{-1} was measured while TRMM derived precipitation data showed an annual precipitation of 1671 mm during the same period, resulting in a runoff coefficient of 0.71 and an evapotranspiration of around 478 mm (Fig. 4.3).

4.3.2. TSS and nutrient yields

The montane forest experienced an average calculated TSS yield (average of the three different methods) of 0.8 t ha^{-1} yr^{-1} (Fig. 4.4 a). However, the different methods to calculate TSS yields showed high variation with the highest TSS yield being more than 5 times higher than the lowest obtained TSS yield. The highest TSS yield was calculated by the method T1, the linear regression between TSS and turbidity extrapolated to a whole year, with a value of 1.6 t ha^{-1} yr^{-1}. However, the TSS – turbidity relationship is driven by one TSS concentration at a higher turbidity value (Fig. 4.2). To improve this relationship, data from other studies with the same sensor could be proposed. However, by including the TSS and turbidity values from the Miombo stream of Chapter 3, it is obvious that the data between the two sites cannot be compared (Fig 4.2) and thus the linear model with only the montane data was used. Lowest TSS yields was obtained with the method T3, using average TSS concentration for the whole hydrological year, with 0.3 t ha^{-1} yr^{-1}. Since the methods to calculate PN, TPP and PIP yields rely on the calculated TSS values, the uncertainty of these yields are as big as for the TSS yields. Calculated PN yields range from 1.93 kg N ha^{-1} yr^{-1} (method 3, assuming average PN concentrations) to 12.7 kg N ha^{-1} yr^{-1} (based on the TSS values obtained from the turbidity measurements) with an average PN yield of 5.7 ka N ha^{-1} yr^{-1}. DON yields showed smaller ranges, with higher calculated yield (9.6 kg N ha^{-1} yr^{-1}, method 1: correlation DON - Q) being 1.5 times higher compared to the lower calculated yield (6.3 kg N ha^{-1} yr^{-1}, method 2: average DON concentrations) resulting in an average DON yield of 8.0 kg N ha^{-1} yr^{-1} (Fig. 5.4 b). Calculated DIN yields showed even lower variabilities, with higher yield (2.7 kg N ha^{-1} yr^{-1}, method 1) only being 9% higher than the lower yield (2.4 kg N ha^{-1} yr^{-1}, method 2).

PIP and TPP showed similar calculated yields (avg. PIP: 0.9 kg P ha^{-1} yr^{-1}; avg. TPP: 0.9 kg P ha^{-1} yr^{-1}) and uncertainties (Fig. 4.4 b). Highest PIP yield (method 1; 1.9 kg P ha^{-1} yr^{-1}) is 7.2 times higher as the lowest PIP yield (method 3; 0.3 kg P ha^{-1} yr^{-1}), while the highest TPP yield (method 1; 1.9 kg P ha^{-1} yr^{-1}) is 5.5 times higher than the lowest TPP yield (method 3; 0.3 kg P ha^{-1} yr^{-1}). Average calculated DOP yield is similar to the particulate P yields (0.8 kg P ha^{-1} yr^{-1}), with lower yield calculated by method 2 (0.6 kg P ha^{-1} yr^{-1}) and higher yield calculated by method 1 (1.0 kg P ha^{-1} yr^{-1}). Average DIP yield was the lowest P yield with 0.3 kg P ha^{-1} yr^{-1}, with both methods reporting same yields (Table 4.1).

4.4. Discussion

The montane forest catchment showed with an average TSS yield of 0.8 t ha^{-1} yr^{-1} similar yields as other tropical montane forest catchments (Chapter 2, Table 2.1) and would be up to 3 times higher than yields from the lowland forest and Miombo woodland catchment. With the highest possible export of 1.6 t ha^{-1} yr^{-1} the montane site would experience the second highest TSS yield reported from a tropical montane forest catchment, after a site in Malaysia, which still reported TSS yields twice as high (Clarke & Walsh, 2006). Assuming lowest possible TSS yield of 0.3 t ha^{-1} yr^{-1} is only marginally larger than yields from the lowland forest and Miombo woodland site.

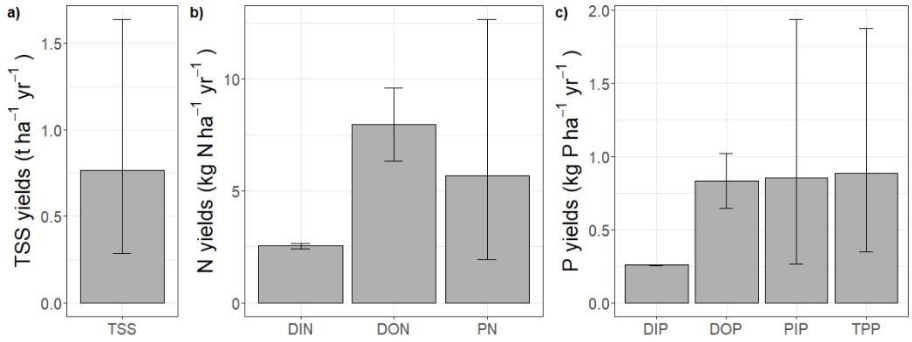

Fig. 4.4 Average yields over all methods described in section 4.2.3. Error bars show the lowest and highest yields calculated for each constituent. a) average calculated total suspended sediment (TSS) of the montane forest catchment. b) average yields of dissolved inorganic N (DIN) dissolved organic N (DON) and particulate N (PN). c) average yields of dissolved inorganic phosphorus (DIP), dissolved organic P (DOP), particulate inorganic P (PIP) and total particulate P (TPP).

Table 4.1 Calculated yields in kg ha^{-1} yr^{-1} (* t ha^{-1} yr^{-1} for TSS yields) for the montane, lowland and Miombo forest. For the montane forest, average values and lower- and upper limits of the different yield calculation methods are reported.

	Montane				
	average	lower	upper	**Lowland**	**Miombo**
TSS*	**0.8**	0.3	1.6	**0.3**	**0.2**
TN	**16.2**	10.7	24.9	**7.4**	**3.0**
PN	**5.7**	1.9	12.7	**3.3**	**1.3**
DON	**8.0**	6.3	9.6	**2.3**	**1.4**
DIN	**2.5**	2.4	2.7	**1.8**	**0.3**
TP	**2.0**	1.2	3.2	**0.5**	**0.3**
TPP	**0.9**	0.3	1.9	**0.2**	**0.1**
PIP	**0.9**	0.3	1.9	**0.1**	**0.1**
DOP	**0.8**	0.6	1.0	**0.3**	**0.2**
DIP	**0.3**	0.3	0.3	**0.1**	**0.0**

However, higher sediment export is expected in the montane catchment, due to a steeper catchment and higher rainfall erosivity (Bagalwa et al., 2021) compared to the rather flat catchments of the lowlands. This high erosivity in the region indicates that calculating TSS yields by assuming average TSS concentration from all the baseflow samples, is not a reliable way to estimate sediment exports. Another indication is that baseflow TSS concentrations are not representative for high flow conditions, as indicated by high turbidity values during storm flow (Fig. 4.3). Given the available turbidity data, the calculated average of TSS yield is probably underestimating the true TSS export and real yields are likely to be at the higher end of our error margin.

The high uncertainty in the TSS yields is reflected in the PN yields as well. The range of prediction is large and highest PN yield predictions are more than five times higher than lowest predictions (Table 4.1). Assuming lower end TSS yields are underestimating sediment export, also lower end PN yield are most likely underestimating the PN export. PN yields of 12.7 kg N ha^{-1} yr^{-1} (upper end of predictions; Table 4.1) are not unusual and similar PN exports have been reported from tropical forests of Costa Rica (14.6 kg N ha^{-1} yr^{-1}; Taylor et al., 2015). Yields of dissolved N species, were quantified quite reliably, due to the similar results using different calculation methods (Table 4.1). They were higher compared to the two other major forest types of the Congo Basin (Table 4.1). DON losses of the montane forest are high and in the same range as PN losses. Dissolved inorganic N yields which were studied previously at the same montane forest in a different catchment were

about double compared to this new study (5.2 kg N ha $^{-1}$ yr^{-1}; Bauters et al., 2019), In contrast, their DON loss estimates were much lower than what was measured in this new study (2 vs. 8.0 kg N ha $^{-1}$ yr^{-1}). Even with the most conservative TN yield prediction, the montane site showed higher TN export (10.7 kg N ha^{-1} yr^{-1}) compared to the lowland (7.4 kg N ha $^{-1}$ yr^{-1}) and Miombo (3.0 kg N ha^{-1} yr^{-1}). With the average TN prediction (16.2 kg N ha $^{-1}$ yr^{-1}) the montane site showed more than double the TN export than the lowland forest, and with the highest prediction (24.9 kg N ha $^{-1}$ yr^{-1}) it is even more than three times higher (Table 4.1). Like for lowland and Miombo forests, TN export of the montane forest was driven by the high organic and particulate losses. Overall, our findings stand in stark contrast to the paradigm of montane forests being limited in nitrogen, since they show higher N losses compared to the supposedly N rich lowland forest.

For P exports the same trend as for N export is visible (Fig. 4.4 & Table 4.1): particulate forms show higher uncertainty between lower and upper end of yield predictions, while for the dissolved forms the predictions seemed to produce more reliable results. Even if we assume the most conservative values of P yields, the montane forest still exported more P in all different forms compared to the lowland and Miombo forest (Table 4.1). This is especially striking for the DIP export, where the montane site exported more than five times more than the lowland forest. While the lowland forest exported 75% of TP compared to the montane forest, the Miombo only exported 16% (Table 4.1). While the lowland forest mainly exported P in organic forms, the montane forest is predominantly exporting P in inorganic forms (DIP and PIP). This is an indicator for the general higher P availability in the montane forest due to younger soils (Reed et al., 2011).

The high uncertainty that came along with the nutrient yield calculations mainly come from the fact that storm event samples of these nutrients were missing. Although the discharge monitoring got interrupted several times due to technical failures and theft of monitoring material (Fig. 4.3), almost a full hydrological year of uninterrupted discharge data was available. Unfortunately, reliable turbidity data was only available for two and a half months. Furthermore, the turbidity data is only useful if a robust correlation with TSS concentrations are possible. In this case, only one sample at turbidity value of 27 NTU was available, and that value was driving the linear relation of the TSS – turbidity prediction (Fig. 4.2). During the two and a half months of turbidity monitoring, values rose up to 280 NTU, which was 10 times higher than the highest sample available for the relationship in Fig. 4.2, highlighting how uncertain the TSS prediction with the turbidity values was. The same is true for the nutrient yields, reliable annual exports of nutrients are not possible with only nutrient concentrations of baseflow conditions. As it was shown in Chapters 2 and 3 of this thesis, storm events are driving sediment and nutrient exports, especially the organic forms. Thus, it is not astonishing that the highest uncertainties in the yield predictions are from particulate and dissolved organic forms of N and P (Table 4.1).

Conclusion and Outlook

Besides the high uncertainty of nutrient yield calculations, the montane forest experienced high fluvial N and P exports, mainly driven by substantial losses of organic and particulate forms of N and P. The availability of only baseflow concentration data was responsible for the lack of confidence of the yield predictions. To gain more reliable numbers on aquatic nutrient exports of this forest catchment, sampling of storm events is crucial. The remoteness of the site and security concerns are a big challenge to set up a storm event sampling system, however, already a few samples during peak storm flow would increase the predictability of nutrient exports enormously.

Part IV - Effect of erosion on soil N

Chapter 5: Stable isotope signatures of soil nitrogen on an environmental-geomorphic gradient within the Congo Basin

This chapter was originally published as: Baumgartner, S., Bauters, M., Barthel, M., Drake, T. W., Ntaboba, L. C., Bazirake, B. M., Six, J., Boeckx, P., Van Oost, K.: Stable isotope signatures of soil nitrogen on an environmental-geomorphic gradient within the Congo Basin. *SOIL*, 7, 83-94, 2021.

Abstract

Nitrogen (N) availability can be highly variable in tropical forests on regional and local scales. While environmental gradients influence N cycling on a regional scale, topography is known to affect N availability on a local scale. We compared natural abundance of ^{15}N isotopes of soil profiles in tropical lowland forest, tropical montane forest, and subtropical Miombo woodland within the Congo Basin as a proxy to assess ecosystem-level differences in N cycling. Soil $\delta^{15}N$ profiles indicated that N cycling in the montane forest is relatively more closed and dominated by organic N turnover, whereas the lowland forest and Miombo woodland experienced a more open N cycle dominated by inorganic N. Furthermore, we examined the effect of slope gradient on soil $\delta^{15}N$ within forest types to quantify local differences induced by topography. Our results show that slope gradient only affects the soil $\delta^{15}N$ in the Miombo forest, which is prone to erosion due to a lower vegetation cover and intense rainfall at the onset of the wet season. Lowland forest, on the other hand, with a flat topography and protective vegetation cover, showed no influence of topography on soil $\delta^{15}N$ in our study site. Despite the steep topography, slope angles do not affect soil $\delta^{15}N$ in the montane forest, although stable isotope signatures exhibited higher variability within this ecosystem. A pan-tropical analysis of soil $\delta^{15}N$ values (i.e. from our study and literature) reveals that soil $\delta^{15}N$ in tropical forests is best explained by factors controlling erosion, namely mean annual precipitation, leaf area index, and slope gradient. Erosive forces vary immensely between different tropical forest ecosystems and our results highlight the need of more spatial coverage of N-cycling studies in tropical forests, to further elucidate the local impact of topography on N cycling in this biome.

5.1. Introduction

The nutrient status of forests is an important determinant for the allocation of sequestered carbon (C) to biomass (Vicca et al., 2012), with nitrogen (N) and/or phosphorus (P) limitation potentially constraining net primary productivity (NPP) (Alvarez-Clare et al., 2013; Fernández-Martínez et al., 2014; Townsend et al., 2011; Vitousek et al., 2010). In addition, models show that the increase of primary production due to CO_2 fertilization will be constrained by nutrient limitations (Wieder et al., 2015). Therefore, understanding nutrient cycling in forests globally is key to assess present and future forest productivity (Townsend et al., 2011; Wieder et al., 2011). Given their major role in the global C cycle (Lewis, 2006; Malhi & Grace,

2000), quantifying nutrient supply and availability is especially important for tropical forests.

To date, research has revealed a high diversity of nutrient cycles with substantial variation from regional to local scales throughout the tropics. Old and highly weathered soils in tropical lowland forests are typically considered to be rich in N and poor in rock-derived P (e.g. Vitousek, 1984). In contrast, tropical montane forests that lie on steep terrain are subjected to geomorphic processes that rejuvenate soils with bedrock nutrients through uplift and erosion. In regions with a moderate uplift, P depletion is unlikely to occur due to this rejuvenation (Porder et al., 2007). As a result of reduced N supply in higher altitudes, due to slower N mineralization processes at lower temperatures, it is more likely that plant growth is limited by N availability in tropical montane forests (Bauters et al., 2017; Soethe et al., 2008; Tanner et al., 1998). Thus, it is important that nutrient availability in tropical forests is not generalized across these different ecosystems. Therefore, analyses of N cycling within ecological gradients are necessary. The "openness of the N cycle" is a good metric to describe cycling differences across ecosystems with contrasting N availabilities. While in N limited ecosystems (i.e. closed N cycle) the internal cycling and recycling rates of N are relatively more important than the absolute in- and outputs (inputs: N_2-fixation and N deposition; outputs: gaseous and leaching losses), the opposite is true for ecosystems that are rich in N (i.e. open N cycle) (Boeckx et al., 2005).

Furthermore, at a local scale, topography has been identified as a main determinant for both biogeochemical and ecological variability in tropical forests (Asner et al., 2015; Hofhansl et al., 2020) in part through its effect on geomorphic processes. In an intact forest, slope gradient is the main control on physical erosion intensity at the hillslope scale (Roering et al., 2001). Accumulated topsoil N has shown to be affected by physical erosion (Amundson et al., 2003; Hilton et al., 2013; Perakis et al., 2015; Weintraub et al., 2015), resulting in a close relation between nutrient availability and geomorphic process rates. Therefore, while at regional scales mainly climatic and environmental gradients are responsible for differences in nutrient availabilities (Prescott, 2002; Read, 1991), hydro-geomorphic gradients seem to be a main determinant of N cycling at the local scale (Amundson et al., 2003). Some studies from geomorphic active regions of the tropics (e.g. Taiwan and Costa Rica) found lower N availability in steeper sloping positions suggesting that erosion substantially affects local N balances (Hilton et al., 2013; Weintraub et al., 2015). However, the magnitude of this effect in more stable landscapes is unknown and calls for a consistent study across geomorphic gradients in the tropics.

The natural abundance of the stable ^{15}N isotopes ($\delta^{15}N$) of plant and soil pools is a useful proxy to assess N cycling (Amundson et al., 2003; Martinelli et al., 1999). Craine et al. (2015a) synthesized global soil $\delta^{15}N$ data to understand patterns of N cycling and showed how soil $\delta^{15}N$ values give insight into input and output pathways of N in the system (Högberg, 1990; Högberg & Johannisson, 1993). The isotopic composition of soil N is influenced by a multitude of processes and therefore interpretation of soil $\delta^{15}N$ values is challenging. The main processes controlling soil

$\delta^{15}N$ values are nitrification, denitrification N mineralization, N_2-fixation, and N leaching. Nitrification has a large isotope fractionation effect, with fractionation factors ranging from 15 to 35 ‰ (Blackmer & Bremner, 1977; Högberg, 1997). On the other hand, fractionation during denitrification is variable with fractionation factors reported ranging from 0 to 33 ‰ (Högberg 1997). Nitrification and denitrification result in a gradual enrichment of soil $\delta^{15}N$. The process of N mineralization is believed to fractionate only marginally, however, in a system with high N mineralization rates, isotopic fractionation due to mineralization can be important (Nadelhoffer and Fry 1994). N_2-fixation depletes soil $\delta^{15}N$ values, as it imports atmospheric N that has an isotopic value of 0 ‰ by default (Högberg, 1997). Aside from these processes, site- and soil-specific characteristics can control soil $\delta^{15}N$. In addition, climatic conditions such as rainfall (Austin & Vitousek, 1998; Boeckx et al., 2005), mean annual temperature (Boeckx et al., 2005) and soil moisture (Handley et al., 1999) all influence soil $\delta^{15}N$. Generally, soil $\delta^{15}N$ signals the openness of the N cycle, with more enriched values in an open system that is more prone to N losses, compared to an more closed system (with the assumption that input $\delta^{15}N$ are similar in both systems) (Boeckx et al., 2005). On a local scale, soil erosion alters the soil $\delta^{15}N$ and leads to more depleted values (Hilton et al., 2013; Weintraub et al., 2015). Because soil erosion is a non-fractionating process, the combined fractionation of a system decreases when soil erosion becomes more important relative to fractionating N losses, such as denitrification. In this case, the $\delta^{15}N$ of the remaining N in the system more closely resembles the signature of the N inputs compared to systems with less erosion.

The objectives of this study were 1) to assess the differences in N availability and N openness in three different forest types along an environmental-geomorphic gradient in the Congo Basin and 2) evaluate the extent and 3) drivers of physical erosion and its effects on N availability in these forests. To achieve these objectives, soil N content and the stable N isotope compositions were measured in soil profiles taken from different topographical positions in three different forest ecotypes. We used soil $\delta^{15}N$ as a proxy that integrates N transformations for differences in N availability and the openness of a system. We hypothesized that soil $\delta^{15}N$ values are highest in lowland tropical forest, which would be an indication for a higher N availability and openness of N cycle. Furthermore, we hypothesized that $\delta^{15}N$ of topsoil N would be lower on steeper slopes compared to $\delta^{15}N$ of topsoil N on less steep slopes and more enriched compared to deeper soil layers of the same profile, and that this effect would be more pronounced in the montane and Miombo forests, where the erosional forces are higher compared to the lowland forest.

5.2 Methods

5.2.1. Site description

We selected representative sites for the Congo Basin's major forest ecotypes (tropical montane forest, tropical lowland forest, and the semi-dry Miombo woodland). The montane forest site is situated in the Kahuzi-Biéga National Park (2.344° S, 28.746° E), northwest of the city of Bukavu in the eastern part of Democratic Republic of the Congo (DRC). Two forest subtypes are present in the

Park: montane mixed forest and monodominant bamboo forest. Soil samples were taken in the mixed forests. Soils are classified as Ferralsols/Acrisols (Bauters et al., 2019) (Table 5.1) and was formed on basalt rock (Van Engelen et al., 2006). The topography of the sampled forest is characterized by steep slopes (Fig. 5.1). Mean annual temperature is ~15°C and mean annual rainfall is ~1970 mm (Fick & Hijmans, 2017). Rainfall is seasonal with two peaks in April and October and a dry season that lasts from June to September.

Samples from the tropical lowland forest were taken in the Yoko Forest Reserve (0.291° N, 25.295° E), south of the city of Kisangani. The Yoko Forest Reserve consists of two forest subtypes: a mixed lowland tropical forest and a monodominant forest, where the *Gilbertiodendron dewevrei* species comprises more than 60% of the basal area. Soil samples in the lowland forest were taken from random points within the catchment, where both forest types are present. Soils in this area are classified as deeply weathered Ferralsols (Van Ranst et al., 2010) on fluvio-aeolian deposits (Van Engelen et al., 2006). The sampling site exhibited low variation in elevation and contained mainly gentle slopes (Fig. 5.1). Samples were taken between altitudes of 440 – 460 m a.s.l. Mean annual temperature is ~24°C and mean annual rainfall is ~1760 mm (Fick & Hijmans, 2017) (Table 5.1). Yoko experiences a short wet season from March to May and a longer one from August to November.

For the Miombo woodland, a site 50 km north of the city of Lubumbashi was selected (11.212° S, 27.233° E). A pristine Miombo is characterized by deciduous woodland dominated by trees of the *Brachystegia, Julbernardia* and *Isoberlinia* genera (Campbell, 1996). As charcoal production and seasonal fires are a common occurrence, soil sampling in areas with recent charcoal production activities was avoided. We classified the soils as Acrisols and Cambisols and the parent material was identified as shales (Van Engelen et al., 2006). The topography is mostly flat and the elevation ranges between 1260 and 1310 m a.s.l (Fig. 5.1). This region experiences a wet season from October to April, with a peak rainfall in December. Mean annual rainfall is ~1250 mm and mean temperature is ~21°C (Fick & Hijmans, 2017)(Table 5.1).

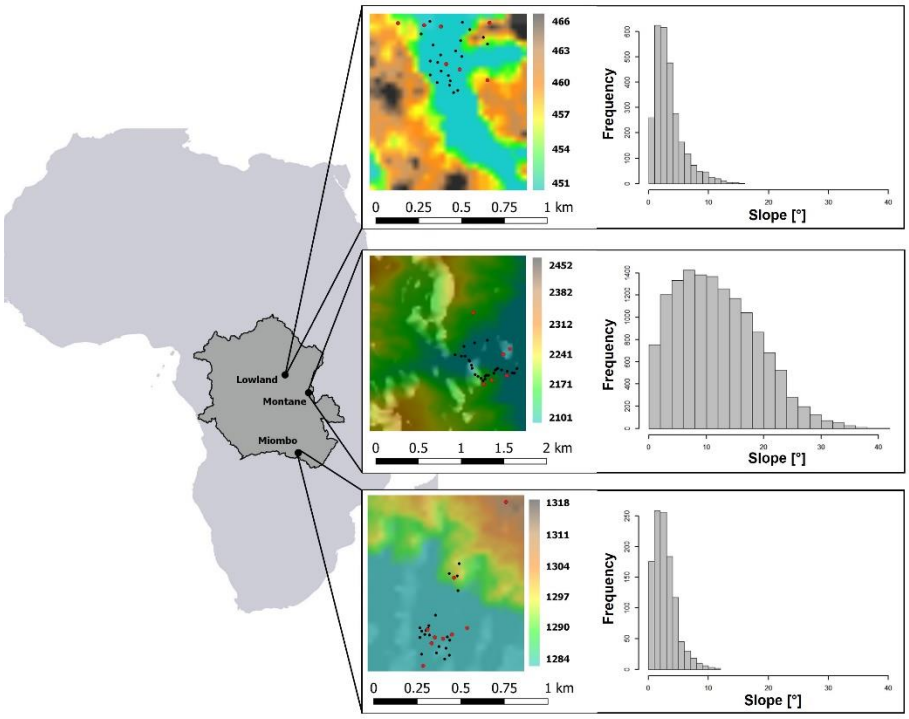

Fig. 5.1 Location of the sampling sites; from left to right: dark grey area indicates the Congo Basin within Africa with forest site locations, red dots indicate locations of 1m soil profiles within each forest site, black dots indicate locations of topsoil sampling positions (0-20 cm). Colors from the 30-m DEMs (source: DEM, NASA JPL) represent elevation (in m above sea level). Histograms on the right show the slope distribution of the respective sampling site.

Table 5.1 Site characteristics of the three forest types. The range of altitudes of the sampled profiles and topsoil samples is shown. The slope indicates the average slope ± standard deviation from all the samples taken at the respective forest site. MAP is the mean annual precipitation and MAT is the mean annual temperature extracted from the WorldClim database (average MAP for the years 2010-2018). EC represents the mean erosion coefficient values calculated from equation 5.2. LSI is the landslide hazard risk for each site extracted from the Global Landslide Hazard Map (Worldbank). LAI is the mean annual leaf area index, extracted from the Copernicus LAI-300m database (European Environment Agency).

Forest Type	Latitude (°)	Longitude (°)	Altitude (m a.s.l.)	Slope (°)	MAP (mm)	MAT (°C)	EC	LSI	Soil type	LAI
Montane	-2.344	28.746	2020 - 2180	22.8 ± 8.0	1970	15	2.79	3.96	Ferralsols/Acrisols	5.42
Lowland	0.291	25.295	440 - 460	4.3 ± 2.3	1760	24	1.22	1	Ferralsols	4.15
Miombo	-11.212	27.233	1260 - 1310	3.9 ± 2.2	1250	21	20.11	1	Acrisols/Cambisols	0.83

5.2.2. Sampling

To analyze differences in soil N cycling between forest sites, soil samples were taken from soil profiles at different slope positions in the catchments (slope, shoulder, and ridge) in order to better represent the catchment as a whole. Nine soil profiles were dug and sampled in both the lowland and Miombo forests. Due to difficult terrain within the montane forest, only six soil profiles were sampled (Fig. 5.1). For each 1 m-profile, soil samples from nine different depths were taken (0-2 cm, 2-4 cm, 4-6 cm, 6-10 cm, 10-15 cm, 15-20 cm, 20-30 cm, 30-50 cm and 50-100cm). To calculate N stocks, bulk density of the soil was determined at five depths of each soil profile using a 100 cm^3 bulk density ring. The bulk density samples were dried at 105°C for 48h and then weighed. To analyze the effect of surface slope angles on stable isotopic signature of soil $\delta^{15}N$, additional topsoil samples (bulk sample from the top 0-20 cm) were taken from throughout the catchments at locations with varying slopes (montane: n=27; lowland: n=24; Miombo: n=21) (Fig. 5.1). Profile- and topsoil sample positions were recorded with a GPS (GPSMAP 60CSx; Garmin; accuracy <5m) and slope angles were estimated using 30-m SRTM derived digital elevation models (DEM) (NASA JPL) which were smoothed with a low-pass filter. In addition, leaf samples from different trees were randomly collected at the lowland and montane forest site and a composite sample for each site was used to analyze foliar $\delta^{15}N$.

5.2.3. Sample analysis

Soil samples were air dried and subsequently sieved through a 2 mm sieve to remove roots and organic residues. To homogenize, soil samples were milled and analyzed for C and N content and ^{15}N isotopes using an elemental analyzer (Automated Nitrogen Carbon Analyzer; SerCon; Crewe, UK) interfaced with an Isotope Ratios Mass Spectrometer (IRMS; 20-20, SerCon). $\delta^{15}N$ laboratory standards used had a certified value of 7.81 ‰ with an uncertainty across runs of 0.07 ‰. Stable isotope ratios are reported in delta notation:

$$\delta^{15}N = \frac{R_{SMP} - R_{STD}}{R_{STD}} \qquad \text{(Eq. 5.1)}$$

with R_{SMP} denoting the $^{15}N/^{14}N$ ratio of the sample and R_{STD} that of the international reference standard AIR-N_2. N stocks were calculated using mass-based N content, multiplied by the bulk density of the respective depth and integrated over the whole profile depth.

5.2.4. Inter-site comparison

For a better inter-site comparison of the erosional effect, we estimated a soil loss coefficient. In addition to slope, soil erosion is controlled by vegetation cover and rainfall characteristics. To incorporate these additional factors, we calculated an erosion coefficient (EC) for each surface soil sample. To calculate the EC, we used the empirical model for sediment detachment (kg m^{-2} yr^{-1}) from Pelletier (2012):

$$EC = S^{\frac{5}{4}} R_a e^{-L_a} \quad \text{(Eq. 5.2)}$$

Where S is the tangent of the mean hillslope gradient of all samples, R_a the mean annual precipitation (MAP), and L_a the mean annual leaf area index (LAI). Numerical values for LAI were extracted from the Copernicus LAI-300m satellite images produced by the Earth Observation program of the European Commission (European Environment Agency) for the year 2019. MAP data were extracted from the WorldClim database and averaged for the years 2010-2018 (Fick & Hijmans, 2017).

For a pan-tropical comparison, data points from Costa Rica (Weintraub et al., 2015) and Taiwan (Hilton et al., 2013) were extracted from the supporting material of the representative studies. Only these two studies were selected for a pan-tropical comparison, as other datasets containing soil $\delta^{15}N$ from tropical forests do not contain information on slope angles and LAI. Furthermore, in other studies, the reported coordinates are not sufficiently precise to extract slope values from global DEMs, resulting in a neglection of within site variability of slope effects.

5.2.5. Statistical analysis

To assess the effect of forest type and soil depth on $\delta^{15}N$ and mass-based C:N ratio, linear mixed effects models were fitted, controlling for topographic position via a random intercept. A third model was fitted for N-stocks. Since stocks are integrated over the whole soil profile, soil depth was omitted as an explanatory variable in the third model, including only the effect of forest type as a fixed effect, while controlling for topographic position via a random intercept. All models were fitted using maximum likelihood methods via the *lmerTest* package (Kuznetsova et al., 2017). To assess the relation between slope angle and $\delta^{15}N$ of the spatial surface samples, linear regressions were applied.

Furthermore, a structural equation model (SEM) was applied to examine the relative direct and indirect importance of different variables on the soil $\delta^{15}N$ values of the five tropical forests. A SEM was chosen because it allows to include dependencies between variables. In soil sciences, SEMs have been used for different applications, for example by implementing different pedological process information in soil mapping approaches (Angelini et al., 2017). The variables considered to explain $\delta^{15}N$ were MAP, MAT, LAI, slope, and soil C content. The SEM model was generated using the *lavaan* package version 0.6 (Rosseel, 2012) for R. All statistical analyses were conducted using the R-software (R Development Core Team, 2019).

5.3. Results

The montane forest showed the highest N stock with mean value (mean ± standard deviation (SD)) of 1.47 ± 0.61 t N ha^{-1}. N stocks were lower in the lowland forest and Miombo woodland, with 0.87 ± 0.11 and 0.73 ± 0.30 t N ha^{-1}, respectively (Table 5.2). The montane forest and Miombo woodland soils exhibited similar C:N ratios with 11.4 ± 1.1 in the montane and 11.2 ± 1.8 in the Miombo, while the C:N ratio in the lowland forest was lower with a mean value of 7.4 ± 0.5 (Table 5.2). Average bulk N and C:N values over the whole profile are reported in Appendix C2. In general, soil

profiles of the Miombo woodlands showed the lowest $\delta^{15}N$ values (3.59 ± 0.73 ‰, average for 0 - 100 cm) than the montane forest (5.83 ± 1.30 ‰) and the lowland forest (7.62 ± 0.63 ‰), while the lowland forest displayed higher $\delta^{15}N$ values, especially in topsoils (Fig 5.2). Lowland values increased steadily until a depth of 10 cm and decreased from there again until 100 cm depth. $\delta^{15}N$ in the Miombo woodlands showed the highest enrichment at a depth of 30 cm. $\delta^{15}N$ values of the montane forest varied considerably (large confidence intervals, Fig. 5.2), but showed a general steady enrichment with increasing depth (Fig 5.2). Spatial topsoil samples from each catchment (0 - 20 cm) reflected those of the soil profiles, showing highest $\delta^{15}N$ values in the lowland forest (mean ± SD; 7.55 ± 0.69 ‰), while the montane forest displayed slightly lower values (6.48 ± 1.42 ‰), the Miombo woodland was most depleted in $\delta^{15}N$ (2.93 ± 0.46 ‰) (Fig. 5.2b). The topsoil samples from the montane forest showed highest variability in $\delta^{15}N$ values, ranging from 3.71 – 10.72 ‰ with a SD of 1.43, whereas the Miombo showed a SD of 0.46 and the lowland forest a SD of 0.70. Slope angle did not have a significant effect on topsoil $\delta^{15}N$ in the lowland and montane forests ($p=0.8$ for lowland and $p=0.57$ for montane forest, respectively; Fig. 5.3). In contrast, topsoil $\delta^{15}N$ significantly decreased with increasing sloping angles in the Miombo ($r^2=0.30$, Fig. 5.3). The Miombo woodland displayed the highest average EC (20.11), whereas the montane (2.77) and lowland (1.22) forests showed clearly lower values (Table 3.1).

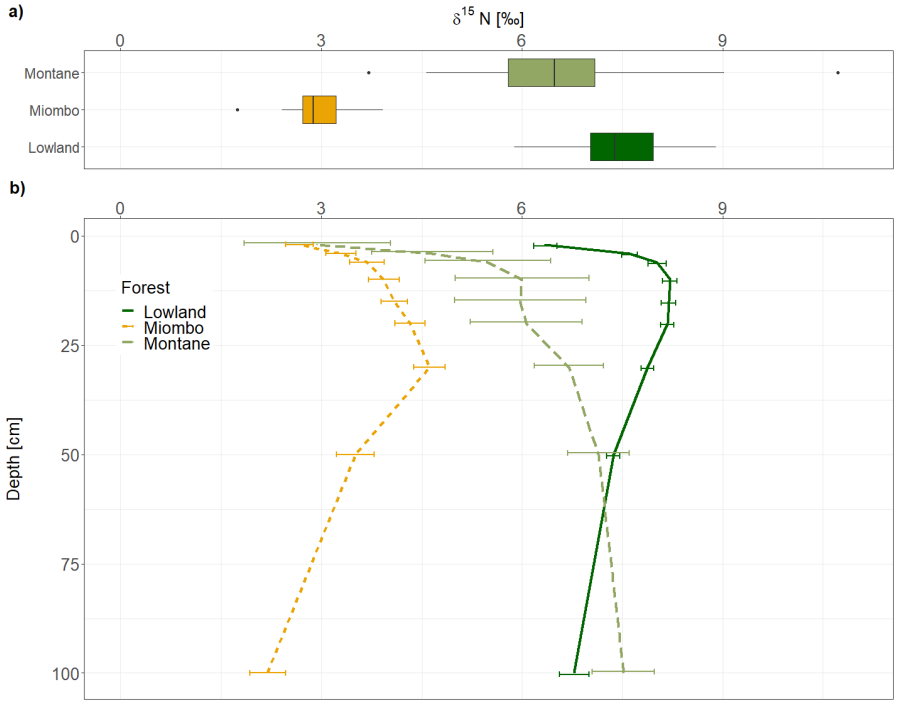

Fig. 5.2 a) Boxplots of the $\delta^{15}N$ of the topsoil (0-20 cm) samples from the montane, lowland and Miombo forest sites. b) $\delta^{15}N$ profiles from the different forest types. Lines showing the means of the replicates from one sampling site. Error bars indicating standard errors.

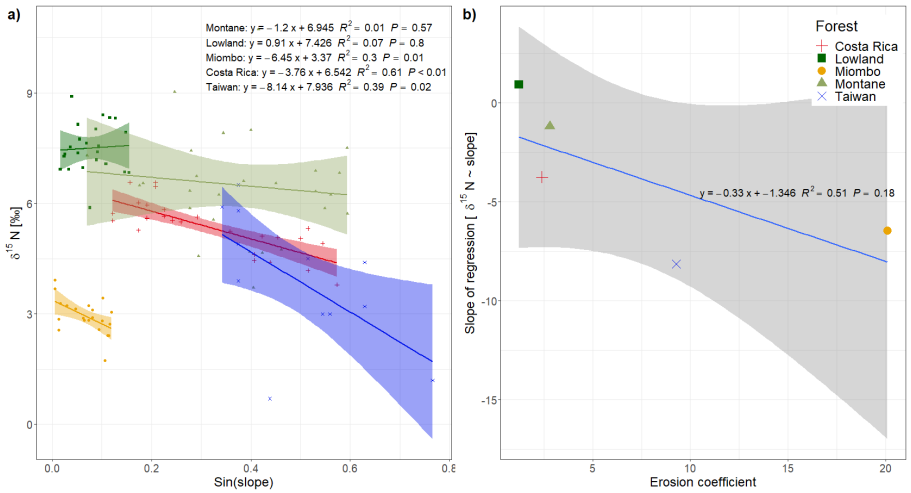

Fig. 5.3 a) Soil $\delta^{15}N$ values vs sinus of the slope from the spatial sampling of topsoil (0-20 cm) in DRC, including data from Costa Rica (Weintraub et al., 2015) and Taiwan (Hilton et al., 2013); b) slope of the regressions from panel (a) plotted against the mean erosion coefficient (Eq. 2) of each study site.

5.4. Discussion

5.4.1. Using soil $\delta^{15}N$ to assess differences in ecosystem N-turnover

At present, relatively little information on $\delta^{15}N$ data for soils in tropical forests is available. This holds especially for Central Africa, where almost no data is reported. Rütting et al. (2015) is one of the few studies that reported on $\delta^{15}N$ from montane tropical forests in Rwanda. Their values for topsoil (0-5 cm) range between 3.6 and 4.6 ‰ and are similar to the values reported in this study for the montane forest (mean of 4.4 ‰ for 0-6 cm depth in this study) and are also in the same range reported from topsoil in Rwanda by Bauters et al. (2017). Lower values were found in an old-growth montane forest topsoil (0-10 cm) in Ethiopia (-3 to 1 ‰, Eshetu & Högberg, 2000) and in semi-natural montane forests in Tanzania (0-4 ‰, Gerschlauer et al., 2019). $\delta^{15}N$ values from tropical mountain forests of Taiwan are also in the same range, with a mean value of 4 ‰ for the upper 10 cm of the soil profile (Hilton et al., 2013). Jamaican soils from tropical montane forests are much more depleted in ^{15}N, with values from -1.6 to 1.5 ‰ for depths down to 20 cm (Brearley, 2013). Top soils from an altitudinal gradient in Borneo were also more depleted, with a mean value of 1.6 ‰ (Kitayama & Iwamoto, 2001). $\delta^{15}N$ values reported for tropical lowland forests are available for soils in Costa Rica where top soils (0-10 cm) showed values of 4.7 ‰ (Osborne et al., 2017) and a mean value of 5.9 ‰ for soils from 0-20 cm depth (Weintraub et al., 2015). Higher erosion, due to high rainfall and uplift rates (1.7-8.5 mm yr^{-1}), may explain why these values of lowland forest in Costa Rica are more depleted in the heavier N isotope compared to the lowland forest in Yoko from this study (7.55 ± 0.69 ‰ for 0 – 20 cm soil samples) because the residence time of soil N decreases with erosion and hence soil rejuvenation (Amundson et al., 2003).

The $\delta^{15}N$ reported here for the Miombo woodland (2.68 – 4.32 ‰ between 0 – 20 cm, Figure 2) falls within the same range as values reported by Wang et al. (2013) from a moist woodland savanna in Zambia (2.6 – 4.8 ‰) and a mature Miombo woodland in Tanzania (3.5 – 3.8 ‰, Mayes et al., 2019), but are lower compared to values reported from a dry forest in the Cerrado Savanna of Brazil (6.3 – 10.8 ‰, Bustamante et al., 2004).

Soil $\delta^{15}N$ is related to the residence time of ecosystem N. Higher rates of mineralization, nitrification and dentification leaves enriched N in the remaining soil organic matter (SOM), while the more depleted mineral N is removed via plant uptake or denitrification and transported down into deeper soil layers by leaching (Handley et al., 1999; Hobbie & Ouimette, 2009). Over the whole profile, the Miombo woodland showed highest depletion of ^{15}N (Fig. 5.2), which would indicate a slower N turnover and a more closed N cycle compared to the lowland and montane forest. However, as the $\delta^{15}N$ signatures are also influenced by soil N inputs, the Miombo woodland, dominated by the legume tree *Brachystegia*, likely receives relatively more depleted ^{15}N through biological N_2-fixation. Previous studies have shown that N_2-fixation is a more important process in tropical woodlands than in tropical forests (Hogberg & Alexander 1995), where less trees of the Fabaceae family are present (Malmer & Nyberg, 2008). Furthermore, it is reported that symbiotic N_2-fixation is downregulated in old-growth tropical lowland forest (Bauters et al., 2016), thus $\delta^{15}N$ of top soil in these forests is less likely to be affected by N_2-fixation, which is clearly indicated by more enriched top soil $\delta^{15}N$ values. Beside N_2-fixation, topsoil $\delta^{15}N$ is also influenced by the isotopic signature of incoming litter fall, inputs through roots and N deposition (Craine et al., 2015b), while downward transport processes and transformation of SOM influences the $\delta^{15}N$ in deeper soil layers (Baisden et al., 2002). In this study, the Miombo woodland showed slightly lower $\delta^{15}N$ values for the topsoil (0-2 cm, 2.66 ‰) than the montane forest (2.94 ‰), while the lowland forest showed a more enriched signature (6.35 ‰). The foliar $\delta^{15}N$ presented in Table 3 show that the values in the Miombo and montane forest are substantially lower than in the lowland forest and that $\delta^{15}N$ inputs from plants lower the soil $\delta^{15}N$ values in these forests more compared to the lowland forest. Whereas the strong depletion of the Miombo woodland can be related to atmospheric N_2-fixation, the shift of plant and topsoil $\delta^{15}N$ to more depleted values in the montane forest could also be an altitudinal effect. Depletion of $\delta^{15}N$ with increasing elevation in tropical forests, have been observed in the Neotropical and Afrotropical forests and were linked to a more conservative N cycle at high altitudes (Bauters et al., 2017).

Soil $\delta^{15}N$ profiles of the lowland forest and the Miombo woodland showed a $\delta^{15}N$ enrichment peak at 10 cm and 30 cm depths (Fig. 5.2b), respectively, indicating the highest microbial activity and/or leaching of soil N in this layer. Montane forest showed a similar peak at the same depth, indicating high turnover or leaching in this soil layer as well. However, from 20 cm onwards $\delta^{15}N$ enrichment increased even further to the highest values at 100 cm depth (Fig. 5.2b). Hobbie & Ouimette (2009) presented a conceptual model for processes that influence $\delta^{15}N$ values in a profile. According to this model, a profile with higher $\delta^{15}N$ values in the root layers and decreasing $\delta^{15}N$ in subsequent depths (similar to the lowland and Miombo profiles)

is more likely to occur in an open system with lower N limitation and more inorganic N cycling (Hobbie & Ouimette, 2009). Denitrification and associated gaseous N losses cause the increase of soil $\delta^{15}N$ at intermediate depth. Leaching and subsequent microbial assimilation of depleted NO_3 at lower depths result in the more depleted $\delta^{15}N$ signature of lower soil layers compared to the intermediate depth (Hobbie and Ouimette, 2009). This is also in line with the higher N_2O fluxes that were observed in the lowland forests of Yoko and in Miombo woodlands in Tanzania compared to montane forests in Kahuzi-Biéga (Table 5.3), indicating generally a higher N turnover (especially nitrification and denitrification) occurring at these sites. Moreover, Bauters et al. (2019) showed indication of mineral N excess in the Yoko lowland forest, which is also due to high atmospheric N depositions in the central African lowlands (Table 5.3). Overall, the soil $\delta^{15}N$ profiles of the lowland forest and the Miombo woodland seem to have a more open N cycle due to excess N availability, which is most likely due to high N depositions in the lowland and high N_2-fixation in the Miombo.

On the other hand, a soil profile where ^{15}N continuously increases with depth (i.e. the case of the montane forest) is indicative of an N-limited ecosystem or dominated by organic N cycling. In these systems, assimilation of leachate (depleted in $\delta^{15}N$) in deeper soil-layers is less common, thus the $\delta^{15}N$ steadily increases with depth. Although, we found highest N stocks in the montane forest, higher foliar C:N ratios of tropical forests with increasing altitude (Bauters et al., 2017) indicate that this ecosystem experiences lower N availability and is dominated by organic N cycling. In Rwandan and Ecuadorian forests, Bauters et al. (2017) concluded from leaf $\delta^{15}N$ altitudinal gradients that N-cycling becomes more closed with increasing elevation and hypothesized that organic N sources for plants become more important in ecosystems with lower temperatures. Furthermore, very high mineralization rates have been measured in the montane forests of Kahuzi-Biéga, which indicates a high organic matter turnover in these forests (Bauters et al., 2019) which is supported by the high aquatic total dissolved N (TDN) and dissolved organic N (DON) exports from this forest (Table 5.3).

Table 5.1 Foliar plant $\delta^{15}N$ [‰] values, N deposition rates (kg N ha^{-1} yr^{-1}), aquatic TDN and DON losses (kg N ha^{-1} yr^{-1}) for the three study sites. Aquatic TDN losses and DON losses are preliminary results from measurements by the authors of this study at the respective study sites (methods see Appendix C1).

	Lowland	Montane	Miombo
Foliar $\delta^{15}N$ (‰)	3.42	0.58	-0.74 [1]
N deposition (kg N ha^{-1} yr^{-1})	18.2 [2]	21.2 [2]	3-5 [1]
Aquatic TDN loss (kg N ha^{-1} yr^{-1})	3.87	6.50	0.84
Aquatic DON loss (kg N ha^{-1} yr^{-1})	2.37	4.46	0.73
N_2O-flux (kg N ha^{-1} yr^{-1})	1.38 [3]	0.59 [3]	1.16 [4]

References: 1) Mayes et al., 2019 (Miombo woodland Tanzania); 2) Bauters et al., 2019 (Lowland forest in Yoko, DRC; Montane forest in Kahuzi-Biéga, DRC); 3) Barthel et al., (2022); 4) Rees et al., 2006 (Miombo Woodland Tanzania)

Table 5.2 Fixed effects estimates for $\delta^{15}N$, N-stocks and C:N ratios. Fixed effects include forest type (Lowland, Montane and Miombo) and soil depth in cm (for $\delta^{15}N$ and C:N). N-stocks are for top 100 cm of the soils. For each effect, estimated standard error and estimated P-values is given, along with the estimated marginal (m) and conditional (c) R^2adj (Nakagawa & Schielzeth, 2013)

Response	Effect	Effect size	SE	P-value	$R^2_{adj,m}$	$R^2_{adj,c}$
$\delta^{15}N$ (‰)	Intercept: Lowland	7.72	0.10	< 0.001	0.65	0.65
	Montane	-1.82	0.18	< 0.001		
	Miombo	-4.08	0.16	< 0.001		
	depth	-0.002	0.00	0.26		
C:N	Intercept: Lowland	7.96	0.16	< 0.001	0.57	0.58
	Montane	3.94	0.26	< 0.001		
	Miombo	4.20	0.22	< 0.001		
	depth	-0.02	0.00	< 0.001		
N (kg m^{-2})	Intercept: Lowland	1.47	0.17	< 0.001	0.36	0.36
	Montane	0.65	0.27	0.160		
	Miombo	-0.35	0.24	0.03		

5.4.2. Influence of topography on soil $\delta^{15}N$

A possible effect of topography on soil $\delta^{15}N$ is most likely due to higher erosion of steeper slopes compared to flat landscapes, because we assume that within a site other factors controlling soil $\delta^{15}N$ (such as temperature, precipitation and vegetation cover) do not vary with topography. In contrast to the Costa Rican tropical lowland forests (Weintraub et al., 2015), slope angle was found to have no effect on $\delta^{15}N$ in the lowland forest of this study (Fig. 5.3a). In contrast to the Costa Rican site, there are no steep slopes in the lowland forest of this study (max. slope sampled 9°) and thus, there is a low potential for physical erosion. This is also indicated by a lower EC (1.22) in the lowlands compared to Costa Rica (2.39) (Table 5.1). Although the Miombo woodland is located in an area, with similar topography to the lowland forest (Fig. 5.1), the EC from this area is much higher (20.11). This can be explained by the fact that the forest cover in the Miombo is less dense than the tropical forests and this increases the exposure of the soil surface to the energetic input of rainfall. Furthermore, the loss of understory vegetation from fire, which occurs frequently during the dry season (Campbell, 1996), leaves the soil unprotected from erosion at the onset of the rainy season. The spatial topsoil samples of the Miombo woodland clearly indicate a significant effect of slope angles on $\delta^{15}N$ (Fig. 5.3a). The $\delta^{15}N$ values in the montane forest, situated on steep terrain, tend to decrease with increasing slope angle, however, the visible trend is not statistically significant (*P*-value of 0.57, Fig. 5.3a). Furthermore, we found a higher variability in $\delta^{15}N$ values of the soil samples in the montane forest (SD of 1.43 ‰) compared to the Miombo (SD of 0.46 ‰) and lowland forest (SD of 0.70 ‰). While slope angle is a commonly used predictor of soil erosion potential, the curvature of the land surface (i.e. convex or concave) has also been shown to affect soil erosion at a local scale (Stefano et al., 2000). The specific hydrology seems to control the erosive mechanism, as slope gradients have been found to influence the rate of soil erosion through overland flow, while curvatures affect diffusive processes, such as splash erosion (Stefano et al., 2000). However, while a trend of lower $\delta^{15}N$ on more convex landscapes in the montane forest is visible (Appendix C2), no statistical significance was found either, as samples were not equally distributed over the range of curvatures. In addition, because our sampling strategy was focused on the slopes, sample sites were biased towards concave curvatures.

Comparing the effect of slope angles on topsoil $\delta^{15}N$ of the study sites from the Congo Basin with the effect observed in tropical forests of Costa Rica (Weintraub et al., 2015) and Taiwan (Hilton et al., 2013) shows that the magnitude of the effect is related to the mean erosion coefficient in these ecosystems (Fig. 5.3b). Sites with a high erosion coefficient show a higher slope of the regression *$\delta^{15}N$ ~slope angles* compared to sites with a low erosion coefficient, implying a bigger effect on soil $\delta^{15}N$ in more geomorphic active sites. As the dense tropical lowland forests of the Congo Basin do not represent high EC values, the local effect of erosion on soil $\delta^{15}N$ seems negligible. Although the montane forest shows a moderate EC, due to the steep topography, the high variability in soil N likely masks the potential effect of topography on $\delta^{15}N$ in our dataset. The estimation of EC based on equation 5.2 assumes that splash and overland flow are the dominant erosion processes but this

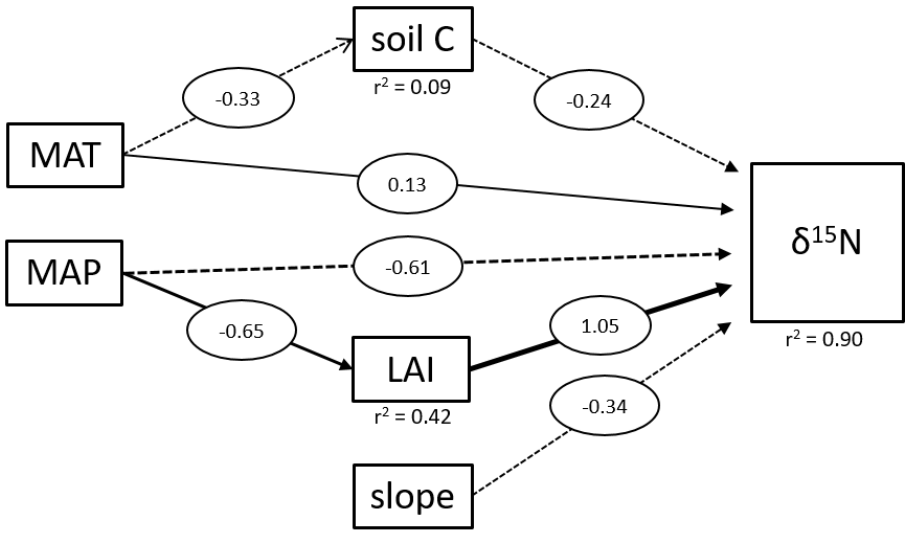

Fig. 5.4 Structural equation model of direct and indirect effects on tropical soil $\delta^{15}N$ values. The diagram shows all significant relationships. MAT represents the mean annual temperature in °C, MAP the mean annual precipitation in mm and LAI the leaf area index. Soil C is the carbon content of the soil samples and slope the slope angles of the sampling site. Numbers represent the strength of each effect.

may underestimate erosional forces at higher hillslope angles (Pelletier, 2012). At higher hillslope angles, landslides will be more important erosional processes than overland flow. This might indicate that at sites with high risks of landslides (as shown in the landslide hazard index (LSI) in Table 5.1) are even more prone to physical soil loss than the EC would indicate. In this case especially the forest in Taiwan (LSI of 4), the montane forest (LSI of 3.96) and the forest in Costa Rica (LSI of 3.65) experience a high risk of landslides and total soil loss in this forest might even be higher than predicted by the EC.

We applied a SEM to assess the driving factors of the topsoil $\delta^{15}N$ variability between different tropical forest sites (Fig. 5.4). On a global scale, soil $\delta^{15}N$ is reported to be mainly influenced by climatic factors (MAT and MAP) and soil properties, such as soil C and clay content (Craine et al., 2015). Our results showed that soil C had only a marginal influence (lower coefficient compared to slope, MAP and LAI) on tropical soil $\delta^{15}N$ and is only significantly influenced by MAT and not MAP. Soil $\delta^{15}N$ in these tropical forests seems to be primarily influenced by factors controlling erosion (MAP, LAI and slope). Beside the direct effect of MAP on soil $\delta^{15}N$, there is also a significant indirect effect visible, where sites with higher MAP experience also higher LAI values (Fig. 5.4). It was not possible to analyze the effect of clay content on $\delta^{15}N$ because the data were not available for all the sites. Although our data showed only for the Miombo a significant effect of topography on the soil $\delta^{15}N$ values, our pantropical analysis suggests that especially in geomorphic active regions, erosion needs to be taken into account to explain local differences in soil $\delta^{15}N$ values. However, it is

important to state that the SEM with only 112 samples from 5 different ecosystems represents an overly simple model and more data is needed for a more precise outcome. Unfortunately, additional $\delta^{15}N$ data, that includes topographical variability is not available, to the best of our knowledge.

5.5. Conclusion

The three tropical forest ecosystems in the Congo Basin each showed a distinct $\delta^{15}N$ soil profile. The $\delta^{15}N$ soil profiles in the montane forest indicate a closed N cycle, which supports the common theory of decreasing N availability at higher altitudes. In contrast, the $\delta^{15}N$ soil profiles indicated that the lowland forest and Miombo woodland tended to have more open N cycles, which were mostly dominated by inorganic N cycling. The Miombo woodland showed the lowest $\delta^{15}N$ values, which is most plausibly explained by enhanced N_2-fixation due to the tree species composition dominated by the legume *Brachystegia*. Furthermore, topsoil $\delta^{15}N$ signatures across our and literature sites of the tropics suggests that a significant amount of the observed variability can be explained by erosional processes. Rainfall, vegetation cover, and topography are the main factors to explain $\delta^{15}N$ variability between five different tropical forest sites. Within the Congo Basin, only the Miombo woodland showed an influence of slope on soil $\delta^{15}N$, whereas in the lowland forest, the comparably low MAP, dense vegetation, and flat topography likely limit erosion and resulted in the lack of a correlation between the $\delta^{15}N$ of soil N and slope angle. In general, this study highlights the possible importance of soil erosion on N budget in tropical forests However, not all sites are similarly impacted. Therefore, soil erosion has to be taken into account while interpreting of soil $\delta^{15}N$ values as a proxy for N cycling. It underlines the importance of further spatial field studies in the tropics given the observed high variabilities between different tropical forest types.

Acknowledgments

We thank the authorities and park rangers of the *Institute Congolais pour la Conservation de la Nature* (ICCN) for the help in accessing the field site in the Kahuzi-Biéga National Park. We are grateful for Serge Alebadwa, Nadine Bahizire, Claudino Sumaili, Degra Ngoy, Christ Ibrahimu and Rosine Bakengere for assistance during the fieldwork. We are also thankful for Katja Van Nieuland and Samuel Bodé for the help with sample analysis. This research has been funded by the Fonds de la Recherche Scientifique FNRS project numbers T.0059.18 and J.0167.19.

Supporting information

Supporting information to this chapter can be found in Appendix C

Appendix C1: Methods for aquatic TDN and DON export

Appendix C2: $\delta^{15}N$ in topsoil (0 – 20 cm) plotted against the curvature of the sampling spot. Positive curvature values represent concave landforms, while negative values represent convex landforms.

Appendix C3: a) Profiles of average bulk N values in g cm^{-3} for the three different forest sites. b) Profiles of average C:N ratios for the different forest sites. Error bars indicate standard error.

Part V – Influence of land use on aquatic N export

Chapter 6: Agricultural land-use increases riverine organic N and particulate P yields in the tropics of Central Africa

After: Baumgartner, S., Drake, T. W., Bauters, M., Barthel, M., Alebadwa, S., Bahizire, N., Boeckx, P., Six, J. & Van Oost, K.: Agricultural land-use increases riverine organic N and particulate P yields in the tropics of Central Africa. *(due for submission)*

Abstract

Land use change and deforestation impose a serious threat on pristine tropical forest ecosystems. Due to the increasing population, the Congo Basin experiences an expansion of shifting agriculture (slash-and-burn agriculture) and loss of primary tropical forests. Land use changes can have immense effects on the carbon (C) and nutrient status of the ecosystems and are reported to enhance losses of soil C and nutrients. To assess the difference of the aquatic nutrient export of a forest and agricultural catchment, we conducted a paired watershed study in the lowlands of the Congo Basin and analysed annual exports of dissolved and particulate nitrogen (N) and phosphorus (P). We found higher dissolved organic N (DON; 106% higher concentrations and 117% higher yields in the agricultural stream compared to forest stream) and particulate inorganic P (PIP; 110% higher concentrations and 116% higher yields in the agricultural stream) concentrations and yields in the agricultural stream, while nitrate (NO_3^-) concentrations (-60%) and yields (-59%) were lower. Shifting agriculture is known to impose N losses and the lower NO_3^- yields are mirroring the lower N content in the agricultural catchment, while higher DON export is associated with a shift in sources of dissolved organic matter. The higher particulate P export, mainly as inorganic P, showed that mineral soils were more prone to erosion in the agricultural system, which was also visible in the C:N ratios of the particulate matter. Sediment yields were most likely underestimated, by missing of storm event samples. Turbidity measurements indicated that storm events have even higher impact on the sediment and particulate nutrient export in the agricultural than in the forested stream catchment (+86.6%). Also dissolved organic N and P exports were driven by storm events, indicated by continuous fDOM measurements, which were 360% higher in the agricultural compared to the forest catchment. Our results highlight the hydrological nutrient losses with deforestation and the subsequently more conservative nutrient cycling within a deforested catchment of the tropics. Furthermore, storm events were identified as driver of sediment and nutrient exports and need to be well examined.

6.1. Introduction

Tropical forests play an important role in the global carbon (C) cycle; they are responsible for one-half of the total terrestrial C sink (Pan et al., 2011). Furthermore, tropical forests are hotspots for biodiversity (Gaston, 2000) and provide livelihood for regional populations (Chhatre & Agrawal, 2009). However, the increase of population in tropical regions and the resulting increase in agriculturally driven

deforestation are putting these precarious ecosystems under pressure. Globally, estimations of pan-tropical forest loss in the 2000s are around 7.6 million ha yr^{-1}, with highest deforestation rates observe in Central and South America (Archard et al., 2014). In the Americas, this high deforestation rate is mostly due to industrial logging and large-scale agricultural practices (Rudel et al., 2009). In the Congo River Basin (CRB) of central Africa, host to the second largest tropical forests, pressure on pristine forests mainly arises from small-scale subsistence farming and shifting agriculture, which is also known as slash-and-burn agriculture (Curtis et al., 2018). However, due to an estimated population increase of around 280% by 2050 alone in the Democratic Republic of the Congo (DRC), this pressure is increasing and driving faster rates of primary forest loss (Tyukavina et al., 2018).

It is well reported that deforestation and land-use change (LUC) increases soil respiration and subsequently enhances the loss of soil organic C (SOC) storage (Don et al., 2011; Guo & Gifford, 2002; Houghton, 1999). Furthermore, LUC effects on the availability on soil nutrients have been widely shown. LUC mainly decreased soil fertility (Templer et al., 2005) and conversions of forests to pasture resulted in lower concentrations of ammonium (NO_3^-) but higher concentrations of nitrate (NH_4^+) and lower rates of N-mineralization rates (Neill et al., 1995; Reiners et al., 1994). Especially for shifting agricultures, losses of total soil N and C and available P were reported (Hölscher et al., 1997; McGrath et al., 2001; Murty et al., 2002). Most losses occur at the beginning of a clearing cycle: removal of biomass by logging and fires are triggering nutrient losses through timber harvesting, erosion, outgassing and hydrological leaching (McGrath et al., 2001). Those losses especially seem to affect soil N, with N cycling rates declining with pasture age and young secondary forests are more prone to N limitations (Davidson et al., 2004; Davidson & Martinelli, 2013). These effects of LUC are also visible the composition of organic matter and dissolved nutrients in streams draining these ecosystems. In tropical regions, mobilization of older and more nitrogen-rich DOM (Drake et al., 2019) and an increase of total and dissolved inorganic forms of nitrogen (N) and phosphorus (P) (Biggs et al., 2004; Bringhurst & Jordan, 2015; Williams & Melack, 1997) were found. Different in sources of DOM are mirrored in different stable isotopic signatures, such as $\delta^{13}C$ (Drake et al., 2019). Furthermore, hydrological patterns, such as evapotranspiration (ET) and runoff coefficients are altered with LUC. A decrease in ET with increasing forest loss increases runoff coefficients of watersheds and increase the water discharge (Coe et al., 2009; Neill et al., 2006). This increases physical erosional forces on surface soils, especially in tropical regions, where rainfall intensities are high. Erosion is known to influence biogeochemical cycles and nutrient availabilities (Taylor et al., 2015; Weintraub et al., 2015), thus changes in erosional forces due to LUC can lead to an even higher degradation of the nutrient status of soils in the tropics (Tully et al., 2015).

Impacts of LUC on soil and riverine biogeochemistry in the tropics has been well studied, however, geographical bias resulted in an underrepresentation of studies within tropical Africa, especially for the Congo Basin. Furthermore, riverine studies covering nutrient exports have mainly focused on dissolved fractions of all nutrients, ignoring particulate forms of N and P. To tackle these regional and methodological

bias, we conducted a paired watershed study in the lowlands of the Congo Basin. We quantified annual yields of total N and P, including both dissolved and particulate forms from a pristine primary forest catchment and from an agricultural catchment. Furthermore, we used C stable isotopes and C:N ratios of particulate organic matter (POM) to identify possible differences in sources of the exported sediments. We hypothesized that the sediment associated forms of N and P are higher in the agricultural stream, due to higher sediment exports. Furthermore, the yields of bioavailable inorganic N and P were hypothesized to be lower in the agricultural dominated catchment, due to the lower availability of those nutrients.

6.2. Material and Methods

6.2.1. Site description

To compare the aquatic export of nutrients from a pristine forest catchment (forest) and a predominantly agricultural catchment (Ag), two headwater streams in the lowlands of the central CRB were selected. Both sites lie in the vicinity of the city of Kisangani in the Tshopo province of the DRC. The forest stream lies within the Yoko Forest Reserve around 35 km south of Kisangani (0.293°N, 25.295°E). The whole catchment consists of 99.3 % of pristine primary tropical mixed forest intercepted with patches of monodominant forests, where the species *Gilbertiodendron dewevrei* consist of more than 60 % of the basal area. Catchment area was determined using digital elevation models (DEM) derived from the 30 m Shuttle Radar Topographic Mission (SRTM, NASA Jet Propulsion Laboratory). The catchment spans an area of 3.1 km^2 and has an elevational range between 440- 475 m a.s.l. with an average slope of 4.3°. The Ag stream is situated in the village of Balifi, around 8 km south of Kisangani (0.422°N, 25.182°E). The Ag catchment area is with 9.7 km^2 with elevations range from 415 – 475 m a.s.l. with similar slopes as the forest catchment. The catchment consists of around 75% of cropland and 22% secondary forests (Fig. 6.1). The whole area is used for shifting agriculture, meaning that forests are cyclically deforested, converted into agricultural land, cropped for a few years, abandoned, and then allowed to regrow. These lands undergo several of those clearing-regrowth cycles.

6.2.2. Monitoring and sampling

For reliable continuous discharge measurements, concrete flumes with fixed widths (forest: 1.6 m; Ag: 5 m) were built. At the bottom in the centre of each flume a pressure transducer (CS451, Campbell Scientific, USA) connected to a datalogger (CR1000, Campbell Scientific, UK) was installed to measure water level in 5-min intervals. Water discharge was measured manually biweekly using a mechanical flowmeter (Model 2030, General Oceanics Inc., USA) to obtain a water level – discharge rating curve for both sites. In addition to the pressure transducer, probes with turbidity and fluorescent dissolved organic matter (fDOM) sensors and internal loggers (YSI-EXO2, Xylem, USA) were deployed at both sites, measuring at 15-min

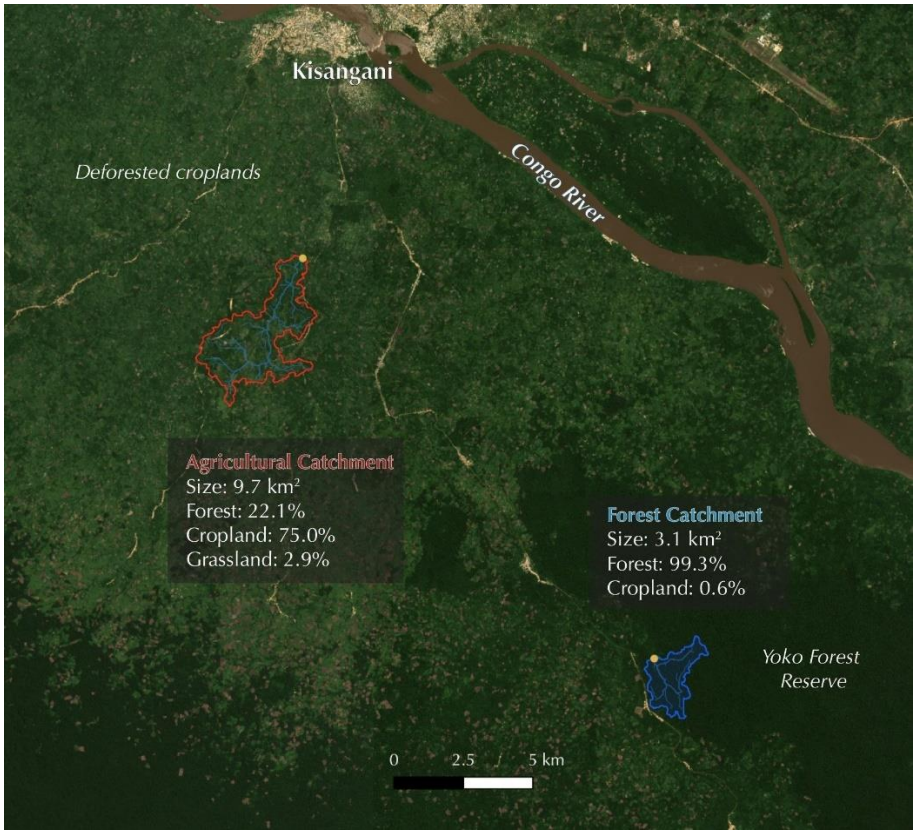

Fig. 6.1 Locations and extent of the agricultural (red) and forest (blue) catchments. Yellow dots indicate the flume positions.

intervals. Turbidity and fDOM probes were precalibrated the same way for both sites and cross-checked to assure comparability of the optical measurements between the two sites. In order to avoid biofouling on the optical sensors of the turbidity and fDOM probe, both YSIs were equipped with an on-board wiper, which cleaned both sensors every 15 min before every measurement. YSIs were deployed at both sites on the 3rd of April 2019 and was running for a full year at the Forest site. At the Ag site, the YSI had to be removed on the 9th of March 2020 due to security issues.

Water samples to measure concentrations of total suspended sediments (TSS), particulate C (PC), particulate N (PN), dissolved organic N (DON), NO_3^-, NH_4^+, total particulate P (TPP), particulate inorganic P (PIP), dissolved organic P (DOP), and phosphate (PO_4^{3-}) were taken bi-weekly in 2L HDPE bottles. Furthermore, dissolved nitrous oxide (N_2O) of the stream water was sampled using the headspace equilibrium technique. A 12 mL plastic syringe was used to inject 6 mL of air bubble-free water into a 12 mL N_2-flushed exetainer (Labco, UK). 50 µl of 50% $ZnCl_2$ solution within the exetainer was used to limit biological activity within the water samples. During each sampling day, both catchments were sampled within a 4-hour period.

6.2.3. Chemical analysis

After sampling both catchments, all the samples were returned to the laboratory of the University of Kisangani, where the water samples were filtered immediately after return. Before filtration, water bottles were agitated to resuspend sediments. Water samples were filtered on pre-combusted and pre-weighed glass-fibre filters (0.7 µm, GF/F, Whatmann, USA). The filtrate was stored in acid washed 250 ml HDPE bottles. Sediment-loaded filters and bottles containing the filtrate were immediately frozen after filtration and transported in batches to Europe for chemical analysis every two to four months.

All filters were dried before analysis at 60°C for 48 h. TSS concentrations were determined by dividing the weight difference of the filters before filtration and the dried filter after filtrations with the amount of water filtered. PN and PC concentrations and the stable isotopic signatures of ^{13}C and ^{15}N were determined by feeding the whole filters to an elemental analyser (Automated Nitrogen Carbon Analyzer, SerCon; Crewe, UK) interfaced with an isotope ratio mass spectrometer (IRMS; 20-20, SerCon, Crewe, UK). ^{13}C values were reported in the delta notation against the reference standard VPDB and ^{15}N against the reference standard AIR-N_2. To measure TPP and PIP concentrations, the filters were first rinsed with 5 mL of Na_2SO_4 solution to remove all dissolved P that was adsorbed to the particles. Afterwards, the filters were digested in 20 mL of 3% $K_2S_2O_8$ at 120°C for 30 minutes (for TPP) and in 20 mL of 1M HCl for 24 hours at room temperature on a shaker bath in the dark (for PIP). The residues within the digestion solutions were removed using a 0.45 µm syringe filter. PO_4^{3-} concentrations in the filtered digestion solutions were measured colorimetrically (see below).

We measured dissolved NO_3^-, NH_4^+ and PO_4^{3-} concentrations in the filtered water samples colorimetrically using a continuous flow analyser (AA3, Bran+Leubbe, Germany). NO_3^- was reduced to nitrite by a copper-cadmium reduction at pH 8, together with sulfanilamide, the nitrite reacts to form a diazo compound which then couples with N-l-napthylenediamine dihydrochloride to form a reddish-purple color compound which was measured at 520 nm. The NH_4^+ in the water sample reacted with salicylate and dichloroisocyanuric acid to produce a blue compound, which was measured at 660 nm. And the PO_4^{3-} reacted with molybdate and ascorbic acid to form a blue compound which was also measured at 660 nm. Total dissolved N (TDN) and total dissolved P (TDP) were determined by converting all N and P in the filtered water samples to NO_3^- and PO_4^{3-}, respectively, using an oxidizing solution of NaOH, H_3BO_3 and $K_2S_2O_8$. A 1:1 mixture of filtered water sample and oxidizing solution was autoclaved for 1 h at 121°C and subsequently measured for NO_3^- and PO_4^{3-} concentrations. Dissolved inorganic N (DIN) was determined as the sum of NO_3^- and NH_4^{3+}, while dissolved inorganic P (DIP) is defined as the PO_4^{3-} concentrations. DON and DOP were retrieved by subtracting all inorganic N and P concentrations from the TN and TP concentrations.

To measure dissolved N_2O concentrations, the headspace of the exetainer was analysed for N_2O concentration at ETH Zürich, using a gas chromatograph (456-GC,

Scion Instruments, UK). Dissolved N_2O concentrations in the water samples were obtained using Henry's law.

6.2.4. Yield calculations and statistical analysis

For each sampling event, instantaneous yields for all measured concentrations were calculated by multiplying the concentrations by the instantaneous water discharge divided by the catchment area. For a better comparison of the measured turbidity and fDOM values between the two sites, turbidity and fDOM yields were calculated for each 15-min interval, by multiplying the measured turbidity and fDOM values with the obtained discharge value at the same time dividing the sum by the catchment area. Possible statistical differences between the yields of the discrete sampling from the two sites were found by applying paired t-tests using the GraphPad Prism 9 software. For the differences between the fDOM and turbidity values, a t-test was applied as with all the 15-min interval measurements.

6.3. Results

6.3.1. Hydrology

Due to the close vicinity of the two catchments, daily satellite derived precipitation data for the monitoring period (GPM, Huffman et al., 2019) are the same for both sites. The precipitation for the monitoring period was 2031 mm. During this period the forest catchment drained 665 mm and the Ag catchment 1216 mm, resulting in runoff coefficients of 0.33 and 0.60 for the forest and the Ag catchment, respectively. Throughout the hydrological year, turbidity and fDOM sensors measured higher yields at the Ag stream compared to the forest stream (Fig. 6.2). Turbidity yields showed an 86.6% increase for the agricultural stream compared to the forest stream, while for fDOM the difference was even more pronounced, with a 360% increase in fDOM yield for the Ag stream.

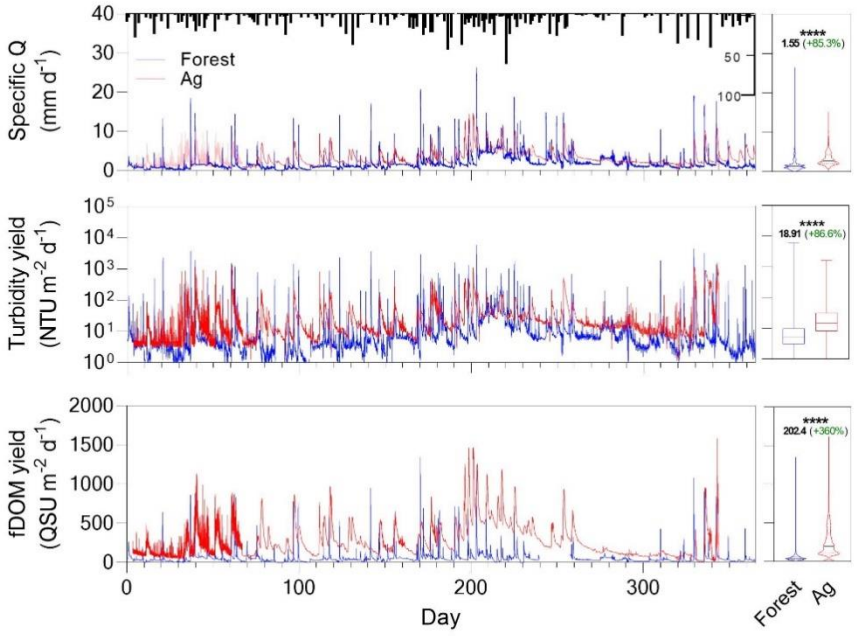

Fig. 6.2 Top row: specific discharge in mm per day for the forest stream (blue) and agricultural stream (red). Black bars indicate the daily rainfall, derived from GPM satellite data. Middle row: timeseries of measured turbidity yields for the forest and agricultural stream. Bottom row: timeseries of fluorescent dissolved organic matter (fDOM) yields from the two streams. Violin and boxplots to the right of the timeseries plots show the medians and inner quartiles. Stars represent the significance determined by the paired t-tests. Numbers indicate the changes between the means of the two streams with the relative changes indicated by the green value in paratheses.

6.3.2. Sediment and nutrient yields

Mean instantaneously measured TSS yields were slightly higher in the Ag stream with, 12.44 ± 9.61 mg ha^{-1} s^{-1} (mean ± SD) compared to mean yield of 9.79 ± 6.65 mg ha^{-1} s^{-1} in the forest stream, however, the paired t-test showed no significant difference between the two catchments (Fig. 6.3). Particulate and dissolved N concentrations in both streams did not show any seasonality (Appendix D4). Mean PN yields were identical for both sites, where the Ag stream yielded 0.07 ± 0.07 mg N ha^{-1} s^{-1} and the forest stream 0.07 ± 0.06 kg N ha^{-1} s^{-1} (Fig. 3). DON yields were significantly higher (117%) in the forest stream (0.10 ± 0.08 kg N ha^{-1} s^{-1}) compared to the Ag stream (0.24 ± 0.21 kg N ha^{-1} s^{-1}), while NO_3^- yields were lower by 59% in the forest stream (0.06 ± 0.04 kg N ha^{-1} s^{-1}) than in the Ag stream (0.02 ± 0.02 kg N ha^{-1} s^{-1}). The lower NO_3^- yields resulted in lower (-50%) DIN yields, while NH_4^+ and N_2O yields showed no significant differences between the two catchments (Fig. 6.4).

TN yields showed no significant difference between the two streams, however, the Ag stream yielded slightly higher TN (0.36 ± 0.30 kg N ha^{-1} s^{-1}) than the forest stream (0.25 ± 0.17 kg N ha^{-1} s^{-1}) on average (Fig. 6.4).

Like PN, particulate P concentrations did not show any seasonality, however, DIP showed higher concentrations during the wet seasons in both streams (Appendix D4). Only the particulate forms of P experienced a significantly higher export in the Ag stream (Fig. 6.5). TPP yields were 85% higher in the Ag stream (0.009 ± 0.008 mg P ha^{-1} s^{-1}) than in the forest stream (0.005 ± 0.004 mg P ha^{-1} s^{-1}). PIP yields showed an even higher difference with 116% higher yields from the Ag stream (0.005 ± 0.003 mg P ha^{-1} s^{-1}) compared to the forest stream (0.002 ± 0.002 mg P ha^{-1} s^{-1}) (Fig. 6.5). DOP and DIP yields showed no significant difference between sites, however the forest stream generally experienced higher yields (0.007 ± 0.012 mg P ha^{-1} s^{-1} DOP; 0.003 ± 0.005 mg P ha^{-1} s^{-1} DIP) compared to the Ag stream (0.003 ± 0.008 mg P ha^{-1} s^{-1} DOP; 0.002 ± 0.003 mg P ha^{-1} s^{-1} DIP) (Fig. 6.5). Both, DOP and DIP concentrations, were often (> 50%) below detection limit. These samples were omitted for analysis. TP yields showed similar values for both catchments: 0.014 ± 0.013 and 0.013 ± 0.011 mg P ha^{-1} s^{-1} for the forest and Ag stream, respectively.

6.3.3. Composition of POM

The C:N ratio of the suspended sediments from the forest stream were 5% higher with an average value of 12.11 ± 0.91 than the C:N ratio of the suspended sediments from the Ag stream (11.50 ± 0.63). The suspended sediments showed no significant difference in the stable isotopic compositions between the two streams (Fig. 6.6). The mean $\delta^{13}C$ for the forest stream were -30.25 ± 0.90 ‰ and -29.98 ± 0.73 for the Ag stream, respectively. Mean observed $\delta^{15}N$ were 5.81 ± 0.88 ‰ and 6.42 ± 2.17 ‰ in the forest and the Ag stream (Fig. 6.6).

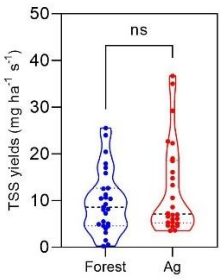

Fig. 6.3 Comparison of total suspended sediment (TSS) yields between the agricultural (red) catchment and the forest (blue) catchment. Dotted black lines indicate the median value for each site, and the dotted blue and red lines indicate the 25% and 75% quartiles.

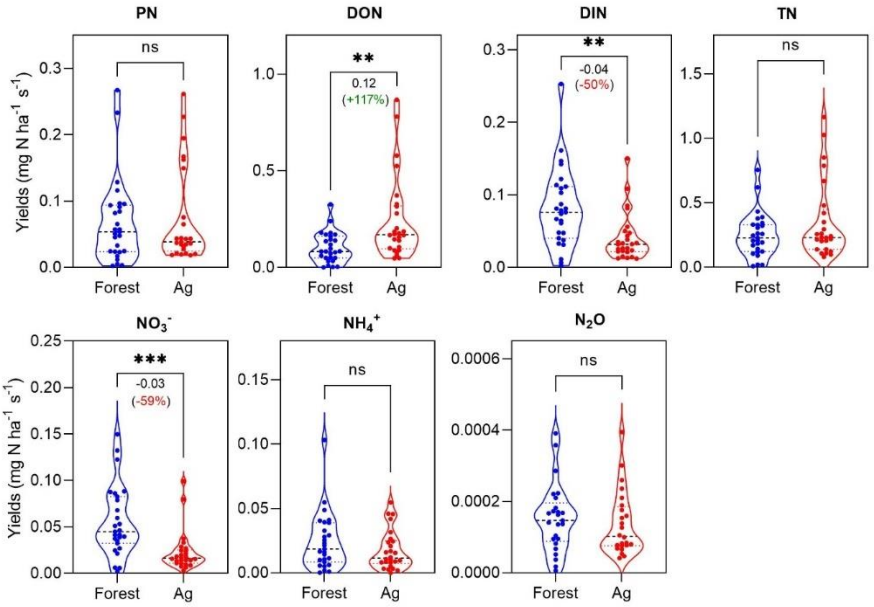

Fig. 6.4 Comparison of yields of particulate nitrogen (PN), dissolved organic nitrogen (DON), dissolved inorganic nitrogen (DIN), total nitrogen (TN), nitrate (NO_3^-), ammonia (NH_4^+), and nitrous oxide (N_2O) between the forest (blue) and agricultural (red) catchments. Stars indicate the significance obtained from the paired t-test, numbers show the differences between the means and the values between parentheses show the relative changes in yields. Dotted black lines indicate the median value for each site, and the dotted blue and red lines indicate the 25% and 75% quartiles.

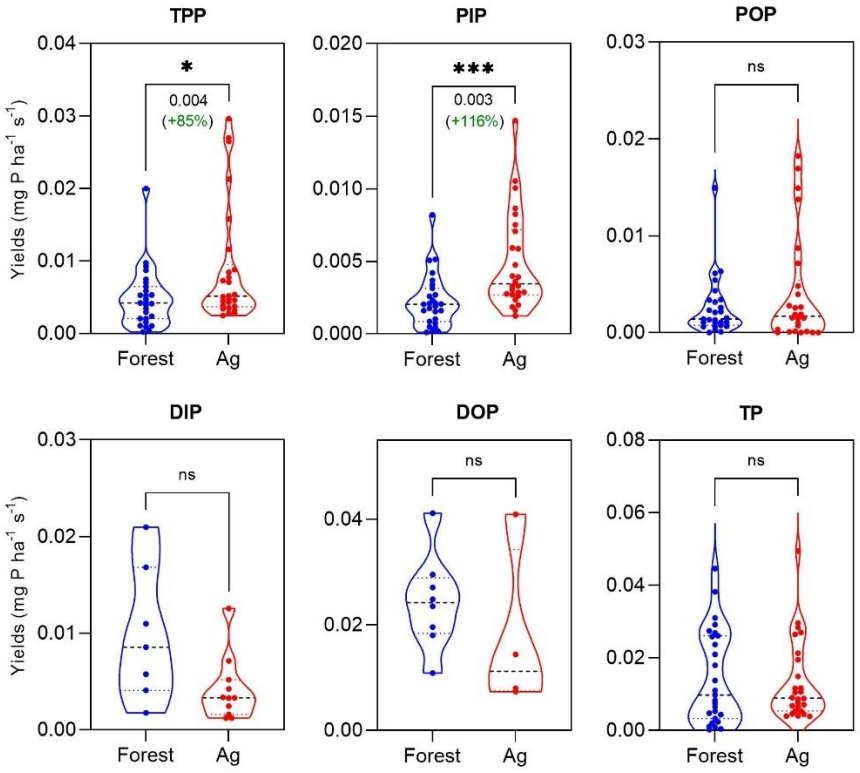

Fig. 6.5 Comparison of yields of total particulate phosphorus (TPP), particulate inorganic phosphorus (PIP), particulate organic phosphorus (POP), dissolved inorganic phosphorus (DIP), dissolved organic phosphorus (DOP), and total phosphorus (TP) between the forest (blue) and agricultural (red) catchments. Stars indicate the significance obtained from the paired t-test, numbers show the differences between the means and the values between parentheses show the relative changes in yields. Dotted black lines indicate the median value for each site, and the dotted blue and red lines indicate the 25% and 75% quartiles.

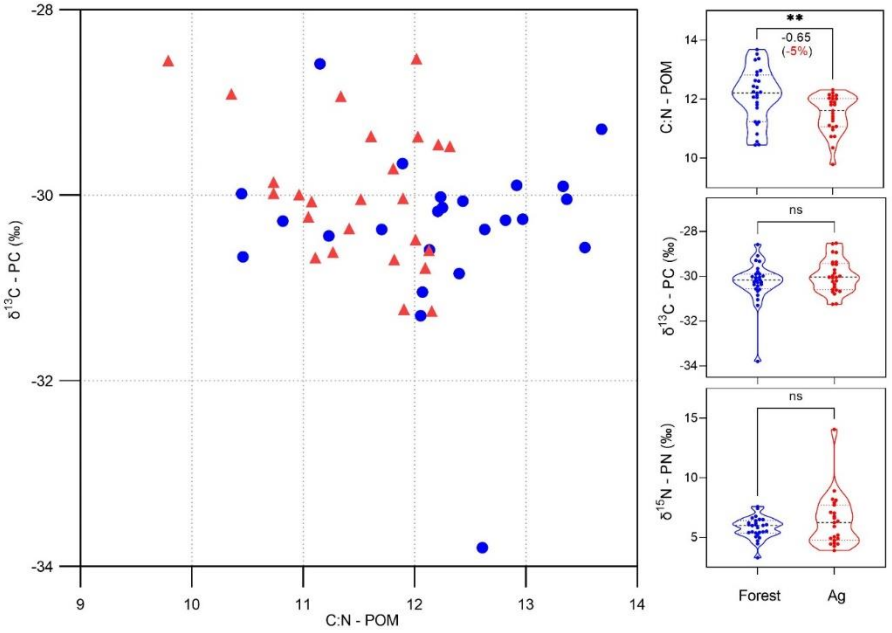

Fig. 6.6 Left panel: stable carbon isotope signature ($\delta^{13}C$) of the particulate organic C plotted against the C:N ratio of the particulate organic matter (POM). Triangles represent POM samples of the agricultural catchment, while round dots represent samples of the primary forest catchment. Right panels: C:N values of the POM samples from both catchments (top). $\delta^{13}C$ of the PC samples from both catchments (middle panel). $\delta^{15}N$ of the PN samples from both catchments (bottom panel). Stars indicate the significance obtained from the paired t-tests, numbers show the differences between the means and the values between parentheses show the relative changes in yields.

6.4. Discussion

6.4.1. Hydrology

Due to the proximity of the two catchments, we can assume that they received similar amounts of rainfall during the monitoring period. Although they received approximately same amount of rainfall, the drainage of the Ag catchment is higher compared to the forest catchment, resulting in a 60% higher ET within the forest catchment (Fig. 6.2), if we assume that there are no changes in water storage throughout the monitoring period at both sites. Higher ET within the forest was expected, because ET is driven by vegetation cover (Bosch & Hewlett, 1982), and increasing water yields up to 47% after LUC were observed in the tropics of Malaysia (Abdul Rahim, 1988). In contrast to other studies, where higher and more intense peak flow during storm events were observed in the Ag stream (da Silva et al., 2018), we observed higher specific peak flows for most of the events in the forest stream

(Fig. 6.2). This observation is most plausibly explained by the size difference of the catchment areas, as bigger catchments tend to have larger soil water storage capacities and longer response times, which buffer peak specific discharge during an event (Iroumé et al., 2005). Furthermore, the travel time of the water is greater in a bigger catchment resulting in longer but flatter storm event peaks, compared to the forest site where the short travel time resulted in quick but high Q peaks (Fig. 6.2). While higher ET within the forest catchment buffers the total annual discharge, higher soil water storage capacities and longer travel times buffer peak event specific Q during the short storm events.

6.4.2. Nutrient yields

In this section we discuss the influence of land use on the aquatic nutrient export during the ambient conditions that were sampled fortnightly. This grab sampling interval resulted in concentrations that were biased towards baseflow conditions, since storm events only occurred 5% of the year. The influence of storm events and the uncertainty that comes with missing peak flow samples will be discussed in the following section.

Lower nitrate export in the Ag stream

The only N yields that differed by land use were DON and NO_3^- (Fig. 6.4). While others reported differences in yields only due to an increase in water discharge and no difference in concentrations (Riskin et al., 2017), in this study the concentrations of DON and NO_3^- significantly differed as well with LUC (Appendix D1). There is a trend in the literature to higher concentrations of riverine DOM after deforestation (Gücker et al., 2016; Yamashita et al., 2010). This can have different reasons and mainly is attributed to a change in DOM sources with LUC (Yamashita et al., 2010). For example: it was shown that agricultural streams experienced higher allochthonous exports from agricultural areas to streams, as there is higher degradation of SOM stocks. Furthermore, in cropping systems, more DOM from root exudations is expected (Gücker et al., 2016). Higher DOM concentrations can explain the higher DON concentrations and yields in the agricultural stream of this study (Fig. 6.4). Ecosystems tend to lose a significant amount of N during deforestation, through the export of wood and burning of biomass and thus experience a tighter N cycle (Davidson et al., 2004). On the other hand, primary forests of the lowlands in the CRB are known to be rich in ecosystem N (Bauters et al., 2019; Chapter 5). NO_3^- is under strong biological control and ecosystems with a high N demand tend to lose less N in forms of NO_3^- (Vitousek & Reiners, 1975). This explains the higher NO_3^- concentrations and yields in the forest stream compared to the agricultural stream. TN yields did not significantly differ, but as seen in Appendix D2, the proportions of different N species changed: in the forest DIN, DON and PN contribute more evenly to TN yields while in the Ag stream TN export is dominated by DON, with a lower share of the DIN constituents. Although deforestation is known to increase physical soil erosion and sediment transport (Borrelli et al., 2017), no significant increase in PN yields in the Ag catchment was observed. Sediment exports in tropical headwater streams are known to be driven by storm events (Chapter 5; Taylor et al., 2015), thus total PN yields, and potentially the resulting total difference between the two study

catchments, was likely underestimated by our sampling approach that was biased toward baseflow conditions (see section 6.4.3).

Higher PIP yields in the Ag catchment

Agricultural land use resulted in higher TPP yields (Fig. 6.5). TPP yields from the Ag stream were 85% higher compared to the forest stream, mainly due to the increase in PIP (+116%). The particulate organic fraction did not show any difference (Fig. 6.5). PIP is mostly comprised of occluded phosphates incorporated into iron-hydroxides (Walker & Syers, 1976). Thus, agricultural land-use appears to result in higher yields of mineral particles even under baseflow conditions, due to higher susceptibility of the soils to erosion in the agricultural sites compared to the forested soils. That no difference was observed in POP export agrees well with the fact that PN yields also did not exhibit a significant difference. These results indicate that LUC mainly results in higher exports of mineral particulates under baseflow conditions.

For dissolved P, the same pattern is expected as for dissolved N: inorganic P, in form of DIP, is under biological control and demand is higher under shifting agriculture (Maranguit et al., 2017). The trend of lower DIP export in the Ag stream was observed, however, there is no significant effect (Fig. 6.5). A detectable and significant effect might have been precluded by the low concentrations of DIP in the stream water, which were close to the detection limit of the measurement method. In the forest stream, only seven samples out of 21 showed PO_4^{3-} concentrations exceed the detection limit of 0.01 mg L^{-1}, whereas in the Ag stream 11 samples exhibited detectable concentrations. We faced the same problem with the DOP samples, however, there even fewer samples that exceeded the detection limit (seven in the forest stream and four in the Ag stream).

6.4.3. Missing storm event samples drive uncertainty

Although it is known that deforestation leads to higher erosion rates and subsequently higher TSS yields (Messina & Biggs, 2016; Riskin et al., 2017), no differences were observed in our paired watershed when comparing instantaneous yields derived from fortnightly concentration samples. However, sampling was only conducted during baseflow and thus the influence of storm events was mostly excluded from our dataset. Nonetheless, the availability of continuous turbidity and fDOM data allows a window into the behaviour of our catchments during storm events.

Turbidity is a good proxy for sediment exports in our streams. To compare turbidity timeseries between the two sites, we normalized the measured NTU values to the catchment area to get a measure of "turbidity yield" (Fig. 6.2). With this we were able to show that annual turbidity yields were indeed significantly higher (+87%) in the Ag stream compared to the forest stream. Thus, real annual TSS yields are most likely also higher in the same order of magnitude. For the forest catchment, it was previously shown that sediment and PN exports were disproportionally driven by storm events (Chapter 2). Given the lower protection due to less vegetation cover and the more pervasive soil disturbance in the agricultural catchment, an 85%

increase in TSS export driven by storm events is plausible. Because PN is generally proportional to TSS (Taylor et al., 2015), turbidity also is a proxy for sediment associated PN export. Thus, although no difference was seen for baseflow PN yields (Fig. 6.4), the inclusion of storm events most likely also results in higher PN exports by around 85 % due to land use (Fig. 6.2).

In the same way that turbidity is a proxy for the concentrations of particulates, fDOM tracks the changes in DOM concentrations, thus having a close relationship to DON (Appendix D3). While during baseflow DON yield was 117% higher in the Ag stream (Fig. 4), fDOM yields throughout the hydrological year were 360% higher in the Ag stream compared to the forest stream (Fig. 6.2). By applying linear models between fDOM and DON concentrations, the annual DON yield calculated with the fDOM values is around 250% higher in the Ag stream than in the forest stream. However, as fDOM is an optical measurement, results are influenced by the turbidity of the stream water. At high turbid water conditions, measured fDOM generally underestimate the real fDOM values (de Oliveira et al., 2018). Due to the general higher turbidity values in the Ag stream, the real fDOM yield was probably even higher than the 360% increase. This indicates that the inclusion of storm events likely doubles the increase of DON yields compared to only the baseflow data, highlighting that storm events are also crucial for the transport of dissolved organic constituents.

6.4.4. POM sources

The analysis of the chemical and isotopic composition of the POM showed that there is only a marginal difference between the POM originated from the forest and the POM originated from the agricultural site (Fig. 6.6). The $\delta^{13}C$ and C:N ratios indicates that in both sites, the POM mainly originates from organic materials of surface vegetation (Chapter 2). The slight shift of lower C:N ratios of the Ag stream POM, indicates a slight shift to a POM source that comes from slightly deeper soil layers, compared to the forest POM. Other studies showed much more pronounced changes in isotopic and chemical signatures of organic material exported (Drake et al., 2019; Moyer et al., 2013; Zhang et al., 2021), however, all these studies were conducted in steeper catchments, where erosion rates were much higher.

Conclusion

Although no differences in TN and TP exports were detectable between a headwater stream draining shifting agricultural land and a headwater stream draining pristine lowland forest, a significant shift from more DIN export in the forest stream to more DON export in the Ag stream visible. Slash and burn practices are known to promote loss of available N in an ecosystem and we were able to show this with higher NO_3^- concentrations and yields in the forest stream, while the agricultural stream exported more DON. Although sediment exports were similar in both catchments, the agricultural stream yielded significantly higher particulate forms of P. This was mainly attributed to an increase in PIP, which showed that LUC triggered the loss of mineral particles. This trend was also corroborated by the generally lower C:N ratios of the agricultural POM. The monitoring of storm events with in-situ sensors allowed

us to conclude, that the measured differences of TSS and DOM export, are most likely underestimated due to the sampling approach that only covered baseflow samples.

Acknowledgments

We thank the villagers of Balifi and Yoko for their support and hospitality towards our research project and Héritier Ololo Fundji for his assistance and organizational talent throughout the monitoring years. We also thank Katja Van Nieuland and Samuel Bodé for their help with the sample analysis. This research has been funded by the Fond de la Recherche Scientifique – FNRS (project numbers: T.0059.18 and J.0167.19) and ETH Zürich core funding.

Supporting information

Supporting information to this chapter can be found in Appendix D

Appendix D1: Comparison of different N and P concentrations between the forest (blue) and agricultural (red) catchments. Stars indicate the significance obtained from the paired t-test, numbers show the differences between the means and the values between parentheses show the relative changes in yields. Dotted black lines indicate the median value for each site, and the dotted blue and red lines indicate the 25% and 75% quartiles

Appendix D2: Average measured instantaneous yields of different nitrogen (top) and phosphorus (bottom) constituents for the forest catchment (blue) and the agricultural catchment (red). Error bars indicating standard deviation of the mean. Percentages show the relative contribution of each constituent to the total N or P yields.

Appendix D3: Relations between fluorescent dissolved organic matter (fDOM) and dissolved organic nitrogen (DON) from the forest stream (left) and the agricultural stream (right). Blue lines indicate the linear regression with its confidence intervals in grey.

Appendix D4: Timeseries of measured water discharge and measured concentrations of particulate nitrogen (PN), dissolved organic nitrogen (DON), dissolved inorganic nitrogen (DIN), total particulate phosphorus (TPP), particulate inorganic phosphorus (PIP), dissolved organic phosphorus (DOP), and phosphate (PO_4^{3-}) from the agricultural stream and the forest stream. Red values indicate the Ag samples and blue values the Forest samples.

Conclusions & Outlook

Chapter 7: Synthesis

7.1 Erosion and aquatic nutrient export

Physical erosion is known as a threat to soil fertility, especially in landscapes under no natural vegetation. However, the influence of erosion on the biogeochemistry of pristine tropical forests has been widely neglected. For sure, the risk of mass movements, such as landslides, is enormously reduced in pristine forest ecosystems and the total aquatic sediment export is reduced by orders of magnitude. Thus, speaking of physical soil erosion in tropical forests, we must be aware that most landscapes are in a steady state, meaning soil formation- and soil loss processes are balanced out (this is especially true for the geomorphic stable sites of the lowland forest and Miombo woodland). However, by measuring the suspended sediment export at the three study sites of this thesis, we were able to show that TSS yields were substantial and that even the lowland forest and Miombo woodland showed similar sediment exports as tropical montane forests in other regions (Table 2.1). Although for the lowland and montane forests, no direct influence of erosion on the openness of soil N cycling was detectable (Fig. 5.3), the high exports of particulate matter play an important role in the loss of particulate associated nutrients. Surprisingly enough, the site with lower impact of erosion on aquatic nutrient exports (PN and TPP yields were lower in the Miombo than in the lowland forest, although they experienced the same TSS yields) was the only site showing a significant influence of erosion on the openness of soil N cycling (Fig. 5.3). This might be due to the general higher N content in the moist forests, which are due to high atmospheric deposition rates (Bauters et al., 2018), while the Miombo received far less N inputs (Table 3.2). Thus, it is possible, that in a system without high N surplus, the erosional losses of soil PN can lead to locally more conservative N cycling in steeper slopes, where the soils are more prone to erosion. For the lowland and montane forest, the N surplus is likely too high for erosion to affect soil N on topographical scale (especially in the montane forest with higher erosion rates). However, we have to be aware of the limitations of the methods applied in Chapter 5. To assess the influence of erosion on N cycling the ^{15}N signatures of topsoil samples from 0-20 cm were analyzed. In retrospect this approach was not ideal, as the $\delta^{15}N$ values in the top 20 cm of the soil profiles are quite variable (Fig. 5.2) and samples from the top 0-2 cm of the soil profiles would have been better to tackle our research questions. Furthermore, to assess differences in N cycling and N availabilities on a topographical scale, a more in-depth sampling approach covering (gross) N turnover rates (mineralization-, nitrification- and denitrification rates) is necessary, as it was done in tropical forests of Costa Rica (Weintraub et al., 2015). Furthermore, this thesis did not cover erosion induced differences in P cycling. It has to be stated that measurements of mineralization rates of organic P in soils are not easy to conduct due to the rapid sorption of mineralized P. Thus, isotopic tracers in incubation experiments are needed (Bünemann, 2015).

Even though, we could not find any evidence that erosion has a negative impact on the availability of nutrients in wet tropical forests of the Congo Basin, particulate forms of these nutrients are important constituents in total aquatic losses. Although

the Central African tropics receive much less precipitation than tropical forests in south America and southeast Asia, we were able to highlight the importance of aquatic particulate nutrient exports in low erosive systems. By analyzing the underlying mechanisms of the sediment exports in Chapter 2, we were able to highlight the importance of storm events on the annual sediment yields. This influence of storm events is also the reason for the limitations of Chapter 6. Due to security issues, the installed autosampler at the agricultural stream was never able to perform its duty. But given the results from Chapters 2 and 3, it is obvious that calculated yields of organic and particulate nutrients were underestimated with only the baseflow samples. However, our study approach revealed that more DON and PIP get exported in the agricultural stream even during baseflow conditions. In the future, the Congo Basin is projected to experience increase in primary forest loss (Tyukavina et al., 2018) and in rainfall intensity (Haensler et al., 2013). The results of this thesis showed that both changes will affect the aquatic nutrient export, by increasing the losses of mainly dissolved organic and particulate forms of N and P.

In the introduction, a link to earth system models (ESM) was made. For example, from the ESMs that are contributing to the newest Coupled Model Intercomparison Project (CMIP6), at least 10 models incorporate N transformations (Arora et al., 2020). These models consider different N inputs and outputs out of the system. Most of the N losses are calculated through denitrification and leaching losses (Davies-Barnard et al., 2020), while erosional N losses are never considered. However, our results from Chapter 3 showed that PN export are actually counterbalancing a considerable part of the N deposition rates that are considered for ESMs (around 5 kg N ha^{-1} yr^{-1}; Zak et al., 2017; Wang et al., 2018) with the PN losses of 3.3 kg N ha^{-1} yr^{-1} for the lowland forest. By incorporating these PN losses, N accumulation would be drastically reduced in those models with possible important impacts on the overall outcome of those ESMs. However, it has to be mentioned that the used atmospheric deposition of 5 kg N ha^{-1} yr^{-1} is also highly underestimating the measured N depositions at the lowland site (Table 3.2).

Although I was able to collect a rich dataset, not all the obtained results can be yet explained and would need further research to fully understand the underlying processes. For example: In Chapter 3 the N:P ratios of the dissolved organic fraction are low in both streams (mean DON:DOP in Miombo 6.6 and in Lowland 19.5). These ratios raise the question of possible sources of this dissolved organic matter or about possible in stream decomposition processes. To better understand export processes probably incubation studies of river water of these forest streams would be necessary. Furthermore, the results from Chapter 6 only showed the different in aquatic nutrient export of two catchments under different land use. However, if we want to examine the effect of deforestation on aquatic nutrient export, more streams within a succession (from freshly deforested catchments to fields with multiply slash-and-burn cycles) need to be studied. However, this will be challenging as deforestation is happening locally and headwater stream catchments will cover more than one stage of a succession. The most reliable results would be obtained if a catchment consisting of primary forest was monitored before the forest within the

same catchment gets cut and transformed to agricultural land. However, such a study is time intensive and needs close collaboration with local authorities.

7.2 Fate of exported material

This thesis had a narrow focus on headwater streams; thus, a nutrient or sediment export was defined as whatever passed our point of sampling. So far, I did not discuss what happens to these constituents downstream of the flumes. However, it is interesting to think about the fate of these nutrients and sediments on a bigger scale. The export out of the forest ecosystem means that these constituents are entering other systems. Sediments are either ending up in larger waterbodies (the Congo River and then the Atlantic Ocean) or are deposited somewhere in floodplains, most likely in the Cuvette Centrale or Pool Malebo (Laraque et al., 2009; Mushi et al., 2019). By upscaling the TSS and PN yields from the headwater streams (Chapters 2 and 3) to the Congo Basin (assuming 35% of the basin is covered with evergreen forest – similar to the lowland forest of this study- and 35% is covered with deciduous broadleaved forest – similar to the Miombo site (Verhegghen et al., 2012)), those headwater streams would be responsible for a total sediment export of 6.4 Tg and a PN export of 0.06 Tg over a year at the Congo River outlet. This is around 22% of the annual TSS yield and 28% of the annual PN yield measured by Spencer et al. (2016) at the Congo River in Kinshasa. The underestimation is possible due to the fact that the other 30% of the CRB is covered by grassland and croplands and TSS and PN yields are expected to be higher there compared to pristine forests (Chapter 6).

Furthermore, all these processes in headwater streams influence downstream water quality. High concentrations of dissolved nutrients can lead to eutrophication in streams and especially coastal regions where the riverine water ends up in the ocean (Rabalais et al., 2009). However, also POM in coastal sediments is shown to be susceptible to mineralization and the release of bioavailable forms of N and P was reported (Lønborg et al., 2018). Around 80% of the total riverine organic matter load is ending up in coastal zones of the world's oceans (Gattuso et al., 1998). These coastal zones are hotspots for marine biogeochemistry and ecology and different processes, such as burial and mineralization of the organic matter reduce the export into the open oceans (Bouillon & Connolly, 2009), however, the plume of the Congo River into the Atlantic Ocean can still reach up to 800 km offshore (Schefuß et al., 2004). Thus, changes in riverine exports of particulate and dissolved nutrients, which starts at the headwater scale, will ultimately also affect the biogeochemistry of the coastal zones of the oceans which can influence important ecological processes.

7.3 Rethinking old paradigms

Nutrients play a crucial role in forest functioning and their availability is governing the role of forest ecosystems in the global climate system (Fernández-Martínez et al., 2014; Vicca et al., 2012; Y. P. Wang et al., 2010). In the introduction of this thesis, I described the long-lasting paradigm of N-rich and P-poor tropical forests on old-growth soils of the lowlands, while montane forests on younger soils experience the opposite trend of N-poor and P-rich conditions. Assessing the nutrient availability in forests remains a challenge given the variety and limitations of current methods. For

example, there are different ways to investigate whether a nutrient is cycled in excess or if it is conservatively recycled, such as with foliar ratios of nutrients and C (Townsend et al., 2008), measuring rates of N and P turnover and mineralization in soils (Davidson et al., 2000), or focusing on ecosystem losses of different nutrient species (Hedin et al., 2003). In the case of Hedin et al. (2003), they found that inorganic N losses follow the availability of nutrients in an ecosystem, i.e. higher N availability resulted in higher DIN losses. Assuming higher N availability in the lowland forest, DIN losses should be more important compared with DIN losses in the montane forest. However, measured DIN yields from the montane forest were higher than from the lowland forest and DON export was more important than DIN in both forests (Chapters 3 and 4). The same applies for P: the supposedly P rich montane forest showed the same pattern as the "p-limited" lowland forest, with DOP yields surpassing DIP yields, however, DIP yields of the montane forest were by a factor 5 higher than the lowland forest. These old-lived paradigms occurred due to the lack of quantification of the whole nutrient cycles: mainly bioavailable forms of N and P were considered in biogeochemical studies covering tropical forests. However, when including organic N and P forms, the whole story shifts. The introduction of DON losses by Hedin et al. (2003) lead to the "N leak hypothesis" (see 3.1). By including organic atmospheric N deposition, Bauters et al. (2018) showed that roughly half of the total N deposition is in form of organic N. This means that if the focus was only on reactive inorganic N, the actual deposited N would have been underestimated by more than half. While Taylor et al. (2015) proposed to extend the DON-leak hypothesis with a PN-leak, it was never clear how important particulate forms of nutrient export are in "low-erosive" systems. With the results presented in Chapters 4 and 5 it is now obvious, that big parts of the N-leak of ecosystems is indeed in particulate forms, even in the stable lowland forest. Furthermore, our approach showed that there is also a "P-leak" in forest ecosystems, with DOP and particulate P losses driven by the hydrologic regime.

7.3 Biogeochemistry in the Congo

Biogeochemical cycles in tropical forests are diverse and varying enormously on local and global scale. So far, research focus, for a better understanding of forest functioning, was mainly centered around the Neotropics and tropical regions of south-east Asia, while the Afrotropics received much less attention (Verbeeck et al., 2011). This is especially worrying as there are fundamental differences between Neo- and Afrotropical forests in terms of biodiversity (Slik et al., 2015) and structure (Lewis et al., 2013). This geographical bias occurs not only for research efforts, also financial aids for forest conservation is unequally distributed, with southeast Asia and the Amazon receiving more financial flows into sustainable projects than the African tropics (Atyi et al., 2019), although the high importance of the central African forests on the global climate is well known. This imbalance just recently led politicians and scientists to call for investments into research within the Congo Basin (White et al., 2021). This thesis aimed to counteract those geographical bias by covering the heterogenous landscapes of the Congo Basin. Although missing infrastructure and local insecurities might hinder instalments of monitoring plots, putting this extra effort is invaluable and the possible returns are enormous. I am

happy that I was able to collaborate with different international research groups to conduct research in the Congo and that these groups continue working in the Congo with ongoing and new projects. However, it is crucial that also the local collaborators are involved and that there will be a new generation of local researcher that are leading these research efforts.

The main part of this thesis was centered around the approximately two years of headwater stream monitoring at four different sites in the Congo. This work absorbed me more than I would have liked, as over most of the time, it felt like everything that could go wrong did go wrong. Nonetheless, with some temporal distance after finishing the monitoring work, I am proud of the dataset we were able to generate. I want to use this last paragraph of my thesis to reflect on my approach on the challenging fieldwork and think about how a similar monitoring approach can be improved, with the experience I gained during this PhD. Many challenges were of technical nature, mainly getting reliable power supply for the loggers, sensors and autosamplers. Looking back, I think a monitoring in remote places should be as "low-tech" as possible. For example: We installed CO_2-probes at the lowland sites and connected it to the same datalogger with the pressure transducer. However, the high energy consumption of this probe drained the batteries so fast, that a bi-weekly replacement of the battery was not enough. While sensor data is nice to have, we have to really think about what is necessary. Continuous water level data, and thus discharge data, is invaluable and should be available for longer time. However, there are small pressure transducer with internal battery and logger available and they allow to get reliable discharge data with little risk of data loss due to theft and battery failure. Although turbidity measurements are crucial to measure sediment exports the installation of a turbidity probe is already more problematic as most of the sensors rely on an external battery and datalogger or are just too big and thus more susceptible to theft. For future campaigns in remote regions of the DRC, short but intense field campaigns, with turbidity probes and autosampler, might be the way to go. For example, for just two weeks in each season the installation is fully equipped with turbidity sensor and autosampler to get a high temporal coverage of samples. During these short campaigns, it is easier to guard the expensive equipment and for the rest of the year a simpler setup with just a pressure transducer for discharge measurements and weekly to fortnightly sampling is enough. Furthermore, it is crucial to get the local people of the nearby villages involved as soon as possible. Their knowledge of the region can already help in the site selection and a good relationship with the local population can help in securing the installations. All in all, long term monitoring of headwater streams in the Congo remains a challenge and there will never be a guarantee that the data collection works as planned. However, with some simple measures and precautions, the risk can be reduced.

References

Abdul Ramir, N. (1988). Water yield changes after forest conversion to agricultural landuse in peninsular malaysia. *Journal of Tropical Forest Science 1(1)*, 68-84.

Alsdorf, D., Beighley, E., Laraque, A., Lee, H., Tshimanga, R., O'Loughlin, F., Mah??, G., Dinga, B., Moukandi, G., & Spencer, R. G. M. (2016). Opportunities for hydrologic research in the Congo Basin. *Reviews of Geophysics*, *54*(2), 378–409. https://doi.org/10.1002/2016RG000517

Alvarez-Clare, S., Mack, M. C., & Brooks, M. (2013). A direct test of nitrogen and phosphorus limitation to net primary productivity in a lowland tropical wet forest. *Ecology*, *94*(7), 1540–1551. https://doi.org/10.1890/12-2128.1

Amundson, R., Austin, A. T., Schuur, E. A. G., Yoo, K., Matzek, V., Kendall, C., Uebersax, A., Brenner, D., & Baisden, W. T. (2003). Global patterns of the isotopic composition of soil and plant nitrogen. *Global Biogeochemical Cycles*, *17*(1). https://doi.org/10.1029/2002GB001903

Anache, J. A. A., Wendland, E. C., Oliveira, P. T. S., Flanagan, D. C., & Nearing, M. A. (2017). Runoff and soil erosion plot-scale studies under natural rainfall: A meta-analysis of the Brazilian experience. *Catena*, *152*, 29–39. https://doi.org/10.1016/j.catena.2017.01.003

Angelini, M. E., Heuvelink, B. M., & Kempen, B. (2017). Multivariate mapping of soil with structural equation modelling. *European Journal of Soil Science, 68,* 575-591. https://doi.org/10.1111/ejss.12446

Archard, F., Beuchle, R., Mayaus, P., Stibig, H., Bodart, C., Brink, A., Carboni, S., Desclée, B., Donnay, F., Eva, H. D., Lupi, A., Rasi, R., Seliger, R., & Simonetti, D. (2014). Determination of tropical deforestation rates and related carbon losses from 1990 to 2010. *Global Change Biology, 8(20),* 2540-2554. https://doi.org/10.1111/gcb.12605

Arora, V. K., Katavouta, A., Williams, R. G., Jones, C. D., Brovkin, V., Friedlingstein, P., Schwinger, J., Bopp, L., Boucher, O., Cadule, P., Chamberlain, M. A., Christian, J. R., Delire, C., Fisher, R. A., Hajima, T., Ilyina, T., Joetzjer, E., Kawamiya, M., Koven, C. D., Krasting, J. P., Law, R. M., Lawrence, D. M., Lenton, A., Lindsay, K., Pongratz, J., Raddatz, T., Séférian, R., Tachiiri, K., Tjiputra, J. F., Wiltshire, A., Wu, T., & Ziehn, T. (2020). Carbon-concentration and carbon-climate feedbacks in CMIP6 models and their comparison to CMIP5 models. *Biogeosciences*, *17*, 417-4222. https://doi.org/10.5194/bg-17-4173-2020

Asner, G. P., Anderson, C. B., Martin, R. E., Tupayachi, R., Knapp, D. E., & Sinca, F. (2015). Landscape biogeochemistry reflected in shifting distributions of chemical traits in the Amazon forest canopy. *Nature Geoscience*, *8*(7), 567–575. https://doi.org/10.1038/ngeo2443

References

Atyi, R. E., Liboum, M., Guizol, P., Awono, A., Jungers, Q., D.S.D., P., Sonwa, D. J., Palla, F., Sufo-Kankeu, R., & Djossi, D. (2019). International financial flows to support nature protection and sustainable forest management in Central Africa. *Central African Forest Observatory*, *3*, 1–8. https://www.cifor.org/knowledge/publication/7392

Austin, A. T., & Vitousek, P. M. (1998). Nutrient dynamics on a precipitation gradient in Hawai'i. *Oecologia*, *113*, 519–529. https://doi.org/10.1007/978-3-642-78568-9_6

Baade, J., Franz, S., & Reichel, A. (2012). Reservoir siltation and sediment yield in the kruger national park, South Africa: A first assessment. *Land Degradation and Development*, *23*(6), 586–600. https://doi.org/10.1002/ldr.2173

Bača, P. (2008). Hysteresis effect in suspended sediment concentration in the Rybárik basin, Slovakia. *Hydrological Sciences Journal*, *53*(1), 224–235. https://doi.org/10.1623/hysj.53.1.224

Baccini, A., Walker, W., Carvalho, L., Farina, M., & Houghton, R. A. (2019). Response to Comment on "Tropical forests are a net carbon source based on aboveground measurements of gain and loss." *Science*, *363*(6423), 230–234. https://doi.org/10.1126/science.aat1205

Bagalwa, M., Majaliwa, J. G. M., Bootsma, H., Karume, K., Akello, S., & Kansiime, F. (2021). Spatio-Temporal Variation of Atmospheric Nutrient Deposition in Different Land Uses/Covers around Lake Kivu. *Journal of Water Resource and Protection*, *13*(09), 699–725. https://doi.org/10.4236/jwarp.2021.139037

Bagalwa, R. M., Chartin, C., Baumgartner, S., Mercier, S., Syauswa, M., Samba, V. C., Zabona, M. T., Karume, K., Cizungu, N. L., Barthel, M., Doetterl, S., Six, J., Boeckx, P., & Van Oost, K. (2021). Spatial and seasonal patterns of rainfall erosivity in the Lake Kivu region: Insights from a meteorological observatory network. *Progress in Physical Geography: Earth and Environment*. https://doi.org/10.1177/03091333211001793

Baharuddin, K. (1988). Effect of logging on sediment yield in a hill dipterocarp forest in peninsular Malaysia. *Journal of Tropical Forest Science*, *1*(1), 56–66.

Baharuddin, K., & Abdul, R. N. (1994). Suspended sediment yield resulting from selective logging practices in a small watershed in peninsular Malaysia. *Journal of Tropical Forest Science*, *7*(2), 286–295.

Baisden, W. T., Amundson, R., Brenner, D. L., Cook, A. C., Kendall, C., & Harden, J. W. (2002). A multiisotope C and N modeling analysis of soil organic matter turnover and transport as a function of soil depth in a California annual grassland soil chronosequence. *Global Biogeochemical Cycles*, *16*(4), 82-1-82–26. https://doi.org/10.1029/2001gb001823

Balakrishna, K., & Probst, J. L. (2005). Organic carbon transport and C/N ratio variations in a large tropical river: Godavari as a case study, India.

Biogeochemistry, *73*(3), 457–473. https://doi.org/10.1007/s10533-004-0879-2

Baldwin, D. S., Howitt, J. A., & Beattie, J. K. (2005). Abiotic degradation of organic phosphorus compounds in the environment. In B. L. Turner, E. Frossard, & D. S. Baldwin (Eds.), *Organic Phosphorus in the Environment* (pp. 75–88). CABI. https://doi.org/10.1079/9780851998220.0075

Banin, L., Feldpausch, T. R., Phillips, O. L., Baker, T. R., Lloyd, J., Affum-Baffoe, K., Arets, E. J. M. M., Berry, N. J., Bradford, M., Brienen, R. J. W., Davies, S., Drescher, M., Higuchi, N., Hilbert, D. W., Hladik, A., Iida, Y., Salim, K. A., Kassim, A. R., King, D. A., … Lewis, S. L. (2012). What controls tropical forest architecture? Testing environmental, structural and floristic drivers. *Global Ecology and Biogeography*, *21*(12), 1179–1190. https://doi.org/10.1111/j.1466-8238.2012.00778.x

Barron, A. R., Purves, D. W., & Hedin, L. O. (2011). Facultative nitrogen fixation by canopy legumes in a lowland tropical forest. *Oecologia*, *165*(2), 511–520. https://doi.org/10.1007/s00442-010-1838-3

Barthel, M., Bauters, M., Baumgartner, S., Drake, T. W., Bey, N., Bush, G., Boeckx, P., Botefa, C. I., Dériaz, N., Ekamba, G., Gallarotti, N., Mbayu, F., Mugula, J., Makelele, I., Mbongo, C., Mohn, J., Mandea, J., Mpambi, D., Ntaboba, L., Rukeza, M., Spencer, R., Summerauer, L., Vanlauwe, B., Van Oost, K., Wolf, B., & Six, J. (2022). Low N_2O and variable CH_4 fluxes from tropical forest soils of the Congo Basin. *Nature Communications.*

Baumgartner, S., Barthel, M., Drake, T., Bauters, M., Makelele, I. A., Mugula, J. K., Summerauer, L., Gallarotti, N., Ntaboba, L. C., Van Oost, K., Boeckx, P., Doetterl, S., Werner, R., & Six, J. (2020). Seasonality, drivers, and isotopic composition of soil CO_2 fluxes from tropical forests of the Congo Basin. *Biogeosciences*, 1–22. https://doi.org/10.5194/bg-2020-133

Baumgartner, S., Bauters, M., Barthel, M., Alebadwa, S., Bahizire, N., Sumaili, C., Ngoy, D., Kongolo, M., Mujinya, B., Cizungu, L., Six, J., Boeckx, P., Oost, K. Van, & Drake, T. W. (2022). Fluvial sediment export from pristine forested headwater catchments in the Congo Basin. *Geomorphology*, *398*, 108046. https://doi.org/10.1016/j.geomorph.2021.108046

Baumgartner, S., Bauters, M., Barthel, M., Drake, T. W., Ntaboba, L. C., Bazirake, B. M., Six, J., Boeckx, P., & Van Oost, K. (2021). Stable isotope signatures of soil nitrogen on an environmental-geomorphic gradient within the Congo Basin. *SOIL*, *7*, 83–94. https://doi.org/10.5194/soil-7-83-2021

Bauters, M., Drake, T. W., Verbeeck, H., Bodé, S., Hervé-Fernandez, P., Zito, P., Podgorski, D. C., Boyemba, F., Makelele, I., Ntaboba, L. C., Spencer, R. G. M., & Boeckx, P. (2018). High fire-derived nitrogen deposition on central African forests. *Proceedings of the National Academy of Sciences*, 1–6. https://doi.org/10.1073/pnas.1714597115

References

Bauters, Marijn, Drake, T. W., Wagner, S., Baumgartner, S., Makelele, I. A., Bodé, S., Verheyen, K., Verbeeck, H., Ewango, C., Cizungu, L., Oost, K. Van, & Boeckx, P. (2021). Fire-derived phosphorus fertilization of African tropical forests. *Nature Communications*, 1–8. https://doi.org/10.1038/s41467-021-25428-3

Bauters, Marijn, Mapenzi, N., Kearsley, E., Vanlauwe, B., & Boeckx, P. (2016). Facultative nitrogen fixation by legumes in the central Congo basin is downregulated during late successional stages. *Biotropica*, *48*(3), 281–284. https://doi.org/10.1111/btp.12312

Bauters, Marijn, Taveirne, C., Van Der Heyden, D., Boeckx, P., Verbeeck, H., Demol, M., Bruneel, S., & Cizungu, L. (2017). Parallel functional and stoichiometric trait shifts in South American and African forest communities with elevation. *Biogeosciences*, *14*(23), 5313–5321. https://doi.org/10.5194/bg-14-5313-2017

Bauters, Marijn, Verbeeck, H., Rütting, T., Barthel, M., Bazirake Mujinya, B., Bamba, F., Bodé, S., Boyemba, F., Bulonza, E., Carlsson, E., Eriksson, L., Makelele, I., Six, J., Cizungu Ntaboba, L., & Boeckx, P. (2019). Contrasting nitrogen fluxes in African tropical forests of the Congo Basin. *Ecological Monographs*, *0*(0), 1–15. https://doi.org/10.1002/ecm.1342

Beer, C., Reichstein, M., Tomelleri, E., Ciais, P., Jung, M., Carvalhais, N., Rödenbeck, C., Arain, M. A., Baldocchi, D., Bonan, G. B., Bondeau, A., Cescatti, A., Lasslop, G., Lindroth, A., Lomas, M., Luyssaert, S., Margolis, H., Oleson, K., Roupsard, O., … Papale, D. (2010). Terrestrial Gross Carbon Dioxide Uptake: Global Distribution and Covariation with Climate. *Science*, *329*(August), 834–839.

Benkobi, L., Trlica, M., & Smith, J. (1994). Evaluation of a redefined surface cover subfactor for use in RUSLE. *Journal of Range Management, 47,* 74-78.

Berhe, A. A., Barnes, R. T., Six, J., & Marin-Spiotta, E. (2018). Role of Soil Erosion in Biogeochemical Cycling of Essential Elements: Carbon, Nitrogen, and Phosphorus. *Annual Review of Earth and Planetary Sciences, 46,* 521-548. https://doi.org/10.1146/annurev-earth-082517-010018

Biggs, T. W., Dunne, T., & Martinelli, L. A. (2004). Natural controls and human impacts on stream nutrient concentrations in a deforested region of the Brazilian Amazon basin. *Biogeochemistry*, *68*(2), 227–257. https://doi.org/10.1023/B:BIOG.0000025744.78309.2e

Blackmer, A. M., & Bremner, J. M. (1977). Nitrogen isotope discrimination in denitrification of nitrate in soils. *Soil Biology and Biochemistry*, *9*(2), 73–77. https://doi.org/10.1016/0038-0717(77)90040-2

Bobbink, R., Hicks, K., Galloway, J., Spranger, T., Alkemade, R., Ashmore, M., Bustamante, M., Cinderby, S., Davidson, E., Dentener, F., Emmett, B., Erisman, J. W., Fenn, M., Gilliam, F., Nordin, A., Pardo, L., & De Vries, W. (2010). Global assessment of nitrogen deposition effects on terrestrial plant

diversity: A synthesis. *Ecological Applications*, *20*(1), 30–59. https://doi.org/10.1890/08-1140.1

Boeckx, P., Paulino, L., Oyarzún, C., Cleemput, O. V. A. N., & Godoy, R. (2005). Soil δ 15 N patterns in old-growth forests of southern Chile as integrator for N-cycling. *Isotopes in Environmental and Health Studies*, *41*(3), 249–259.

Borrelli, P., Robinson, D. A., Fleischer, L. R., Lugato, E., Ballabio, C., Alewell, C., Meusburger, K., Modugno, S., Schütt, B., Ferro, V., Bagarello, V., Oost, K. Van, Montanarella, L., & Panagos, P. (2017). An assessment of the global impact of 21st century land use change on soil erosion. *Nature Communications*, *8*(1). https://doi.org/10.1038/s41467-017-02142-7

Bosch, J. M., & Hewlett, J. D. (1982). A review of catchment experiments to determine the effect of vegetation changes on water yield and evapotranspiration. *Journal of Hydrology*, *55*(1–4), 3–23. https://doi.org/10.1016/0022-1694(82)90117-2

Bouillon, S., & Connolly, R. M. (2009). Carbon Exchange Among Tropical Coastal Ecosystems. In I. Nagelkerken (Ed.), *Ecological Connectivity among Tropical Coastal Ecosystems* (pp. 45–70). Springer Netherlands. https://doi.org/10.1007/978-90-481-2406-0_3

Bow, J., Brown, M., & Sayre, R. (2009). African Surficial Lithology Database. Africa Terrestrial Ecological Footprint Mapping Project. *The Nature Conservancy and U.S. Geological Survey.* Arlington and Reston, Virginia.

Brasington, J., & Richards, K. (2000). Turbidity and suspended sediment dynamics in small catchments in the Nepal Middle Hills. *Hydrological Processes*, *14*(14), 2559–2574. https://doi.org/10.1002/1099-1085(20001015)14:14<2559::AID-HYP114>3.0.CO;2-E

Brearley, F. Q. (2013). Nitrogen stable isotopes indicate differences in nitrogen cycling between two contrasting Jamaican montane forests. *Plant and Soil*, *367*(1–2), 465–476. https://doi.org/10.1007/s11104-012-1469-z

Brienen, R. J. W., Phillips, O. L., Feldpausch, T. R., Gloor, E., Baker, T. R., Lloyd, J., Lopez-Gonzalez, G., Monteagudo-Mendoza, A., Malhi, Y., Lewis, S. L., Vásquez Martinez, R., Alexiades, M., Álvarez Dávila, E., Alvarez-Loayza, P., Andrade, A., Aragaõ, L. E. O. C., Araujo-Murakami, A., Arets, E. J. M. M., Arroyo, L., … Zagt, R. J. (2015). Long-term decline of the Amazon carbon sink. *Nature*, *519*(7543), 344–348. https://doi.org/10.1038/nature14283

Bringhurst, K., & Jordan, P. (2015). The impact on nutrient cycles from tropical forest to pasture conversion in Costa Rica. *Sustainable Water Resources Management*, *1*(1), 3–13. https://doi.org/10.1007/s40899-015-0003-x

Brookshire, E. N. J., Gerber, S., Menge, D. N. L., & Hedin, L. O. (2012). Large losses of inorganic nitrogen from tropical rainforests suggest a lack of nitrogen limitation. *Ecology Letters*, *15*(1), 9–16. https://doi.org/10.1111/j.1461-

0248.2011.01701.x

Bruijnzeel, L. A. (1991). Nutrient input—output budgets of tropical forest ecosystems: A review. *Journal of Tropical Ecology*, *7*(1), 1–24. https://doi.org/10.1017/S0266467400005010

Bultot, F. (1971). Atlas Climatique du Bassin Congolais Publications de L'Institut National pour L'Etude Agronomique du Congo (I.N.E.A.C), Deuxieme Partie, Les Composantes du Bilan d'Eau.

Bultot, F., & Griffiths, J.W. (1972). The equatorial wet zone, in *Climates of Africa, World Surv. Climatol.,* vol. 10, edited by J.W. Griffiths, chap. 8, pp. 259-311, Elsevier Publishing Company, Amsterdam, London and New York.

Bünemann, E. K. (2015). Assessment of gross and net mineralization rates of soil organic phosphorus - A review. *Soil Biology and Biochemistry*, *89*, 82–98. https://doi.org/10.1016/j.soilbio.2015.06.026

Bustamante, M. M. C., Martinelli, L. A., Silva, D. A., Camargo, P. B., Klink, C. A., Domingues, T. F., & Santos, R. V. (2004). 15N natural abundance in woody plants and soils of Central brazilian savannas (cerrado). *Ecological Applications*, *14*(4), 200–213. https://doi.org/10.1890/01-6013

Campbell, B. (1996). The Miombo in Transition: Woodlands and Welfare in Africa. In *CIFOR - Center for International Forestry Research*.

Campo, J., Maass, M., Jaramillo, V. J., Martínez-Yrízar, A., & Sarukhán, J. (2001). Phosphorus cycling in a Mexican tropical dry forest ecosystem. *Biogeochemistry*, *53*(2), 161–179. https://doi.org/10.1023/A:1010663516029

Chadwick, O. A., Derry, L. A., Vitousek, P. M., Huebert, B. J., & Hedin, L. O. (1999). Changing sources of nutrients during four million years of ecosystem development. *Nature*, *397*(6719), 491–497. https://doi.org/10.1038/17276

Chhatre, A., & Agrawal, A. (2009). Trade-offs and synergies between carbon storage and livelihood benefits from forest commons. *Proceedings of the National Academy of Sciences of the United States of America*, *106*(42), 17667–17670. https://doi.org/10.1073/pnas.0905308106

Ciais, P. C., Bombelli, A., Williams, M., Piao, S. L., Chave, J., Ryan, C. M., Henry, M., Brender, P., & Valentini, R. (2011). The carbon balance of Africa: Synthesis of recent research studies. *Philosophical Transactions of the Royal Society A: Mathematical, Physical and Engineering Sciences*, *369*(1943), 2038–2057. https://doi.org/10.1098/rsta.2010.0328

Clark, K. E., Hilton, R. G., West, A. J., Malhi, Y., Gröcke, D. R., Bryant, C. L., Ascough, P. L., Robles Caceres, A., & New, M. (2013). New views on “old” carbon in the Amazon River: Insight from the source of organic carbon eroded from the Peruvian Andes. *Geochemistry, Geophysics, Geosystems*, *14*(5), 1644–1659. https://doi.org/10.1002/ggge.20122

Clarke, M. A., & Walsh, R. P. D. (2006). Long-term erosion and surface roughness change of rain-forest terrain following selective logging, Danum Valley, Sabah, Malaysia. *Catena*, *68*(2–3), 109–123. https://doi.org/10.1016/j.catena.2006.04.002

Coe, M. T., Costa, M. H., & Soares-Filho, B. S. (2009). The influence of historical and potential future deforestation on the stream flow of the Amazon River - Land surface processes and atmospheric feedbacks. *Journal of Hydrology*, *369*(1–2), 165–174. https://doi.org/10.1016/j.jhydrol.2009.02.043

Correll, D. L., Jordan, T. E., & Weller, D. E. (1999). Transport of nitrogen and phosphorus from Rhode River watersheds during storm events. *Water Resources Research*, *35*(8), 2513–2521. https://doi.org/10.1029/1999WR900058

Coynel, A., Seyler, P., Etcheber, H., Meybeck, M., & Orange, D. (2005). Spatial and seasonal dynamics of total suspended sediment and organic carbon species in the Congo River. *Global Biogeochemical Cycles*, *19*(4), 1–17. https://doi.org/10.1029/2004GB002335

Craine, J. M., Brookshire, E. N. J., Cramer, M. D., Hasselquist, N. J., Koba, K., Marin-Spiotta, E., & Wang, L. (2015). Ecological interpretations of nitrogen isotope ratios of terrestrial plants and soils. *Plant and Soil*, *396*(1–2), 1–26. https://doi.org/10.1007/s11104-015-2542-1

Craine, J. M., Elmore, A. J., Wang, L., Augusto, L., Baisden, W. T., Brookshire, E. N. J., Cramer, M. D., Hasselquist, N. J., Hobbie, E. A., Kahmen, A., Koba, K., Kranabetter, J. M., Mack, M. C., Marin-Spiotta, E., Mayor, J. R., McLauchlan, K. K., Michelsen, A., Nardoto, G. B., Oliveira, R. S., … Zeller, B. (2015). Convergence of soil nitrogen isotopes across global climate gradients. *Scientific Reports*, *5*, 1–8. https://doi.org/10.1038/srep08280

Curtis, P. G., Slay, C. M., Harris, N. L., Tyukavina, A., & Hansen, M. C. (2018). Classifying drivers of global forest loss. *Science*, *361*(6407), 1108–1111. https://doi.org/10.1126/science.aau3445

da Silva, V. de paulo R., Silva, M. T., Singh, V. P., de Souza, E. P., Braga, C. C., de Holanda, R. M., Almeida, R. S. R., de Assis Salviano de Sousa, F., & Braga, A. C. R. (2018). Simulation of stream flow and hydrological response to land-cover changes in a tropical river basin. *Catena*, *162*(November 2017), 166–176. https://doi.org/10.1016/j.catena.2017.11.024

Davidson, E. A. (1993). Soil water content and the ratio of nitrous oxide to nitric oxide emitted from soil. *Oremland RS (Ed) Biogeochemistry of Global*, 369–386.

Davidson, E A, Ishida, F. Y., & Nepstad, D. C. (2004). Effects of an experimental drought on soil emissions of carbon dioxide, methane, nitrous oxide, and nitric oxide in a moist tropical forest. *Global Change Biology*, *10*(5), 718–730.

https://doi.org/10.1111/j.1529-8817.2003.00762.x

Davidson, Eric A., & Martinelli, L. A. (2013). Nutrient Limitations to Secondary Forest Regrowth. *Amazonia and Global Change*, 299–309. https://doi.org/10.1029/2009GM000905

Davidson, Eric A., Neill, C., Krusche, A. V., Ballester, V. V. R., Markewitz, D., & Figueiredo, R. de O. (2004). Loss of nutrients from terrestrial ecosystems to streams and the atmosphere following land use change in Amazonia. *Geophysical Monograph Series*, *153*, 147–158. https://doi.org/10.1029/153GM12

Davidson, Eric A., Verchot, L. V., Henrique Cattânio, J., Ackerman, I. L., & Carvalho, J. E. M. (2000). Effects of soil water content on soil respiration in forests and cattle pastures of eastern Amazonia. *Biogeochemistry*, *48*(1), 53–69. https://doi.org/10.1023/A:1006204113917

Davies-Barnard, T., Meyerholt, J., Zaehle, S., Friedlingstein, P., Brovkin, V., Fan, Y., Fisher, R. A., Jones, C. D., Lee, H., Peano, D., Smith, B., Warlind, D., & Wilthsire, A. J. (2020). Nitrogen cycling in CMIP6 land surface models: progress and limitations. *Biogeosciences, 17,* 5129-5148. https://doi.org/10.5194/bg-17-5129-2020

Don, A., Schumacher, J., & Freibauer, A. (2011). Impact of tropical land-use change on soil organic carbon stocks - a meta-analysis. *Global Change Biology*, *17*(4), 1658–1670. https://doi.org/10.1111/j.1365-2486.2010.02336.x

Douglas, I. (1999). Hydrological investigations of forest disturbance and land cover impacts in South-East Asia: A review. *Philosophical Transactions of the Royal Society B: Biological Sciences*, *354*(1391), 1725–1738. https://doi.org/10.1098/rstb.1999.0516

Drake, T. W., Van Oost, K., Barthel, M., Bauters, M., Hoyt, A. M., Podgorski, D. C., Six, J., Boeckx, P., Trumbore, S. E., Cizungu Ntaboba, L., & Spencer, R. G. M. (2019). Mobilization of aged and biolabile soil carbon by tropical deforestation. *Nature Geoscience*, *12*(July). https://doi.org/10.1038/s41561-019-0384-9

Ehama, M., Hashihama, F., Kinouchi, S., Kanda, J., & Saito, H. (2016). Sensitive determination of total particulate phosphorus and particulate inorganic phosphorus in seawater using liquid waveguide spectrophotometry. *Talanta*, *153*, 66–70. https://doi.org/10.1016/j.talanta.2016.02.058

Elsenbeer, H. (2001). Hydrologic flowpaths in tropical rainforest soilscapes-A review. *Hydrological Processes*, *15*(10), 1751–1759. https://doi.org/10.1002/hyp.237

Emery, K. O., Wigley, R. L., Bartlett, A. S., Meyer, R., & Barhoorn, E. S. (1967). Freshwater Peat on the Continental Shelf. *Science*, *158*(3806), 1301–1307.

ESA. (2017). Land Cover CCI Product User Guide Version 2. Tech. Rep. Available at: maps.elie.ucl.ac.be/CCI/viewer/download/ESACCI-LC-Ph2-PUGv2_2.0.pdf

Eshetu, Z., & Högberg, P. (2000). Effects of land use on 15N natural abundance of soils in Ethiopian highlands. *Plant and Soil*, *222*(1–2), 109–117. https://doi.org/10.1023/A:1004777301260

Falkowski, P., Scholes, R. J., Boyle, E., Canadell, J., Canfield, D., Elser, J., Gruber, N., Hibbard, K., Hogberg, P., Linder, S., Mackenzie, F. T., Moore, B., Pedersen, T., Rosental, Y., Seitzinger, S., Smetacek, V., & Steffen, W. (2000). The global carbon cycle: A test of our knowledge of earth as a system. *Science*, *290*(5490), 291–296. https://doi.org/10.1126/science.290.5490.291

Fernández-Martínez, M., Vicca, S., Janssens, I. A., Sardans, J., Luyssaert, S., Campioli, M., Chapin, F. S., Ciais, P., Malhi, Y., Obersteiner, M., Papale, D., Piao, S. L., Reichstein, M., Rodà, F., & Peñuelas, J. (2014). Nutrient availability as the key regulator of global forest carbon balance. *Nature Climate Change*, *4*(6), 471–476. https://doi.org/10.1038/nclimate2177

Fick, S. E., & Hijmans, R. J. (2017). WorldClim 2: new 1-km spatial resolution climate surfaces for global land areas. *International Journal of Climatology*, *37*(12), 4302–4315. https://doi.org/10.1002/joc.5086

Fisher, J. B., Sikka, M., Sitch, S., Ciais, P., Poulter, B., Galbraith, D., Lee, J. E., Huntingford, C., Viovy, N., Zeng, N., Ahlström, A., Lomas, M. R., Levy, P. E., Frankenberg, C., Saatchi, S., & Malhi, Y. (2013). African tropical rainforest net carbon dioxide fluxes in the twentieth century. *Philosophical Transactions of the Royal Society B: Biological Sciences*, *368*(1625), 13–17. https://doi.org/10.1098/rstb.2012.0376Fritsch, M., & Sarrailh, M. (1986). Les transports solides dans l'écosysème forestier tropical humide guyanais: eefets du défrichement et de l'aménagement de pâturages. *Cah. ORSTOM, Sér. Pédol.*, *XXII*(1), 209–222.

Fry, B., & Sherr, E. B. (1989). δ13C Measurements as Indicators of Carbon Flow in Marine and Freshwater Ecosystems. In P. W. Rundel, J. R. Ehleringer, & K. A. Nagy (Eds.), *Stable Isotopes in Ecological Research* (pp. 196–229). Springer New York.

Fuka, D. R., Walter, M. T., Archibald, J. A., Steenhuis, T. S., & Easton, Z. M. (2015). *EcoHydRology: A community modeling foundation for Eco-Hydrology. R package version 0.4.12.* (p. 48). http://cran.r-project.org/package=EcoHydRology

Gallarotti, N., Barthel, M., Verhoeven, E., Isadora, E., Pereira, P., Bauters, M., Baumgartner, S., Drake, T. W., Boeckx, P., Mohn, J., Longepierre, M., Kalume, J., Isaac, M., Makelele, A., Cizungu, L., & Johan, N. (2021). In-depth analysis of N 2 O fl uxes in tropical forest soils of the Congo Basin combining isotope and functional gene analysis. *The ISME Journal*. https://doi.org/10.1038/s41396-021-01004-x

Gardner, T. A., Barlow, J., Chazdon, R., Ewers, R. M., Harvey, C. A., Peres, C. A., & Sodhi, N. S. (2009). Prospects for tropical forest biodiversity in a human-modified world. *Ecology Letters*, *12*(6), 561–582. https://doi.org/10.1111/j.1461-0248.2009.01294.x

Garnett Williams. (1989). Sediment Concentration Versus Water Discharge During Single Event.Pdf. In *Journal of Hydrology* (Vol. 111, pp. 89–106).

Gaston, K. J. (2000). Global patterns in biodiversity. *Nature*, *405*(6783), 220–227. https://doi.org/10.1038/35012228

Gattuso, J. P., Frankignoulle, M., & Wollast, R. (1998). Carbon and carbonate metabolism in coastal aquatic ecosystems. *Annual Review of Ecology and Systematics*, *29*, 405–434. https://doi.org/10.1146/annurev.ecolsys.29.1.405

Gerschlauer, F., Saiz, G., Schellenberger Costa, D., Kleyer, M., Dannenmann, M., & Kiese, R. (2019). Stable carbon and nitrogen isotopic composition of leaves, litter, and soils of various ecosystems along an elevational and land-use gradient at Mount Kilimanjaro, Tanzania. *Biogeosciences*, *16*(2), 409–424. https://doi.org/10.5194/bg-16-409-2019

Grayson, R. B., Haydon, S. R., Jayasuriya, M. D. A., & Finlayson, B. L. (1993). Water quality in mountain ash forests - separating the impacts of roads from those of logging operations. *Journal of Hydrology*, *150*(2–4), 459–480. https://doi.org/10.1016/0022-1694(93)90121-O

Gücker, B., Silva, R. C. S., Graeber, D., Monteiro, J. A. F., Brookshire, E. N. J., Chaves, R. C., & Boëchat, I. G. (2016). Dissolved nutrient exports from natural and human-impacted Neotropical catchments. *Global Ecology and Biogeography*, *25*(4), 378–390. https://doi.org/10.1111/geb.12417

Guo, L. B., & Gifford, R. M. (2002). Soil carbon stocks and land use change: A meta analysis. *Global Change Biology*, *8*(4), 345–360. https://doi.org/10.1046/j.1354-1013.2002.00486.x

Haensler, A., Saeed, F., & Jacob, D. (2013). Assessing the robustness of projected precipitation changes over central Africa on the basis of a multitude of global and regional climate projections. *Climatic Change*, *121*(2), 349–363. https://doi.org/10.1007/s10584-013-0863-8

Handley, L. L., Austin, A. T., Robinson, D., Scrimgeour, C. M., Raven, J. A., Heaton, T. H. E., Schmidt, S., & Stewart, G. R. (1999). The 15N natural abundance (δ 15N) of ecosystem samples reflects measures of water availability. *Australian Journal of Plant Physiology*, *26*(2), 185–199. https://doi.org/10.1071/PP98146

Harris, N. L., Gibbs, D. A., Baccini, A., Birdsey, R. A., de Bruin, S., Farina, M., Fatoyinbo, L., Hansen, M. C., Herold, M., Houghton, R. A., Potapov, P. V., Suarez, D. R., Roman-Cuesta, R. M., Saatchi, S. S., Slay, C. M., Turubanova, S. A., & Tyukavina, A. (2021). Global maps of twenty-first century forest carbon

fluxes. *Nature Climate Change*, *11*(March). https://doi.org/10.1038/s41558-020-00976-6

Hecky, R. E., Bootsma, H. A., & Kingdon, M. L. (2003). Impact of land use on sediment and nutrient yields to Lake Malawi/Nyasa (Africa). *Journal of Great Lakes Research*, *29*(SUPPL. 2), 139–158. https://doi.org/10.1016/S0380-1330(03)70544-9

Hedin, L. O., Armesto, J. J., & Johnson, A. H. (1995). Patterns of Nutrient Loss from Unpolluted , Old-Growth Temperate Forests : Evaluation of Biogeochemical Theory Author. *Ecology*, *76*(2), 493–509.

Hedin, L. O., Brookshire, E. N. J., Menge, D. N. L., & Barron, A. R. (2009). The Nitrogen Paradox in Tropical Forest Ecosystems. *Annual Review of Ecology, Evolution, and Systematics*, *40*(1), 613–635. https://doi.org/10.1146/annurev.ecolsys.37.091305.110246

Hedin, L. O., Vitousek, P. M., & Matson, P. A. (2003). Nutrient losses over four million years of tropical forest development. *Ecology*, *84*(9), 2231–2255. https://doi.org/10.1890/02-4066

Heidel, S. G. (1956). The progressive lag of sediment concentration with flood waves. *Eos, Transactions American Geophysical Union*, *37*(1), 56–66. https://doi.org/10.1029/TR037i001p00056

Hilton, R. G., Galy, A., West, A. J., Hovius, N., & Roberts, G. G. (2013). Geomorphic control on the δ15N of mountain forests. *Biogeosciences*, *10*(3), 1693–1705. https://doi.org/10.5194/bg-10-1693-2013

Hobbie, E. A., & Ouimette, A. P. (2009). Controls of nitrogen isotope patterns in soil profiles. *Biogeochemistry*, *95*(2), 355–371. https://doi.org/10.1007/s10533-009-9328-6

Hofhansl, F., Chacón-Madrigal, E., Fuchslueger, L., Jenking, D., Morera-Beita, A., Plutzar, C., Silla, F., Andersen, K. M., Buchs, D. M., Dullinger, S., Fiedler, K., Franklin, O., Hietz, P., Huber, W., Quesada, C. A., Rammig, A., Schrodt, F., Vincent, A. G., Weissenhofer, A., & Wanek, W. (2020). Climatic and edaphic controls over tropical forest diversity and vegetation carbon storage. *Scientific Reports*, *10*(1), 1–11. https://doi.org/10.1038/s41598-020-61868-5

Högberg, P. (1990). Forests losing large quantities of nitrogen have elevated 15N:14N ratios. *Oecologia*, *84*(2), 229–231. https://doi.org/10.1007/BF00318276

Högberg, P. (1997). Tansley review no. 95 natural abundance in soil-plant systems. *New Phytologist*, *137*(2), 179–203. https://doi.org/10.1046/j.1469-8137.1997.00808.x

Hogberg, P., & Alexander, I. J. (1995). Roles of Root Symbioses in African Woodland and Forest : Evidence from 15N abundance and foliar analysis. *Journal of*

Ecology, *83*(2), 217–224.

Högberg, P., & Johannisson, C. (1993). ^{15}N Abundance of forests is correlated with losses of nitrogen. *Plant and Soil*, *157*(1), 147–150.

Hölscher, D., Ludwig, B., Möller, R. F., & Fölster, H. (1997). Dynamic of soil chemical parameters in shifting agriculture in the Eastern Amazon. *Agriculture, Ecosystems and Environment*, *66*(2), 153–163. https://doi.org/10.1016/S0167-8809(97)00077-7

Holtgrieve, G. W., Jewett, P. K., & Matson, P. A. (2006). Variations in soil N cycling and trace gas emissions in wet tropical forests. *Oecologia*, *146*(4), 584–594. https://doi.org/10.1007/s00442-005-0222-1

Hoover, D. J., & MacKenzie, F. T. (2009). Fluvial fluxes of water, suspended particulate matter, and nutrients and potential impacts on tropical coastal water Biogeochemistry: Oahu, Hawai'i. *Aquatic Geochemistry*, *15*(4), 547–570. https://doi.org/10.1007/s10498-009-9067-2

Hou, E., Chen, C., Luo, Y., Zhou, G., Kuang, Y., Zhang, Y., Heenan, M., Lu, X., & Wen, D. (2018). Effects of climate on soil phosphorus cycle and availability in natural terrestrial ecosystems. *Global Change Biology*, *24*(8), 3344–3356. https://doi.org/10.1111/gcb.14093

Houghton, R. A. (1999). The annual net flux of carbon to the atmosphere from changes in land use 1850-1990. *Tellus, Series B: Chemical and Physical Meteorology*, *51*(2), 298–313. https://doi.org/10.3402/tellusb.v51i2.16288

Houghton, R. A. (2003). The Contemporary Carbon Cycle. *Treatise on Geochemistry*, *8–9*, 473–513. https://doi.org/10.1016/B0-08-043751-6/08168-8

Houlton, B. Z., Wang, Y. P., Vitousek, P. M., & Field, C. B. (2008). A unifying framework for dinitrogen fixation in the terrestrial biosphere. *Nature*, *454*(7202), 327–330. https://doi.org/10.1038/nature07028

Hubau, W., Lewis, S. L., Phillips, O. L., Affum-Baffoe, K., Beeckman, H., Cuní-Sanchez, A., Daniels, A. K., Ewango, C. E. N., Fauset, S., Mukinzi, J. M., Sheil, D., Sonké, B., Sullivan, M. J. P., Sunderland, T. C. H., Taedoumg, H., Thomas, S. C., White, L. J. T., Abernethy, K. A., Adu-Bredu, S., … Zemagho, L. (2020). Asynchronous carbon sink saturation in African and Amazonian tropical forests. *Nature*, *579*(7797), 80–87. https://doi.org/10.1038/s41586-020-2035-0

Huffman, G. J., Bolvin, D. T., Nelkin, E. J., & Tan, J. (2019). Integrated Multi-satellitE Retrievals for GPM (IMERG) Technical Documentation. *IMERG Tech Document*, *01*(01). https://gpm.nasa.gov/sites/default/files/document_files/IMERG_doc_190909.pdf

Hughes, A. O., Quinn, J. M., & McKergow, L. A. (2012). Land use influences on

suspended sediment yields and event sediment dynamics within two headwater catchments, Waikato, New Zealand. *New Zealand Journal of Marine and Freshwater Research*, *46*(3), 315–333. https://doi.org/10.1080/00288330.2012.661745

IPCC, 2021: Climate Change 2021: The Physical Science Basis. Contribution of Working Group I to the Sixth Assessment Report of the Intergovernmental Panel on Climate Change [Masson-Delmotte, V., P. Zhai, A. Pirani, S.L. Connors, C. Péan, S. Berger, N. Caud, Y. Chen, L. Goldfarb, M.I. Gomis, M. Huang, K. Leitzell, E. Lonnoy, J.B.R. Matthews, T.K. Maycock, T. Waterfield, O. Yelekçi, R. Yu, and B. Zhou (eds.)]. Cambridge University Press. In Press.

Iroumé, A., Huber, A., & Schulz, K. (2005). Summer flows in experimental catchments with different forest covers, Chile. *Journal of Hydrology*, *300*(1–4), 300–313. https://doi.org/10.1016/j.jhydrol.2004.06.014

Jones, A., Breuning-Madsen, H., Brossard, M., Dampha, A., Deckers, J., Dewitte, O., Gallali, T., Hallett, S., Jones, R., Kilasara, M., Le Roux, P., Micheli, E., Montanarella, L., Spaargaren, O., Thiombiano, L., Van Ranst, E., Yemefack, M., Zougmoré, R. (eds.). (2013). Soil Atlas of Africa. European Commisssion, Publications Office of the European Union, Luxembourg. 176 pp.

Jung, M., Schwalm, C., Migliavacca, M., Walther, S., Camps-Valls, G., Koirala, S., Anthoni, P., Besnard, S., Bodesheim, P., Carvalhais, N., Chevallier, F., Gans, F., S Goll, D., Haverd, V., Köhler, P., Ichii, K., K Jain, A., Liu, J., Lombardozzi, D., … Reichstein, M. (2020). Scaling carbon fluxes from eddy covariance sites to globe: Synthesis and evaluation of the FLUXCOM approach. *Biogeosciences*, *17*(5), 1343–1365. https://doi.org/10.5194/bg-17-1343-2020

Kaspari, M., & Powers, J. S. (2016). Biogeochemistry and geographical ecology: Embracing all twenty-five elements required to build organisms. *American Naturalist,* (188), S62-S73. https//doi.org/10.1086/687576

Kaspari, M., & Yanoviak, S. P. (2009). Biogeochemistry and the structure of tropical brown food webs. *Ecology*, *90*(12), 3342–3351. https://doi.org/10.1890/08-1795.1

Kirschbaum, M. U. F. (1995). The temperature dependence of soil organic matter decomposition, and the effect of global warming on soil organic C storage. *Soil Biology and Biochemistry*, *27*(6), 753–760. https://doi.org/10.1016/0038-0717(94)00242-S

Kitayama, K., & Iwamoto, K. (2001). Patterns of natural 15N abundance in the leaf-to-soil continuum of tropical rain forests differing in N availability on Mount Kinabalu, Borneo. *Plant and Soil*, *229*(2), 203–212. https://doi.org/10.1023/A:1004853915544

Klein, M. (1984). Anti clockwise hysteresis in suspended sediment concentration during individual storms: Holbeck catchment; Yorkshire, England. *Catena*,

11(2–3), 251–257. https://doi.org/10.1016/0341-8162(84)90014-6

Koehler, B., Corre, M. D., Veldkamp, E., Wullaert, H., & Wright, S. J. (2009). Immediate and long-term nitrogen oxide emissions from tropical forest soils exposed to elevated nitrogen input. *Global Change Biology*, *15*(8), 2049–2066. https://doi.org/10.1111/j.1365-2486.2008.01826.x

Kroese, J. S., Quinton, J. N., Jacobs, S. R., Breuer, L., & Rufino, M. C. (2021). Particulate macronutrient exports from tropical African montane catchments point to the impoverishment of agricultural soils. *Soil*, *7*(1), 53–70. https://doi.org/10.5194/soil-7-53-2021

Kuznetsova, A., Brockhoff, P. B., & Christensen, R. H. B. (2017). lmerTest Package: Tests in Linear Mixed Effects Models. *J. Stat. Softw.* 82, 1-26. https://doi.org/10.18637/jss.v082.i13

Labrière, N., Locatelli, B., Laumonier, Y., Freycon, V., & Bernoux, M. (2015). Soil erosion in the humid tropics: A systematic quantitative review. *Agriculture, Ecosystems and Environment*, *203*, 127–139. https://doi.org/10.1016/j.agee.2015.01.027

Lai, F. S. (1993). Sediment yield from logged, steep upland catchments in Peninsular Malaysia. *Hydrology of Warm Humid Regions*, *216*, 219–230.

Lamb, A. L., Wilson, G. P., & Leng, M. J. (2006). A review of coastal palaeoclimate and relative sea-level reconstructions using δ13C and C/N ratios in organic material. *Earth-Science Reviews*, *75*(1–4), 29–57. https://doi.org/10.1016/j.earscirev.2005.10.003

Lapola, D. M., Oyama, M. D., & Nobre, C. A. (2009). Exploring the range of climate biome projections for tropical South America: The role of CO2 fertilization and seasonality. *Global Biogeochemical Cycles*, *23*(3), 1–16. https://doi.org/10.1029/2008GB003357

Laraque, A., Bricquet, J. P., Pandi, A., & Olivry, C. (2009). A review of material transport by the Congo River and its tributaries. *Hydrological Processes*, *23*, 3216–3224. https://doi.org/10.1002/hyp.7395

Lesack, L. F. W. (1993). Water balance and hydrologic characteristics of a rain forest catchment in the central Amazon Basin. *Water Resources Research*, *29*(3), 759–773. https://doi.org/10.1029/92WR02371

Levy-Varon, J. H., Batterman, S. A., Medvigy, D., Xu, X., Hall, J. S., van Breugel, M., & Hedin, L. O. (2019). Tropical carbon sink accelerated by symbiotic dinitrogen fixation. *Nature Communications*, *10*(1), 1–8. https://doi.org/10.1038/s41467-019-13656-7

Lewis, S. L. (2006). Tropical forests and the changing earth system. *Philosophical Transactions of the Royal Society B: Biological Sciences*, *361*(1465), 195–210. https://doi.org/10.1098/rstb.2005.1711

Lewis, S. L., Sonké, B., Sunderland, T., Begne, S. K., Lopez-Gonzalez, G., van der Heijden, G. M. F., Phillips, O. L., Affum-Baffoe, K., Baker, T. R., Banin, L., Bastin, J. F., Beeckman, H., Boeckx, P., Bogaert, J., De Cannière, C., Chezeaux, E., Clark, C. J., Collins, M., Djagbletey, G., … Zemagho, L. (2013). Above-ground biomass and structure of 260 African tropical forests. *Philosophical Transactions of the Royal Society B: Biological Sciences*, *368*(1625). https://doi.org/10.1098/rstb.2012.0295

Lewis, W. M. (1986). *Nitrogen and Phosphorus Runoff Losses from a Nutrient-Poor Tropical Moist Forest*. *67*(5), 1275–1282.

Lewis, W. M., Melack, J. M., McDowell, W. H., McClain, M., & Richey, J. E. (1999). Nitrogen yields from undisturbed watersheds in the Americas. *Biogeochemistry*, *46*(1–3), 149–162. https://doi.org/10.1007/BF01007577

Lewis, W.M., Hamilton, S.K., & Saunders, J. F. (1995). Rivers of Northern South America. Pages 219-256, in: *River and stream ecosystems.* Edited by: Cushing, C. E., Cummins, K. W., & Minshall, G. W. Elsevier, Amsterdam.

Lewis, W. M., Saunders, J. F., Biogeochemistry, S., & May, N. (1989). *Concentration and Transport of Dissolved and Suspended Substances in the Orinoco River Published by : Springer Stable URL : https://www.jstor.org/stable/1468846 REFERENCES Linked references are available on JSTOR for this article : reference # references* . *7*(3), 203–240.

Lewis, W. M., Saunders, J. F., Levine, S. N., & Weibezahn, F. H. (1986). Organic carbon in the Caura River, Venezuela. *Limnology and Oceanography*, *31*(3), 653–656. https://doi.org/10.4319/lo.1986.31.3.0653

Liaw, A., & Wiener, M. (2002). Classification and Regression by randomForest. *R News*, *2*(3), 18–22. https://cran.r-project.org/doc/Rnews/

Lloret, E., Dessert, C., Pastor, L., Lajeunesse, E., Crispi, O., Gaillardet, J., & Benedetti, M. F. (2013). Dynamic of particulate and dissolved organic carbon in small volcanic mountainous tropical watersheds. *Chemical Geology*, *351*, 229–244. https://doi.org/10.1016/j.chemgeo.2013.05.023

Lloyd, C. E. M., Freer, J. E., Johnes, P. J., & Collins, A. L. (2016a). Technical Note: Testing an improved index for analysing storm discharge-concentration hysteresis. *Hydrology and Earth System Sciences*, *20*(2), 625–632. https://doi.org/10.5194/hess-20-625-2016

Lloyd, C. E. M., Freer, J. E., Johnes, P. J., & Collins, A. L. (2016b). Using hysteresis analysis of high-resolution water quality monitoring data, including uncertainty, to infer controls on nutrient and sediment transfer in catchments. *Science of the Total Environment*, *543*, 388–404. https://doi.org/10.1016/j.scitotenv.2015.11.028

Lønborg, C., Álvarez–Salgado, X. A., Duggan, S., & Carreira, C. (2018). Organic matter bioavailability in tropical coastal waters: The Great Barrier Reef.

Limnology and Oceanography, *63*(2), 1015–1035. https://doi.org/10.1002/lno.10717

Ludwig, W., Probst, J. L., & Kempe, S. (1996). Predicting the oceanic input of organic carbon by continental erosion. *Global Biogeochemical Cycles*, *10*(1), 23–41. https://doi.org/10.1029/95GB02925

Malhi, Y. (2012). The productivity, metabolism and carbon cycle of tropical forest vegetation. *Journal of Ecology*, *100*(1), 65–75. https://doi.org/10.1111/j.1365-2745.2011.01916.x

Malhi, Y., & Grace, J. (2000). Tropical forests and atmospheric carbon dioxide. *Trends in Ecology and Evolution*, *15*(8), 332–337. https://doi.org/10.1016/S0169-5347(00)01906-6

Malmer, A. (1996). Hydrological effects and nutrient losses of forest plantation establishment on tropical rainforest land in Sabah, Malaysia. *Journal of Hydrology*, *174*, 1–20. papers2://publication/uuid/61171ACD-AFDE-45EF-ABBC-358AFE714896

Malmer, A., & Nyberg, G. (2008). Forest and water relations in miombo woodlands : need for understanding of complex stand management. *Finnish Forest Research Institute*, *98*, 70–86.

Malutta, S., Kobiyama, M., Chaffe, P. L. B., & Bonumá, N. B. (2020). Hysteresis analysis to quantify and qualify the sediment dynamics: State of the art. *Water Science and Technology*, *81*(12), 2471–2487. https://doi.org/10.2166/wst.2020.279

Maranguit, D., Guillaume, T., & Kuzyakov, Y. (2017). Land-use change affects phosphorus fractions in highly weathered tropical soils. *Catena*, *149*, 385–393. https://doi.org/10.1016/j.catena.2016.10.010

Martinelli, L. A., Piccolo, M. C., Townsend, A. R., Vitousek, P. M., Cuevas, E., McDowell, W., Robertson, G. P., Santos, O. C., & Tre. (1999). Nitrogen stable isotopic composition of leaves and soil: Tropical versus temperate forests. *Biogeochemistry*, *46*, 45–65.

Matson, P. A., Mcdowell, W. H., Townsend, A. R., & Vitousek, P. M. (1999). The globalization of N deposition: ecosystem consequences in tropical environments. *New Perspectives on Nitrogen Cycling in the Temperate and Tropical Americas*, 67–83. https://doi.org/10.1007/978-94-011-4645-6_4

Mayes, M., Melillo, J., Neill, C., Palm, C., Mustard, J., & Nyadzi, G. (2019). Nitrogen Cycle Patterns During Forest Regrowth in an African Miombo woodland Landscape. *Journal of Geophysical Research: Biogeosciences*, *124*(6), 1591–1603. https://doi.org/10.1029/2018JG004803

McDowell, W. H., & Asbury, C. E. (1994). Exports of carbon, nitrogen, and major ions from three tropical montane watersheds. *Limnol. Oceanogr.*, *39*(l), 111–

125. http://www.google.co.uk/url?sa=t&source=web&cd=2&ved=0CB0QFjAB&url=http://www.aslo.org/lo/toc/vol_39/issue_1/0111.pdf&rct=j&q=mcdowell carbon puerto rico&ei=kjH5TJaQNs2WhQeajfmBCQ&usg=AFQjCNGbaN6jGzjIg71uoU4WHpS206wyyw&sig2=sg7nQ2JDJIIlbUJQpp7B9g%5Cnpaper

McGrath, D. A., Smith, C. K., Gholz, H. L., & Oliveira, F. D. A. (2001). Effects of land-use change on soil nutrient dynamics in Amazônia. *Ecosystems*, *4*(7), 625–645. https://doi.org/10.1007/s10021-001-0033-0

Messina, A. M., & Biggs, T. W. (2016). Contributions of human activities to suspended sediment yield during storm events from a small, steep, tropical watershed. *Journal of Hydrology*, *538*, 726–742. https://doi.org/10.1016/j.jhydrol.2016.03.053

Moyer, R. P., Bauer, J. E., & Grottoli, A. G. (2013). Carbon isotope biogeochemistry of tropical small mountainous river, estuarine, and coastal systems of Puerto Rico. *Biogeochemistry*, *112*(1–3), 589–612. https://doi.org/10.1007/s10533-012-9751-y

Murty, D., Kirschbaum, M. U. F., Mcmurtrie, R. E., & Mcgilvray, H. (2002). Does conversion of forest to agricultural land change soil carbon and nitrogen? A review of the literature. *Global Change Biology*, *8*(2), 105–123. https://doi.org/10.1046/j.1354-1013.2001.00459.x

Mushi, C. A., Ndomba, P. M., Trigg, M. A., Tshimanga, R. M., & Mtalo, F. (2019). Assessment of basin-scale soil erosion within the Congo River Basin: A review. *Catena*, *178*(February), 64–76. https://doi.org/10.1016/j.catena.2019.02.030

Nadelhoffer, K. J., & Fry, B. (1994). Nitrogen isotope studies in forest ecosystems. In: *Stable Isotopes in Ecology and Environmental Science.* Edited by: Michener, R., & Lajtha, K. Blackwell Scientific Publications, London.

Nakagawa, S., & Schielzeth, H. (2013). A general and simple method for obtaining R2 from generalized linear mixed-effects models. *Methods in Ecology and Evolution*, *4*(2), 133–142. https://doi.org/10.1111/j.2041-210x.2012.00261.x

Nash, J. E., & Sutcliffe, J. V. (1970). River flow forecasting through conceptual models part I - A discussion of principles. *Journal of Hydrology*, *10*(3), 282–290. https://doi.org/10.1016/0022-1694(70)90255-6

Neff, J. C., III, F. S. C., & Vitousek, P. M. (2003). Breaks in the Cycle: Dissolved Organic Nitrogen in Terrestrial Ecosystems. *Frontiers in Ecology and the Environment*, *1*(4), 205. https://doi.org/10.2307/3868065

Neill, C., Deegan, L. A., Thomas, S. M., & Cerri, C. C. (2001). Deforestation for Pasture Alters Nitrogen and. *Ecological Applications*, *11*(6), 1817–1828. https://doi.org/10.1890/1051-0761(2001)011[1817:DFPANA]2.0.CO;2

Neill, C., Deegan, L. A., Thomas, S. M., Haupert, C. L., Krusche, A. V., Ballester, V. M., & Victoria, R. L. (2006). Deforestation alters the hydraulic and biogeochemical characteristics of small lowland Amazonian streams. *Hydrological Processes*, *20*, 2563–2580. https://doi.org/10.1002/hyp.6216

Neill, C., Piccolo, M. C., Steudler, P. A., Melillo, J. M., Feigl, B. J., & Cerri, C. C. (1995). Nitrogen dynamics in soils of forests and active pastures in the western Brazilian Amazon Basin. *Soil Biology and Biochemistry*, *27*(9), 1167–1175. https://doi.org/10.1016/0038-0717(95)00036-EOliveira, P. T. S., Nearing, M. A., & Wendland, E. (2015). Orders of magnitude increase in soil erosion associated with land use change from native to cultivated vegetation in a Brazilian savannah environment. *Earth Surface Processes and Landforms*, *40*(11), 1524–1532. https://doi.org/10.1002/esp.3738

Olson, D. M., Dinerstein, E., Wikramanayake, E. D., Burgess, N. D., Powell, G. V. N., Underwood, E. C., D'Amico, J. A., Itoua, I., Strand, H. E., Morrison, J. C., Loucks, C. J., Allnutt, T. F., Ricketts, T. H., Kura, Y., Lamoreux, J. F., Wettengel, W. W., Hedao, P., & Kassem, K. R. (2004). Terrestrial Ecoregions of the World: A New Map of Life on Earth. *BioScience,* (51), 933-938.

Osborne, B. B., Nasto, M. K., Asner, G. P., Balzotti, C. S., Cleveland, C. C., Sullivan, B. W., Taylor, P. G., Townsend, A. R., & Porder, S. (2017). Climate, Topography, and Canopy Chemistry Exert Hierarchical Control Over Soil N Cycling in a Neotropical Lowland Forest. *Ecosystems*, *20*(6), 1089–1103. https://doi.org/10.1007/s10021-016-0095-7

Palmer, P. I., Feng, L., Baker, D., Chevallier, F., Bösch, H., & Somkuti, P. (2019). Net carbon emissions from African biosphere dominate pan-tropical atmospheric CO2 signal. *Nature Communications*, *10*(1), 3344. https://doi.org/10.1038/s41467-019-11097-w

Pan, Y., Birdsey, R. A., Fang, J., Houghton, R., Kauppi, P. E., Kurz, W. A., Phillips, O. L., Shvidenko, A., Lewis, S. L., Canadell, J. G., Ciais, P., Jackson, R. B., Pacala, S. W., McGuire, A. D., Piao, S., Rautiainen, A., Sitch, S., & Haye. (2011). A Large and Persistent Carbon Sink in the World's Forests. *Science*, *333*, 4.

Pan, Y., Birdsey, R. A., Fang, J., Houghton, R., Kauppi, P. E., Kurz, W. A., Phillips, O. L., Shvidenko, A., Lewis, S. L., Canadell, J. G., Ciais, P., Jackson, R. B., Pacala, S. W., McGuire, A. D., Piao, S., Rautiainen, A., Sitch, S., & Hayes, D. (2011). A large and persistent carbon sink in the world's forests. *Science*, *333*(6045), 988–993. https://doi.org/10.1126/science.1201609

Pelletier, J. D. (2012). A spatially distributed model for the long-term suspended sediment discharge and delivery ratio of drainage basins. *Journal of Geophysical Research: Earth Surface*, *117*(2), 1–15. https://doi.org/10.1029/2011JF002129

Perakis, S. S., & Hedin, L. O. (2002). Nitrogen loss from unpolluted South American forests mainly via dissolved organic compounds. *Nature*, *415*(6870), 416–419.

https://doi.org/10.1038/415416a

Perakis, S. S., Tepley, A. J., & Compton, J. E. (2015). Disturbance and Topography Shape Nitrogen Availability and δ15N over Long-Term Forest Succession. *Ecosystems*, *18*(4), 573–588. https://doi.org/10.1007/s10021-015-9847-z

Pett-Ridge, J. C. (2009). Contributions of dust to phosphorus cycling in tropical forests of the Luquillo Mountains, Puerto Rico. *Biogeochemistry*, *94*(1), 63–80. https://doi.org/10.1007/s10533-009-9308-x

Phillips, J. D. (2010). The convenient fiction of steady-state soil thickness. *Geoderma*, *156*(3–4), 389–398. https://doi.org/10.1016/j.geoderma.2010.03.008

Porder, S., Vitousek, P. M., Chadwick, O. A., Chamberlain, C. P., & Hilley, G. E. (2007). Uplift, erosion, and phosphorus limitation in terrestrial ecosystems. *Ecosystems*, *10*(1), 158–170. https://doi.org/10.1007/s10021-006-9011-x

Potapov, P. V., Turubanova, S. A., Hansen, M. C., Adusei, B., Broich, M., Altstatt, A., Mane, L., & Justice, C. O. (2012). Quantifying forest cover loss in Democratic Republic of the Congo, 2000-2010, with Landsat ETM+ data. *Remote Sensing of Environment*, *122*, 106–116. https://doi.org/10.1016/j.rse.2011.08.027

Prescott, C. E. (2002). The influence of the forest canopy on nutrient cycling. *Tree Physiology*, *22*(15–16), 1193–1200. https://doi.org/10.1093/treephys/22.15-16.1193

Quinton, J. N., Govers, G., Van Oost, K., & Bardgett, R. D. (2010). The impact of agricultural soil erosion on biogeochemical cycling. *Nature Geoscience*, *3*(5), 311–314. https://doi.org/10.1038/ngeo838

R Core Team. (2021). *R: A Language and Environment for Statistical Computing*. https://www.r-project.org/

Rabalais, N. N., Turner, R. E., Díaz, R. J., & Justić, D. (2009). Global change and eutrophication of coastal waters. *ICES Journal of Marine Science*, *66*(7), 1528–1537. https://doi.org/10.1093/icesjms/fsp047

Raymond, P. A., & Saiers, J. E. (2010). Event controlled DOC export from forested watersheds. *Biogeochemistry*, *100*(1), 197–209. https://doi.org/10.1007/s10533-010-9416-7

Read, D. J. (1991). Mycorrhizas in ecosystems. *Experientia*, *47*, 376–391. https://doi.org/10.1016/0006-2952(93)90100-B

Reed, S. C., Townsend, A. R., Taylor, P. G., & Cleveland, C. C. (2011). Phosphorus Cycling in Tropical Forests Growing on Highly Weathered Soils. In E. Brünemann, A. Oberson, & E. Frossard (Eds.), *Phosphorus in Action* (Vol. 26, pp. 215–243). Springer International Publishing. https://doi.org/10.1007/978-3-642-15271-9

Rees, R. M., Wuta, M., Furley, P. A., & Li, C. (2006). Nitrous oxide fluxes from savanna (miombo) woodlands in Zimbabwe. *Journal of Biogeography*, *33*(3), 424–437. https://doi.org/10.1111/j.1365-2699.2005.01423.x

Reiners, W. A., Bouwman, A. F., Parsons, W. F. J., & Keller, M. (1994). Tropical rain forest conversion to pasture: Changes in vegetation and soil properties. *Ecological Applications*, *4*(2), 363–377. https://doi.org/10.2307/1941940

Réjou-Méchain, M., Mortier, F., Basin, J. F., Cornu, G., Barbier, N., Bayol, N., Bénédet, F., Bry, X., Dauby, G., Deblauwe, V., Doucet, J. L., Doumenge, C., Fayolle, A., Garcia, C., Lubamba, J. P. K., Loumeto, J. J., Ngomanda, A., Ploton, P., Sonké, B., Trottier, C., Vimal, R., Yongo, O., Pélissier, R., & Gourlet-Fleury, S. (2021). Unveiling African rainforest composition and vulnerability to global change. *Nature, 593(5),* 90-94. https://doi.org/10.1038/s41586-021-03483-6

Riskin, S. H., Neill, C., Jankowski, K., Krusche, A. V., McHorney, R., Elsenbeer, H., Macedo, M. N., Nunes, D., & Porder, S. (2017). Solute and sediment export from Amazon forest and soybean headwater streams: *Ecological Applications*, *27*(1), 193–207. https://doi.org/10.1002/eap.1428

Roering, J. J., Kirchner, J. W., & Dietrich, W. E. (2001). Hillslope evolution by nonlinear, slope-dependent transport: Steady state morphology and equilibrium adjustment timescales. *Journal of Geophysical Research: Solid Earth*, *106*(B8), 16499–16513. https://doi.org/10.1029/2001jb000323

Rosseel, Y. (2012). lavaan: An R Package for Structural Equation Modeling. *Journal of Statistical Software*, *48*(2), 1–36.

Rudel, T. K., Defries, R., Asner, G. P., & Laurance, W. F. (2009). Changing drivers of deforestation and new opportunities for conservation. *Conservation Biology*, *23*(6), 1396–1405. https://doi.org/10.1111/j.1523-1739.2009.01332.x

Rütting, T., Ntaboba, L. C., Roobroeck, D., Bauters, M., Huygens, D., & Boeckx, P. (2015). Leaky nitrogen cycle in pristine African montane rainforest soil. *Global Biogeochemical Cycles*, *29*, 1754–1762. https://doi.org/10.1111/1462-2920.13280

Saiz, G., Wynn, J. G., Wurster, C. M., Goodrick, I., Nelson, P. N., & Bird, M. I. (2015). Pyrogenic carbon from tropical savanna burning: Production and stable isotope composition. *Biogeosciences*, *12*(6), 1849–1863. https://doi.org/10.5194/bg-12-1849-2015

Santiago, L. S. (2015). Nutrient limitation of eco-physiological processes in tropical trees. *Trees - Structure and Function*, *29*(5), 1291–1300. https://doi.org/10.1007/s00468-015-1260-x

Saunders, T. J., McClain, M. E., & Llerena, C. A. (2006). The biogeochemistry of dissolved nitrogen, phosphorus, and organic carbon along terrestrial-aquatic flowpaths of a montane headwater catchment in the Peruvian Amazon. *Hydrological Processes*, *20*, 2549–2652. https://doi.org/10.1002/hyp.6215

Sayer, A. M., Walsh, R. P. D., & Bidin, K. (2006). Pipeflow suspended sediment dynamics and their contribution to stream sediment budgets in small rainforest catchments, Sabah, Malaysia. *Forest Ecology and Management*, *224*(1–2), 119–130. https://doi.org/10.1016/j.foreco.2005.12.012

Schefuß, E., Versteegh, G. J. M., Jansen, J. H. F., & Sinninghe Damsté, J. S. (2004). Lipid biomarkers as major source and preservation indicators in SE Atlantic surface sediments. *Deep-Sea Research Part I: Oceanographic Research Papers*, *51*(9), 1199–1228. https://doi.org/10.1016/j.dsr.2004.05.002

Schwab, G. O., Fangmeier, D. D. & Elliot, W. J. (1994). *Soil and Water Conservation Engineering (4th ed.).* New York: Wiley.

Sidle, R. C., & Campbell, A. J. (1985). Patterns of Suspended Sediment Transport in a Coastal Alaska Stream. *JAWRA Journal of the American Water Resources Association*, *21*(6), 909–917. https://doi.org/10.1111/j.1752-1688.1985.tb00186.x

Six, J., Conant, R. T., Paul, E. A., & Paustian, K. (2002). Stabilization mechanisms of soil organic matter: Implications for C-saturation of soils. *Plant and Soil*, *241*(2), 155–176.

Slik, J. W. F., Arroyo-Rodríguez, V., Aiba, S. I., Alvarez-Loayza, P., Alves, L. F., Ashton, P., Balvanera, P., Bastian, M. L., Bellingham, P. J., Van Den Berg, E., Bernacci, L., Da Conceição Bispo, P., Blanc, L., Böhning-Gaese, K., Boeckx, P., Bongers, F., Boyle, B., Bradford, M., Brearley, F. Q., … Venticinque, E. M. (2015). An estimate of the number of tropical tree species. *Proceedings of the National Academy of Sciences of the United States of America*, *112*(33), E4628–E4629. https://doi.org/10.1073/pnas.1512611112

Slomp, C. P. (2012). Phosphorus Cycling in the Estuarine and Coastal Zones: Sources, Sinks, and Transformations. In *Treatise on Estuarine and Coastal Science* (Vol. 5). Elsevier Inc. https://doi.org/10.1016/B978-0-12-374711-2.00506-4

Smith, H. G., & Dragovich, D. (2009). Interpreting sediment delivery processes using suspended sediment-discharge hysteresis patterns from nested upland catchments, south-eastern Australia. *Hydrological Processes*, *23*, 2415–2426.

Smith, D. D., & Wischmeier, W. H. (1957). Factors affecting sheet and rill erosion. *Eos, Transactions American Geophysical Union*, *38*(6), 889-896.

Soethe, N., Lehmann, J., & Engels, C. (2008). Nutrient availability at different altitudes in a tropical montane forest in Ecuador. *Journal of Tropical Ecology*, *24*, 397–406. https://doi.org/10.1017/S026646740800504X

Sollins, P., Robertson, G. P., & Uehara, G. (1988). Nutrient mobility in variable- and permanent-charge soils. *Biogeochemistry*, *199*(6), 181–199. https://doi.org/https://doi.org/10.1007/BF02182995

Spencer, R. G. M., Hernes, P. J., Dinga, B., Wbakanghanzi, J. N., Drake, T., & Six, J. (2016). Origins, seasonality, and fluxes of organic matter in the Congo River. *Global biogeochemical cycles, 30,* 1105-1121. https://doi.org/10.1002/2016GB005427

Stefano, C. Di, Ferro, V., Porto, P., & Tusa, G. (2000). Slope curvature influence on soil erosion and deposition processes. *Water Resources Research*, *36*(2), 607–617.

Stenfert Kroese, J., Jacobs, S. R., Tych, W., Breuer, L., Quinton, J. N., & Rufino, M. C. (2020). Tropical Montane Forest Conversion Is a Critical Driver for Sediment Supply in East African Catchments. *Water Resources Research*, *56*(10). https://doi.org/10.1029/2020WR027495

Suzumura, M. (2008). Persulfate chemical wet oxidation method for the determination of particulate phosphorus in comparison with a high-temperature dry combustion method. *Limnology and Oceanography: Methods*, *6*(11), 619–629. https://doi.org/10.4319/lom.2008.6.619

Tanner, E. V. J., Vitousek, P. M., & Cuevas, E. (1998). Experimental investigation of nutrient limitation of forest growth on wet tropical mountains. *Ecology*, *79*(1), 10–22.

Taylor, P. G., Wieder, W. R., Weintraub, S., Cohen, S., Cleveland, C. C., Townsend, A. R., & Templer, P. H. (2015). Organic forms dominate hydrologic nitrogen export from a lowland tropical watershed. *Ecology*, *96*(5), 1229–1241. https://doi.org/10.1890/13-1418.1

Templer, P. H., Groffman, P. M., Flecker, A. S., & Power, A. G. (2005). Land use change and soil nutrient transformations in the Los Haitises region of the Dominican Republic. *Soil Biology and Biochemistry*, *37*(2), 215–225. https://doi.org/10.1016/j.soilbio.2004.07.031

Thornton, P. E., Lamarque, J. F., Rosenbloom, N. A., & Mahowald, N. M. (2007). Influence of carbon-nitrogen cycle coupling on land model response to CO2 fertilization and climate variability. *Global Biogeochemical Cycles*, *21*(4), 1–15. https://doi.org/10.1029/2006GB002868

Toriman, M. E., Mazlin Mokhtar, B. I. N., Karim, O., Barzani Gasim, M., & Taha, R. (2009). Short-term sediment yields from small catchment of Sungai Anak Bangi Selangor. *Bulletin of the Geological Society of Malaysia*, *55*, 55–59. https://doi.org/10.7186/bgsm55200909

Townsend-Small, A., McClain, M. E., Hall, B., Noguera, J. L., Llerena, C. A., & Brandes, J. A. (2008). Suspended sediments and organic matter in mountain headwaters of the Amazon River: Results from a 1-year time series study in the central Peruvian Andes. *Geochimica et Cosmochimica Acta*, *72*(3), 732–740. https://doi.org/10.1016/j.gca.2007.11.020

Townsend, A. R., Asner, G. P., & Cleveland, C. C. (2008). The biogeochemical

heterogeneity of tropical forests. *Trends in Ecology and Evolution*, *23*(8), 424–431. https://doi.org/10.1016/j.tree.2008.04.009

Townsend, A. R., Cleveland, C. C., Houlton, B. Z., Alden, C. B., & White, J. W. C. (2011). Multi-element regulation of the tropical forest carbon cycle. *Frontiers in Ecology and the Environment*, *9*(1), 9–17. https://doi.org/10.1890/100047

Tully, K., Sullivan, C., Weil, R., & Sanchez, P. (2015). The State of soil degradation in sub-Saharan Africa: Baselines, trajectories, and solutions. *Sustainability (Switzerland)*, *7*(6), 6523–6552. https://doi.org/10.3390/su7066523

Tyukavina, A., Hansen, M. C., Potapov, P., Parker, D., Okpa, C., Stehman, S. V., Kommareddy, I., & Turubanova, S. (2018). Congo Basin forest loss dominated by increasing smallholder clearing. *Science Advances*, *4*(11). https://doi.org/10.1126/sciadv.aat2993

Van Engelen, V. W. P., Verdoodt, A., Dijkshoorn, J. A., & Van Ranst, E. (2006). Soil and Terrain Database of Central Africa (DR of Congo, Burundi and Rwanda), ISRIC - World Soil Information, Wageningen.

Van Oost, K., Quine, T. A., Govers, G., De Gryze, S., Six, J., Harden, J. W., Ritchie, J. C., McCarty, G. W., Heckrath, G., Kosmas, C., Giraldez, J. V., Marques Da Silva, J. R., & Merckx, R. (2007). The impact of agricultural soil erosion on the global carbon cycle. *Science*, *318*(5850), 626–629. https://doi.org/10.1126/science.1145724

Van Ranst, E., Baert, G., Ngongo, M., & Mfuka, P. (2010). *Carte pédologique de Yangambi, planchette 2: Yangambi, échelle 1:50.000*. UGent; Hogent; UNILU; UNIKIN.

Verbeeck, H., Boeckx, P., & Steppe, K. (2011). Tropical forests : include Congo basin. *Nature*, *479*, 179.

Vercruysse, K., Grabowski, R. C., & Rickson, R. J. (2017). Suspended sediment transport dynamics in rivers: Multi-scale drivers of temporal variation. *Earth-Science Reviews*, *166*, 38–52. https://doi.org/10.1016/j.earscirev.2016.12.016

Verhegghen, A., Mayaux, P., De Wasseige, C., & Defourny, P. (2012). Mapping Congo Basin vegetation types from 300 m and 1 km multi-sensor time series for carbon stocks and forest areas estimation. *Biogeosciences*, *9*(12), 5061–5079. https://doi.org/10.5194/bg-9-5061-2012

Vicca, S., Luyssaert, S., Peñuelas, J., Campioli, M., Ill Chapin, F. S., Ciais, P., Heinemeyer, A., Högberg, P., Kutsch, W. L., Law, B. E., Malhi, Y., Papale, D., Piao, S. L., Reichstein, M., Schulze, E. D., & Janssens, I. A. (2012). Fertile forests produce biomass more efficiently. *Ecology Letters*, *15*, 520–526. https://doi.org/10.1111/j.1461-0248.2012.01775.x

Vitousek, P. M., Naylor, R., Crews, T., David, M. B., Drinkwater, L. E., Holland, E., Johnes, P. J., Katzenberger, J., Martinelli, L. A., Matson, P. A., Nziguheba, G.,

Ojima, D., Palm, C. A., Robertson, G. P., Sanchez, P. A., Townsend, A. R., & Zhang, F. S. (2009). Nutrient imbalances in agricultural development. *Science*, *324*(5934), 1519–1520. https://doi.org/10.1126/science.1170261

Vitousek, Peter M., Hedin, L. O., Matson, P. A., Fownes, J. H., & Neff, J. (1998). Within-System Element Cycles, Input-Output Budgets, and Nutrient Limitation. *Successes, Limitations, and Frontiers in Ecosystem Science*, 432–451. https://doi.org/10.1007/978-1-4612-1724-4_18

Vitousek, Peter M., & Reiners, W. A. (1975). Ecosystem Succession and Nutrient Retention: A Hypothesis. *BioScience*, *25*(6), 376–381. https://doi.org/10.2307/1297148

Vitousek, Peter M. (1984). Litterfall, nutrient cycling, and nutrient limitation in tropical forests. *Ecology*, 65, 285-298. https://doi.org/10.2307/1939481

Vitousek, Peter M, Porder, S., Houlton, B. Z., & Chadwick, O. a. (2010). Terrestrial phosphorus limitation : mechanisms , implications , and nitrogen – phosphorus interactions. *Ecological Applications, 20*(1), 5–15. https://doi.org/10.1890/08-0127.1

Wager, S. (2014). *randomForestCI: Confidence Intervals for Random Forests*.

Walker, T. W., & Syers, J. K. (1976). The fate of phosphorus during pedogenesis. *Geoderma*, *15*(1), 1–19. https://doi.org/10.1016/0016-7061(76)90066-5

Wang, L., Okin, G. S., D'Odorico, P., Caylor, K. K., & Macko, S. A. (2013). Ecosystem-scale spatial heterogeneity of stable isotopes of soil nitrogen in African savannas. *Landscape Ecology*, *28*(4), 685–698. https://doi.org/10.1007/s10980-012-9776-6

Wang, R., Goll, D., Balkanski, Y., Hauglustaine, D., Boucher, O., Ciais, P., Janssens, I., Penuelas, J., Guenet, B., Sardans, J., Bopp, L., Vuichard, N., Zhou, F., Li, B., Piao, S., Peng, S., Huang, Y., & Tao, S. (2017). Global forest carbon uptake due to nitrogen and phosphorus deposition from 1850 to 2100. *Global Change Biology*, *23*(11), 4854–4872. https://doi.org/10.1111/gcb.13766Wang, Y. P., Law, R. M., & Pak, B. (2010). A global model of carbon, nitrogen and phosphorus cycles for the terrestrial biosphere. *Biogeosciences*, *7*(7), 2261–2282. https://doi.org/10.5194/bg-7-2261-2010

Wang, Y. P., Ciais, P., Goll, D., Huang, Y., Luo, Y., Wang, Y. P., Bloom, A. A., Broquet, G., Hartmann, J., Peng, S., Penuelas, J., Piao, S., Sardans, J., Stocker, B. D., Wang, R., Zaehle, S., & Zechmeister-Boltenstern, S. (2018). GOLUM-CNP v1.0: a data-driven modeling of carbon, nitrogen and phosphorus cycles in major terrestrial biomes. *Geoscientific Model Development, 11,* 3908-3928. https://doi.org/10.5194/gmd-11-3903-2018

Weintraub, S. R., Taylor, P. G., Porder, S., Cleveland, C. C., Asner, G. P., & Townsend, A. R. (2015). Topographic controls on soil nitrogen availability in a lowland tropical forest. *Ecology*, *96*(6), 1561–1574. c:%5CPDfs%5C14-

0834.1.pdf

White, F. (1983). Vegetation of Africa - a descriptive memoir to accompany the Unesco/AETFAT/UNSO vegetetation map of Africa. *Natural Resources Research Report XX*. U. N. Educational, Scientific and Cultural Organization; 7 Place de Fontenoy, 75700 Paris, France; 356 pages.

White, L. J. T., Masudi, E. B., Ndongo, J. D., Matondo, R., Soudan-Nonault, A., Ngomanda, A., Averti, I. S., Ewango, C. E. N., Sonké, B., & Lewis, S. L. (2021). Congo Basin rainforest — invest US$150 million in science. *Nature*, *598*(7881), 411–414. https://doi.org/10.1038/d41586-021-02818-7

Wieder, W. R., Cleveland, C. C., Smith, W. K., & Todd-Brown, K. (2015). Future productivity and carbon storage limited by terrestrial nutrient availability. *Nature Geoscience*, *8*(6), 441–444. https://doi.org/10.1038/NGEO2413

Wieder, W. R., Cleveland, C. C., & Townsend, A. R. (2011). Throughfall exclusion and leaf litter addition drive higher rates of soil nitrous oxide emissions from a lowland wet tropical forest. *Global Change Biology*, *17*(10), 3195–3207. https://doi.org/10.1111/j.1365-2486.2011.02426.x

Williams, J. R., Jones, C. A., & Dyke, P. T. (1984). A modelling approach to determining the relationship between erosion and soil productivity. *Transactions - American Society of Agricultural Engineers*, *27*(1), 129–144. https://doi.org/10.13031/2013.32748

Williams, M. R., & Melack, J. M. (1997). Solute export from forested and partially deforested catchments in the central amazon. *Biogeochemistry*, *38*(1), 67–102. https://doi.org/10.1023/A:1005774431820

Wood, P. A. (1977). Controls of variation in suspended sediment concentration in the River Rother, West Sussex, England. *Sedimentology*, *24*(3), 437–445. https://doi.org/10.1111/j.1365-3091.1977.tb00131.x

Wright, S. J. (2019). Plant responses to nutrient addition experiments conducted in tropical forests. *Ecological Monographs*, *89*(4), 1–18. https://doi.org/10.1002/ecm.1382

Yamashita, Y., Maie, N., Briceño, H., & Jaffé, R. (2010). Optical characterization of dissolved organic matter in tropical rivers of the Guayana Shield, Venezuela. *Journal of Geophysical Research: Biogeosciences*, *115*(G1). https://doi.org/10.1029/2009JG000987

Zak, D. R., Freedman, Z. B., Upchurch, R. A., Steffens, M., & Kögel-Knabner, I. (2016). Anthrogopgenic N deposition increases soil organic matter accumulation without altering its biochemical composition. *Global Change Biology, 23(2),* 933-944. https://doi.org/10.1111/gcb.13480

Zhang, Y., Meng, X., Bai, Y., Wang, X., Xia, P., Yang, G., Zhu, Z., & Zhang, H. (2021). Sources and features of particulate organic matter in tropical small

mountainous rivers (SW China) under the effects of anthropogenic activities. *Ecological Indicators*, *125*, 107471. https://doi.org/10.1016/j.ecolind.2021.107471Ziegler, A. D., Benner, S. G., Kunkel, M. L., Phang, V. X. H., Lupascu, M., & Tantasirin, C. (2016). Particulate carbon and nitrogen dynamics in a headwater catchment in Northern Thailand: hysteresis, high yields, and hot spots. *Hydrological Processes*, *30*(19), 3339–3360. https://doi.org/10.1002/hyp.10840

Ziegler, A. D., Benner, S. G., Tantasirin, C., Wood, S. H., Sutherland, R. A., Sidle, R. C., Jachowski, N., Nullet, M. A., Xi, L. X., Snidvongs, A., Giambelluca, T. W., & Fox, J. M. (2014). Turbidity-based sediment monitoring in northern Thailand: Hysteresis, variability, and uncertainty. *Journal of Hydrology*, *519*(PB), 2020–2039. https://doi.org/10.1016/j.jhydrol.2014.09.010

Zimmermann, A., Francke, T., & Elsenbeer, H. (2012). Forests and erosion: Insights from a study of suspended-sediment dynamics in an overland flow-prone rainforest catchment. *Journal of Hydrology*, *428–429*, 170–181. https://doi.org/10.1016/j.jhydrol.2012.01.039

Appendices

Appendix A

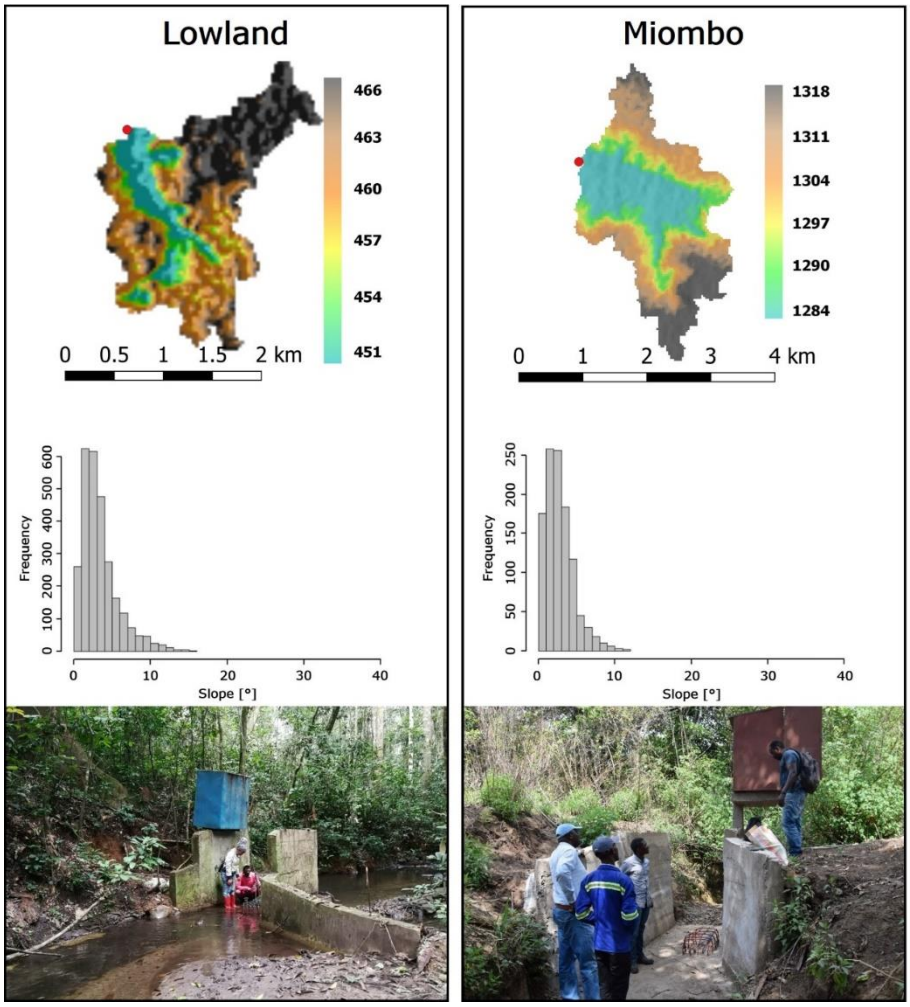

Appendix A1 Topographical maps and slope distributions of the two catchments. Colored values are in meters above sea level. Red dots indicate the locations of the concrete flumes (photos at the bottom). Source DEM: NASA JPL.

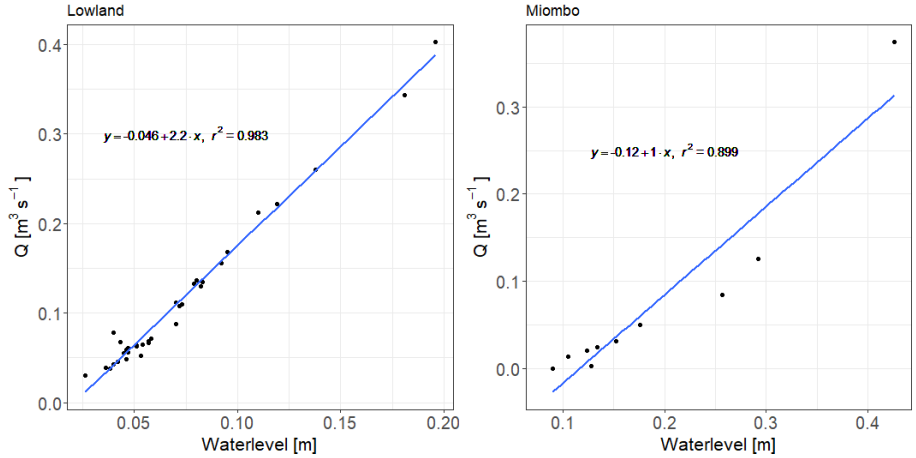

Appendix A2 Rating curves for discharge calculation for the lowland forest catchment (left) and the Miombo woodland catchment (right).

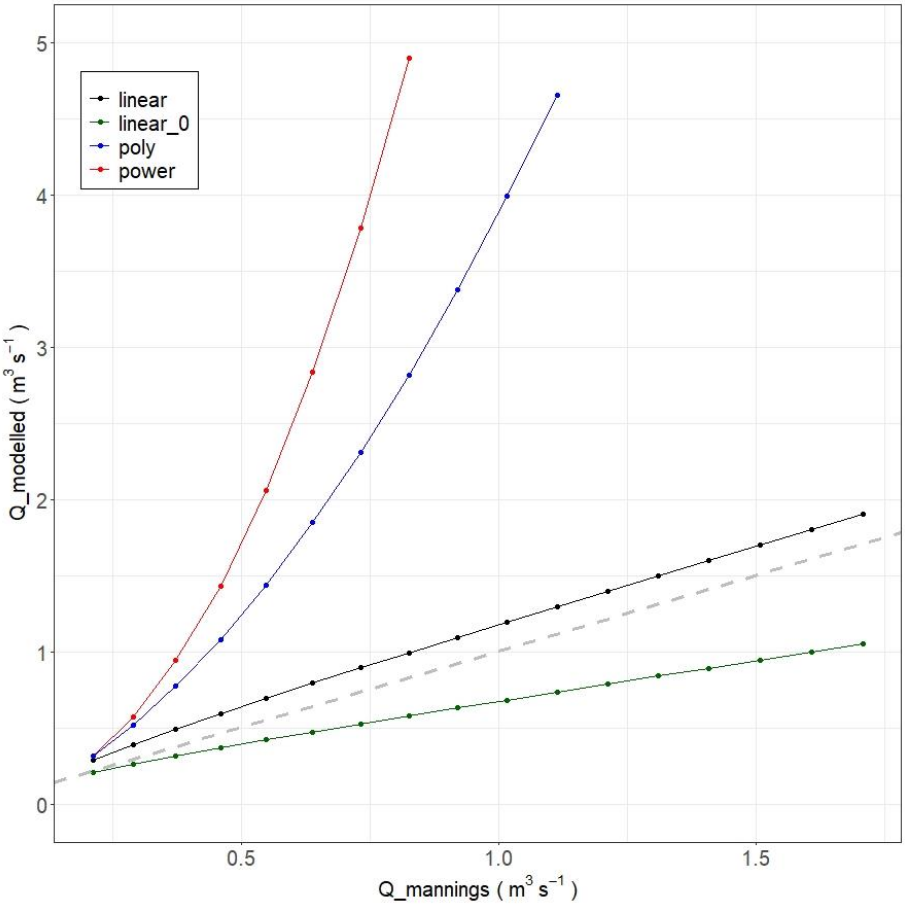

Appendix A3 Comparison between discharge calculated with the Manning's equation and the discharge calculated from the different models obtained from the rating curve in Appendix A2 for the Miombo site. Black is the linear model between water level and Q. Green is the linear model between water level and Q with an intercept 0. Blue is a second order polynomial function between water level and Q and red is a power function between water level and Q. Q were calculated for water levels between 0.5 and 2 m. Grey dashed line indicates the 1:1 line.

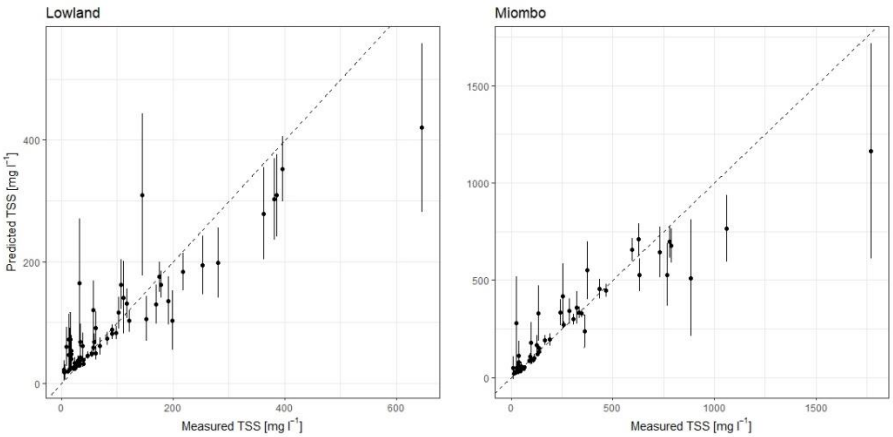

Appendix A4 Comparison between measured and predicted TSS values for the lowland forest and Miombo woodland site. Error bars indicate the standard deviation of the random forest prediction.

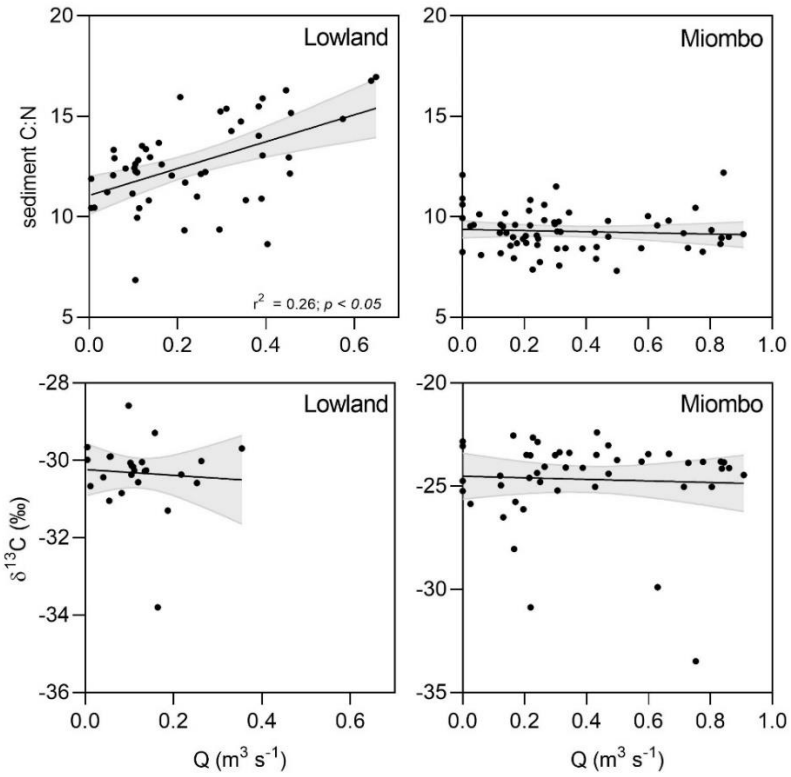

Appendix A5 C:N ratios of sediments plotted against the discharge (Q) values at the respective sampling points (top figures). $\delta^{13}C$ values of Particulate Organic Carbon plotted against the discharge values at the respective sampling points (bottom figures).

Appendix A6 left photo: Miombo woodland at the end of the dry season after seasonal fires. Right photo: Miombo woodland at the end of the rainy season.

Appendix B

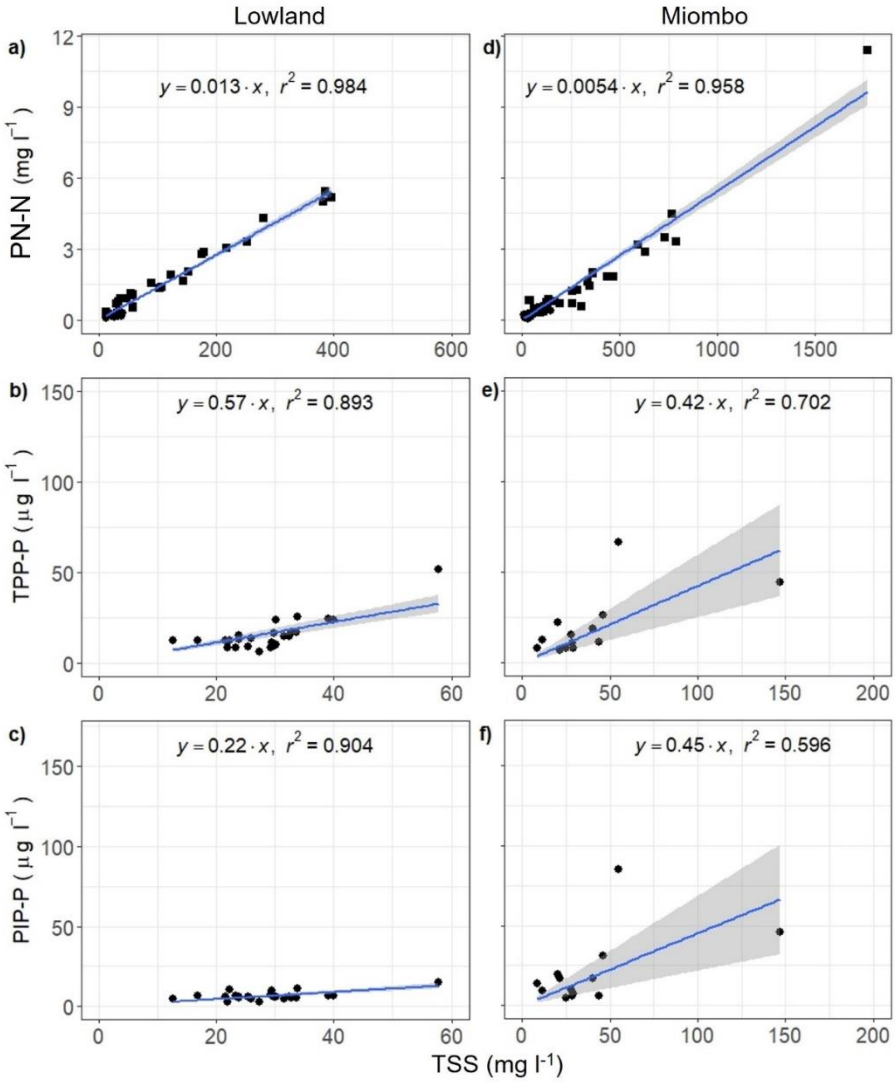

Appendix B1 Particulate nutrient concentrations as a function of total suspended sediment (TSS) concentration at the two forest sites. Round dots represent samples during baseflow campaigns and square dots represent samples taken during storm flow conditions. Blue lines indicate linear regressions with its confidence intervals in grey.

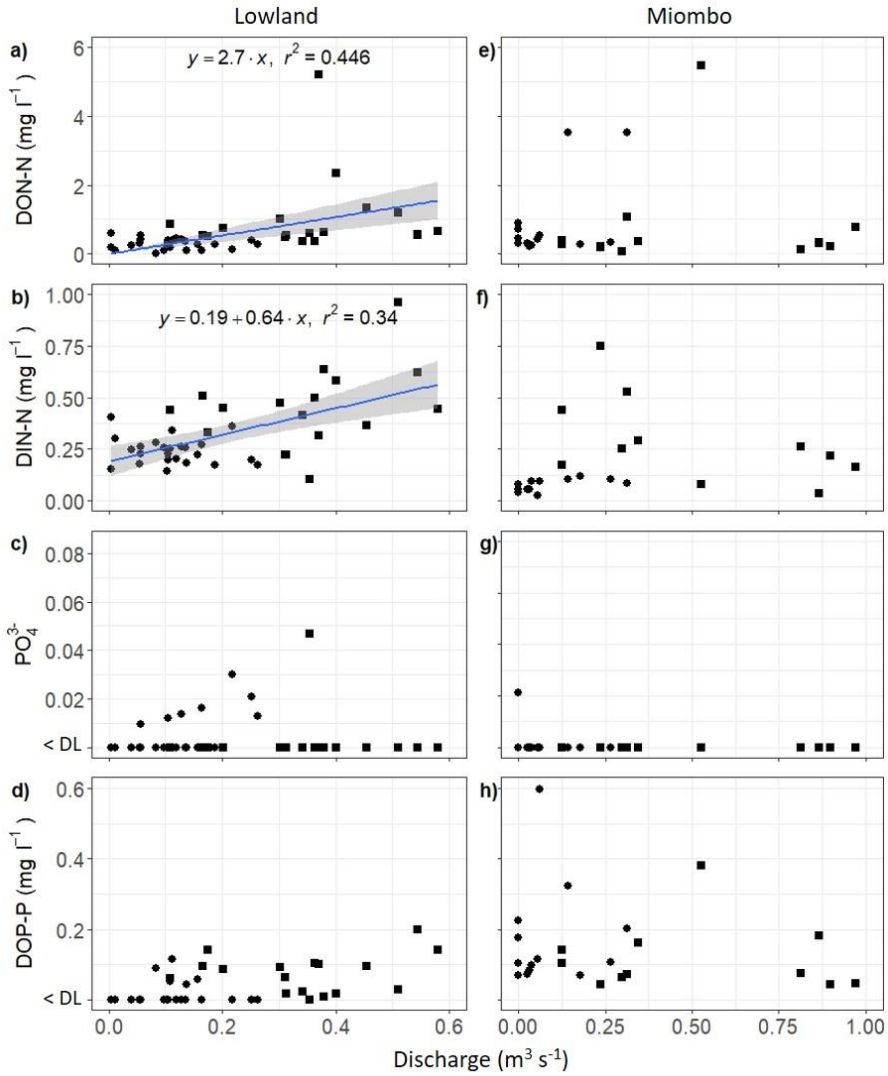

Appendix B2 Dissolved nutrient concentrations as a function of discharge at the two forest sites. Round dots indicate the samples from the baseflow sampling campaign and square dots represent samples during storm-event sampling. Blue lines indicate linear regressions with its confidence intervals in grey. Regression fits are only shown when regressions have a p value < 0.05.

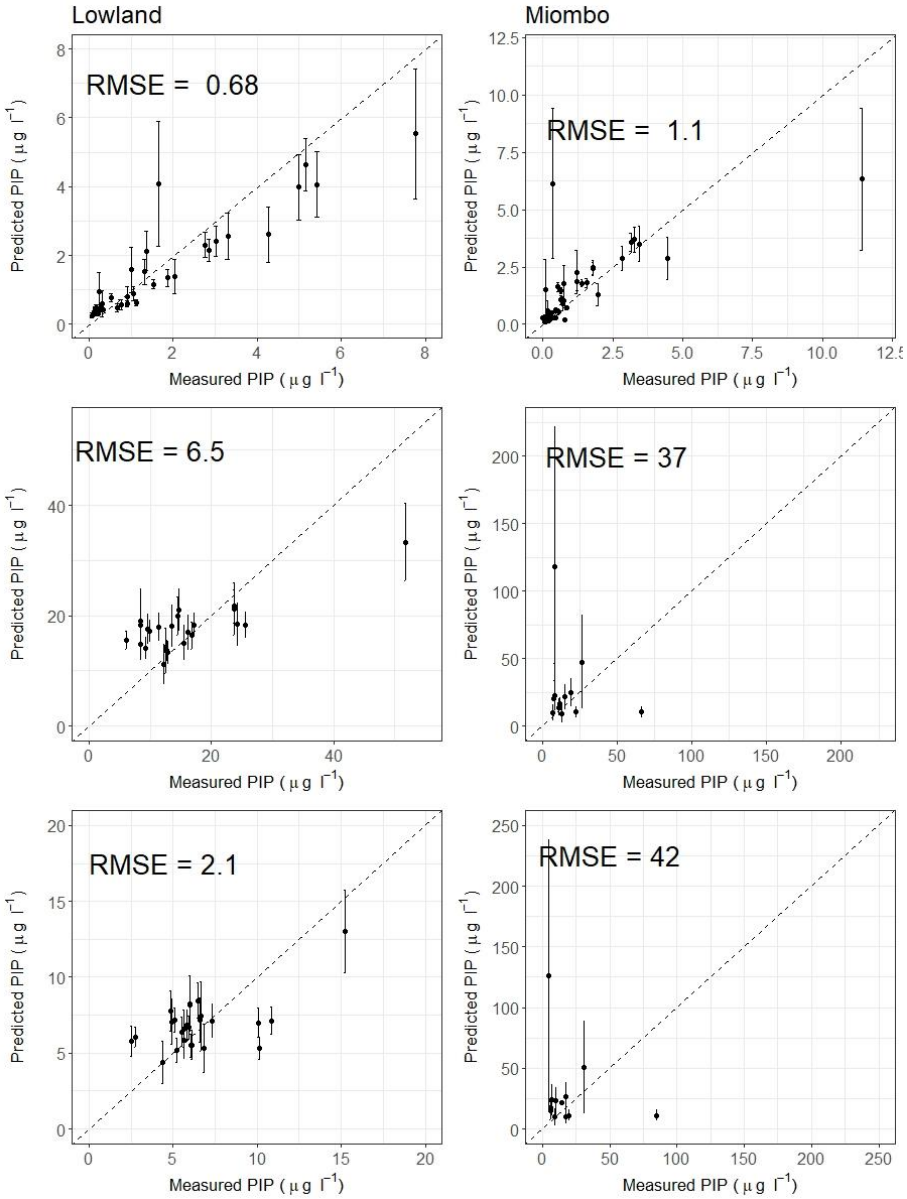

Appendix B3 Comparison of measured particulate nutrients concentrations and predicted concentrations with the doubled modelling approach (turbidity -> TSS -> particulate nutrient concentrations). Values indicate the root mean square errors (RMSE). Dashed line represents the 1:1 line.

Appendix B4 Number of samples taken at baseflow and stormflow conditions for each measurement. Middle columns show the mean values ± standard error of the baseflow and stormflow samples. Root mean square error (RMSE) of model predictions for the constituents which were modelled for yield calculations (see Appendix B1 – B3).

		N° of Samples		mean conc. samples			
		Baseflow	Stormflow	Baseflow	Stormflow	RMSE	Unit
Lowland	TSS	39	49	24.36 ± 1.35	116.88 ± 18.60	48.39 [1]	mg L^{-1}
	PN	29	24	0.17 ± 0.01	2.28 ± 0.34	0.68	mg L^{-1}
	DON	39	16	0.33 ± 0.03	1.05 ± 0.29	0.77	mg L^{-1}
	NO_3^-	39	16	0.17 ± 0.01	0.31 ± 0.04	0.12	mg L^{-1}
	NH_4^+	39	16	0.07 ± 0.01	0.12 ± 0.02	0.06	mg L^{-1}
	TPP	39	0	12.25 ± 1.00	n.a.	6.5	µg L^{-1}
	PIP	39	0	5.58 ± 0.41	n.a.	2.1	µg L^{-1}
	DOP	39	16	21.74 ± 5.85	75.21 ± 13.25	n.a.	µg L^{-1}
	PO_4^{3-}	39	16	7.31 ± 0.87	7.47 ± 2.47	n.a.	µg L^{-1}
Miombo	TSS	18	55	34.89 ± 7.17	271.89 ± 45.33	117.6 [1]	mg L^{-1}
	PN	18	42	0.12 ± 0.02	1.20 ± 0.30	1.1	mg L^{-1}
	DON	19	11	0.81 ± 0.24	0.85 ± 0.47	n.a.	mg L^{-1}
	NO_3^-	19	11	0.02 ± 0.00	0.08 ± 0.02	n.a.	mg L^{-1}
	NH_4^+	19	11	0.05 ± 0.01	0.23 ± 0.06	n.a.	mg L^{-1}
	TPP	18	0	22.28 ± 3.67	n.a.	37	µg L^{-1}
	PIP	18	0	17.54 ± 4.87	n.a.	42	µg L^{-1}
	DOP	19	11	139.82 ± 32.30	119 ± 30	n.a.	µg L^{-1}
	PO_4^{3-}	19	11	6.48 ± 0.90	5 ± 0	n.a.	µg L^{-1}

Appendix C

Appendix C1 Supplement – Methods
Methods for aquatic TDN and DON export

At each forest site, water samples have been taken from a nearby stream with a 2L HDPE bottle. Samples were taken fortnightly (N = 22 for lowland forest, N = 19 for montane forest and N = 5 for Miombo woodland) and discharge was measured at concrete flumes with a fixed width, by measuring water level and discharge with a mechanical flowmeter (General Oceanics Inc, Miami, US). Water samples got filtered through a 0.7 µm glass microfibre filter (Whatman, UK). The filtrated samples were immediately stored in a freezer and transported to Belgium for chemical analysis. NH_4^+ was determined colorimetrically by the salycialte-nitropusside method (Mulvaney 1996) on an autoanalyzer (AA3; Bran and Luebbe, Norderstedt, Germany). NO_3^- was also determined colometrically with the same autoanalyzer in form of NO_2^- after reduction of NO_3^- in a Cd-Cu column followed by the reaction of the NO_2^- with N-l-napthylethylenediamine to produce a chomophore. Total dissolved nitrogen (TDN) was measured by adding 1:1 oxidizing solution of NaOH, H_3BO_3, and $K_2S_2O_8$ to the sample and autoclave it for 1h at 121°C. This process converted NH_4^+ and the dissolved organic N (DON) into NO_3^+ (Lachouani et al. 2010). Yields were calculated by dividing the annual exports by the catchment area. The catchment area was determined using the GPS positions of the flumes and calculating upstream area in a 30-m SRTM derived digital elevation model (DEM) (NASA JPL).

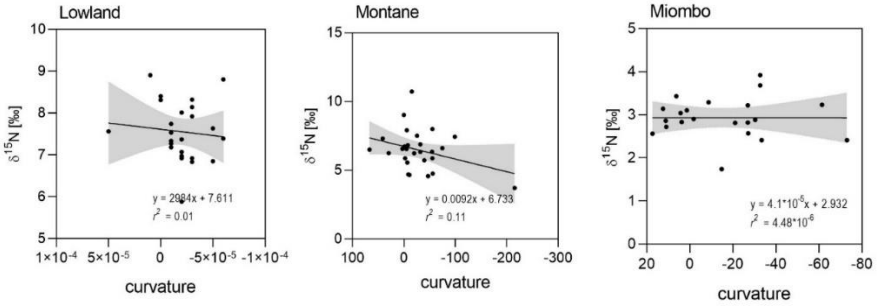

Appendix C2 $\delta^{15}N$ in topsoil (0 – 20 cm) plotted against the curvature of the sampling spot. Positive curvature values represent concave landforms, while negative values represent convex landforms.

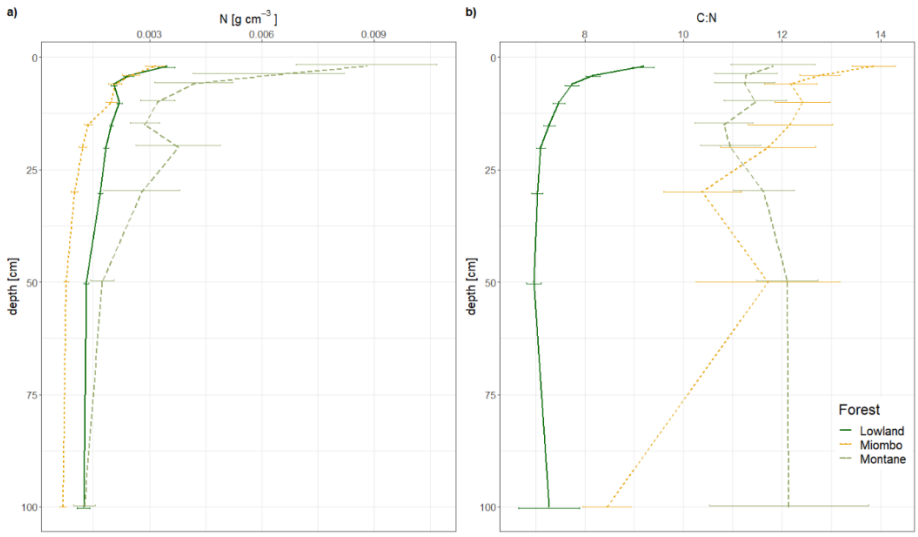

Appendix C3 a) Profiles of average bulk N values in g cm^{-3} for the three different forest sites. b) Profiles of average C:N ratios for the different forest sites. Error bars indicate standard error.

References Appendix C

Lachouani, P., A. H. Frank, and W. Wanek. 2010. A suite of sensitive chemical methods to determine the d15N of ammonium, nitrate and total dissolved N in soil extracts. Rapid Communications in Mass Spectrometry: RCM 24:3615–3623.

Mulvaney, R. L. 1996. Nitrogen—inorganic forms. Pages 1123–1184 in D. L. Sparks, editor. Methods of soil analysis. Part 3. Chemical methods. American Society of Agronomy, Madison, Wisconsin, USA.

Appendix D

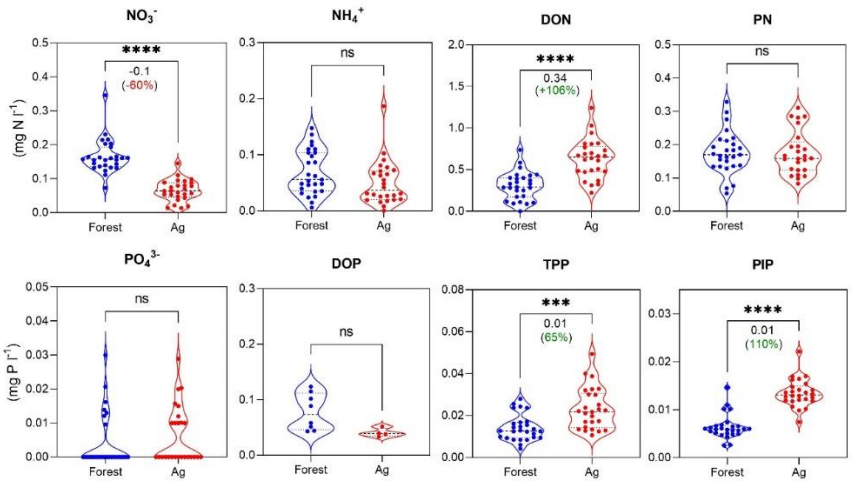

Appendix D1 Comparison of different N and P concentrations between the forest (blue) and agricultural (red) catchments. Stars indicate the significance obtained from the paired t-test, numbers show the differences between the means and the values between parentheses show the relative changes in yields. Dotted black lines indicate the median value for each site, and the dotted blue and red lines indicate the 25% and 75% quartiles

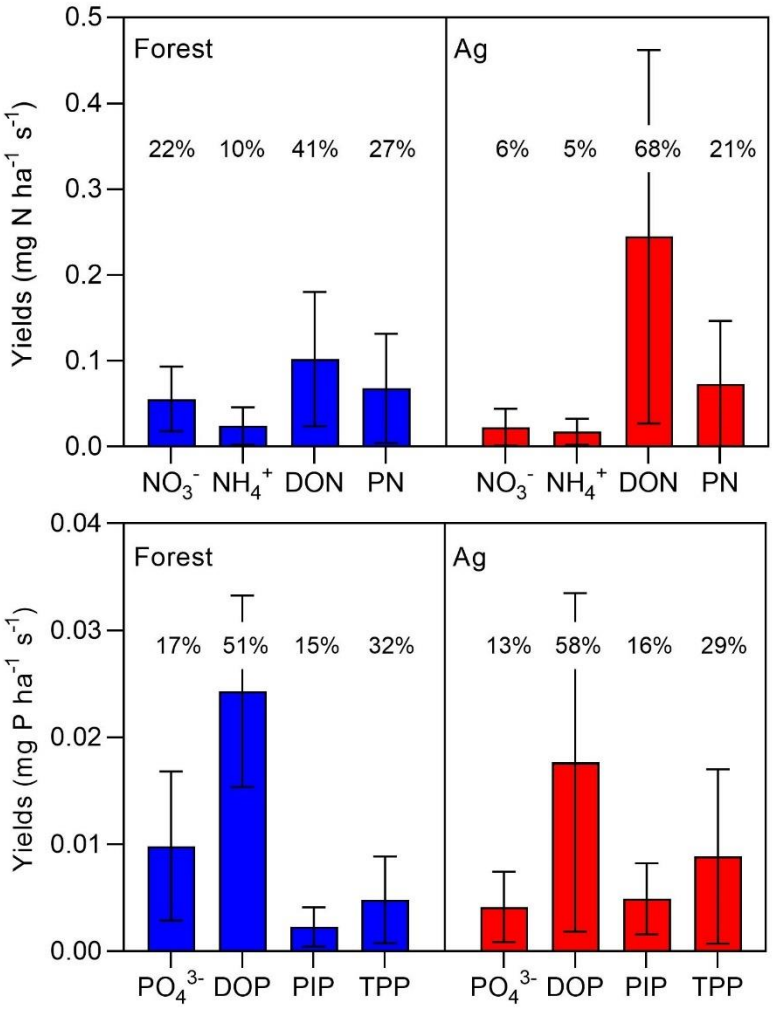

Appendix D2 Average measured instantaneous yields of different nitrogen (top) and phosphorus (bottom) constituents for the forest catchment (blue) and the agricultural catchment (red). Error bars indicating standard deviation of the mean. Percentages show the relative contribution of each constituent to the total N or P yields.

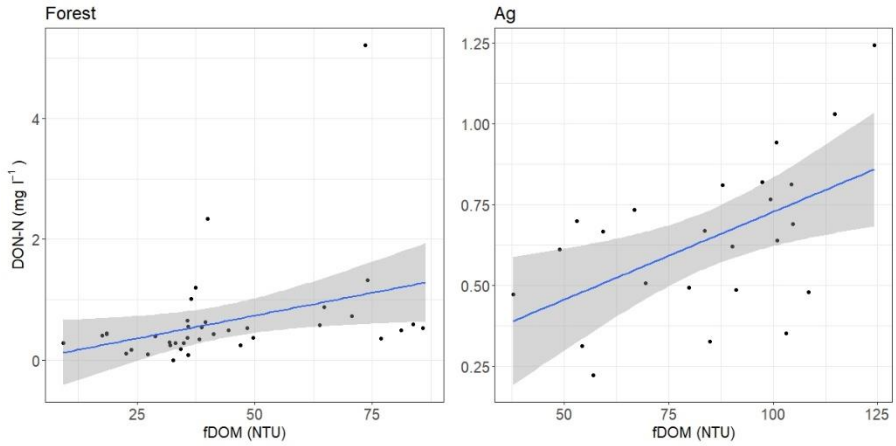

Appendix D3 Relations between fluorescent dissolved organic matter (fDOM) and dissolved organic nitrogen (DON) from the forest stream (left) and the agricultural stream (right). Blue lines indicate the linear regression with its confidence intervals in grey.

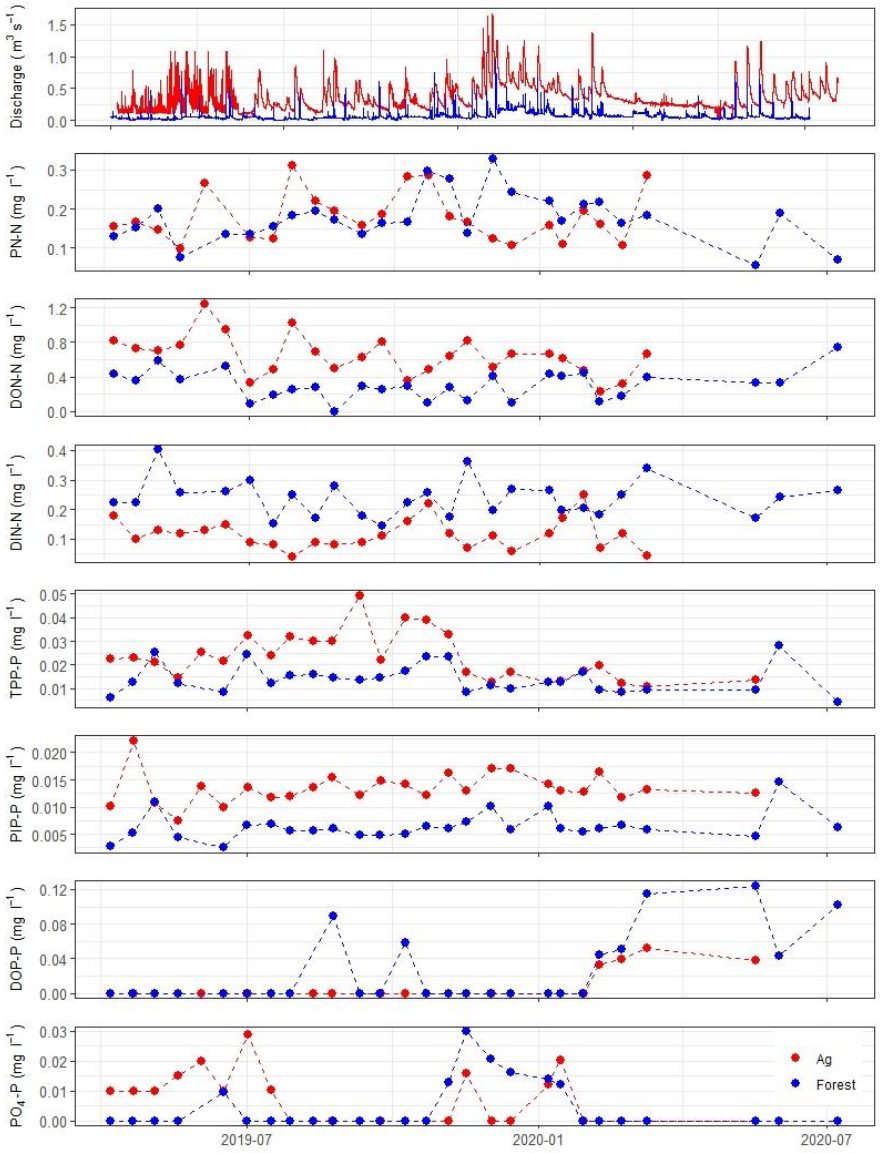

Appendix D4 Timeseries of measured water discharge and measured concentrations of particulate nitrogen (PN), dissolved organic nitrogen (DON), dissolved inorganic nitrogen (DIN), total particulate phosphorus (TPP), particulate inorganic phosphorus (PIP), dissolved organic phosphorus (DOP), and phosphate (PO_4^{3-}) from the agricultural stream and the forest stream. Red values indicate the Ag samples and blue values the Forest samples.

Acknowledgments

My incredible journey on the FORSEDCO project started in March 2018 somewhere in the jungle of Yangambi. Having some Belgium professor (one that I barely knew at that time) on my back, rescuing him from whatever infectious diseases were waiting to take advantage of his injured foot, that he got while scouting for the perfect spot to build a concrete flume in the middle of the forest. I got selected to fulfil this courageous task because his then PhD student and Travis had too close working relationships with that professor. That would have made it awkward for them to carry their boss around on their backs. Maybe it was this heroic rescue mission that got me in a favourable position some months later, when the same professor was in a desperate need to replace said PhD student. Just like that, my next three and a half years of my life were dedicated to the mission to scientifically please that professor, whom I courageously saved on that muggy day in March 2018. My whole PhD was an amazing journey with lots of challenges to overcome. This whole project would not have been possible without the help of so many people that guided and supported me on so many occasions! It is time now to thank all of you from the bottom of my heart:

Kristof. I am very thankful for your support of my special status that I was asking for. I am well aware that we had more discussions about administrative and monetary stuff and that it was not your (mine neither!) favourite thing to do. The more I am glad that we managed everything and that I can finally present you now the fruits of our work. I appreciated your inputs and guidance and patience on my way to fulfil this PhD. To Pascal and Jo, for hosting me in their groups, I really appreciated the times I spent at ISOFYS and SAE. I feel privileged to be able to benefit from your broad expertise and your suggestions were always welcome. I know that all of you three had sometimes different opinions on how to deal and handle with the problems we had during our campaigns and that I sometimes disagreed but let me assure you that we did all our best and I'm really happy with the outcome.

Now to the lovely people who made this project so awesome: Marijn, Matti and Travis. The dream-team. Go Anteaters! Fight Anteaters! I have so many amazing memories with you guys: spending a night on top of Nyiragongo, salt and pepper gluttony, enjoying nice breakfasts over the tea plantations outside Bukavu with hypnotized chickens, afterwork swims in the Ruki (just to name a few!). Marijn, the pioneer of Congolese biogeochemistry! My first encounter with you could not have been more fitting! The Belgian messiah, ascended from the deepest forests of Djolu, saving our lost asses in Bukavu! Our first DRC experience would not have been the same without your experience and thanks to you, I was hooked with the Congo! But not only were you an amazing fieldwork-buddy, also your immense knowledge about nutrients and forest ecology are amazing! Your inputs on my work were so valuable and I extremely profited from your experience.

Matti, I was so happy that we were able to do our first DRC trip together. If you wouldn't have convinced me to do my master thesis with you in Congo, I wouldn't be writing those lines right now! Your support over the years was amazing and I'm really thankful for your encouraging way of dealing with things. As soon as something did not go as planned, you were there and providing solutions and help. Your pragmatic way of live is exemplary.

Travis, the riverine-biogeochemistry god! I was so happy to have you around for my whole PhD. Thank you very much for always being there and dealing with my day-to-day problems of my research. You were always supporting my decisions and you also had to convince our big bosses from time to time that the things that we were doing were not all that bad. Getting my manuscripts Travinated improved the quality immensely and helped me a lot in publishing those!

Fieldwork in the DRC would not be possible without the support of the local people. Basile and Landry, thank you for your support and providing your lab spaces. I was really happy to have you taking the initiative in the constructions of the flumes and providing logistic support throughout the whole project.

I am deeply thankful for the students that were doing the main part of the fieldwork: Serge, Nadine, Christ, Rosine, Rodrigue, Serge, Degra, Claudino and Merveille. Your commitment to the work in the forest is invaluable. I am really glad that all of you were able to defend your own thesis with the work we did together and that some of you are continuing your scientific career. I am looking forward to see you conduct your own biogeochemical research in the Congo!

Work in and around Kisangani would not have been possible without the help of my brother Héritier! The way you guided me through Kisangani, since the first day I arrived there, was just amazing. I was always looking forward to get back to Kisangani. I felt privileged to be around during many important events of your live: the marriage with Florence and the birth of Freddy-Barthel. It is so nice to see your family grow! I really hope that I get the chance to come back and visit you and your family again.

A big thank you goes out to the people who were around in Louvain and Ghent: Especially Marco, Montfort, Guy-David, Pengzhi and Alice from UCL and Samuel, Katja and Saskia from UGhent. You all provided me with administrative, logistical and or scientific support and I highly appreciated this.

Now to the amazing people of the sustainable agroecosystems group. Thank you all for including me, as an external student, to your lovely group. I guess such a nice group mentality cannot be taken for granted. All those nice team outings, afterwork beers, after-afterwork beers Langstrasse-Karaoke-nights, game nights, spikeball sessions etc. etc. This list could be expanded far more, and this really shows the spirit that this group has, and I will really miss this work environment! I really enjoyed my time with all of you!

To my family, who supported me my whole life. I am really grateful that I have parents stand by my side even if I decide to be a long-time student ;). My mom, who

made sure that I was always well prepared for my fieldtrips in terms of first aid kits, really appreciated this service! Also, your warnings to always wear shoes in the jungle whatever happens, probably saved me several times from needing my own piggyback ride into safety :). *Mama und Papa, i dank eu vo ganzem Herze für die Unterstützig woni über all die Johre vo eu erhalte ha! Ohni eu wär die Arbeit nöd möglich gsi und er hönd an sehr grosse Ateil dra, dass i jetzt do stoh woni bi.*

Last but not least I have to acknowledge my better half, Laura. I am well aware that you were not super keen on me continuing my research in the DRC. I guess until now I was not really successful in convincing you that fieldwork in the DRC is safe. All the more I really appreciate that you still supported my work from the beginning, even if it meant that I was gone for longer times. *Viele herzliche Dank für alles! Dini führsorglich Unterstützig über die Johre het mer sehr viel bedüted!*

Curriculum vitae

Personal information

Name:	Simon
Surname:	Baumgartner
Address:	Ueberlandstrasse 28, 8051 Zürich
E-Mail:	s-baumgartner@gmx.ch
Date of birth:	01.07.1991
Civil status:	single
Nationality:	Swiss

Education

09/2015 – 09/2017	Swiss Federal Institute of Technology ETH Zürich Master in Environmental Science Major: Biogeochemistry & Pollutant dynamics
09/2011 – 08/2014	Swiss Federal Institute of Technology ETH Zürich Bachelor in Environmental Science Major: Biogeochemistry & Pollutant dynamics
08/2006 – 07/2010	Kantonsschule Heerbrugg Matura Focus: Chemistry/Biology

Professional experience

Since 09/2018	Université catholique de Louvain, Louvain-la Neuve, Belgium Ghent University, Ghent, Belgium PhD student
12/2017 – 08/2018	Swiss Federal Institute of Technology ETH, Zürich: Scientific assistance Group of Sustainable Agroecosystems
05/2017 – 11/2017	Arcadis Schweiz AG, Schlieren: Internship Group of Contaminated sites and building hazards
09/2015 – 06/2016	Swiss Federal Institute for Forest, Snow and Landscape Research WSL, Birmensdorf: Scientific assistance Group of Rhizosphere Processes

11/2014 – 05/2015	Swiss Federal Institute for Forest, Snow and Landscape Research WSL, Birmensdorf: Civil service

Scientific publications

Baumgartner, S., Bauters, M., Barthel, M., Alebadwa, S., Bahizire, N., Sumaili, C., Ngoy, D., Kongolo, M., Mujinya, B., Cizungu, L., Six, J., Boeckx, P., Oost, K. Van, & Drake, T. W. (2022). Fluvial sediment export from pristine forested headwater catchments in the Congo Basin. *Geomorphology*, *398*, 108046.

Barthel, M., Bauters, M., **Baumgartner, S.**, Drake, T. W., Bey, N., Bush, G., Boeckx, P., Botefa, C. I., Dériaz, N., Ekamba, G., Gallarotti, N., Mbayu, F., Mugula, J., Makelele, I., Mbongo, C., Mohn, J., Mandea, J., Mpambi, D., Ntaboba, L., Rukeza, M., Spencer, R., Summerauer, L., Vanlauwe, B., Van Oost, K., Wolf, B., & Six, J. (2022). Low N_2O and variable CH_4 fluxes from tropical forest soils of the Congo Basin. *Nature Communications.*

Baumgartner, S., Bauters, M., Barthel, M., Drake, T. W., Ntaboba, L. C., Bazirake, B. M., Six, J., Boeckx, P., & Van Oost, K. (2021). Stable isotope signatures of soil nitrogen on an environmental-geomorphic gradient within the Congo Basin. *SOIL*, *7*, 83–94.

Bauters, Marijn, Drake, T. W., Wagner, S., **Baumgartner, S.**, Makelele, I. A., Bodé, S., Verheyen, K., Verbeeck, H., Ewango, C., Cizungu, L., Oost, K. Van, & Boeckx, P. (2021). Fire-derived phosphorus fertilization of African tropical forests. *Nature Communications*, 1–8.

Gallarotti, N., Barthel, M., Verhoeven, E., Isadora, E., Pereira, P., Bauters, M., **Baumgartner, S.**, Drake, T. W., Boeckx, P., Mohn, J., Longepierre, M., Kalume, J., Isaac, M., Makelele, A., Cizungu, L., & Johan, N. (2021). In-depth analysis of N 2 O fl uxes in tropical forest soils of the Congo Basin combining isotope and functional gene analysis. *The ISME Journal*.

Bagalwa, R. M., Chartin, C., **Baumgartner, S.**, Mercier, S., Syauswa, M., Samba, V. C., Zabona, M. T., Karume, K., Cizungu, N. L., Barthel, M., Doetterl, S., Six, J., Boeckx, P., & Van Oost, K. (2021). Spatial and seasonal patterns of rainfall erosivity in the Lake Kivu region: Insights from a meteorological observatory network. *Progress in Physical Geography: Earth and Environment*.

Baumgartner, S., Barthel, M., Drake, T., Bauters, M., Makelele, I. A., Mugula, J. K., Summerauer, L., Gallarotti, N., Ntaboba, L. C., Van Oost, K., Boeckx, P., Doetterl, S., Werner, R., & Six, J. (2020). Seasonality, drivers, and isotopic composition of soil CO_2 fluxes from tropical forests of the Congo Basin. *Biogeosciences*, 1–22.

Zuijdgeest, A., **Baumgartner, S.**, Wehrli, B. (2016). Hysteresis effects in organic matter turnover in a tropical floodplain during a flood cycle. *Biogeochemistry*, 131, 49–63.